Republic of Iraq
Ministry of Higher Education
and Scientific Research
University of Babylon
College of Engineering

The Dynamics of Dual-Spin Spacecraft Using Two Ring Dampers

A Thesis
Submitted to University of Babylon
College of Engineering
in Partial Fulfillment of the Requirements for the Degree of
Master of Science in Mechanical Engineering
(Applied Mechanics)

By

Ameer Abdul mona'm Kadhem Abbas

(B.Sc. 2004)

June - 2009

جمهورية العراق
وزارة التعليم العالي والبحث العلمي
جامعة بابل
كلية الهندسة

ديناميكية المركبة الفضائية ذات البرم المزدوج باستخدام مخمدين حلقيين

رسالة مقدمة إلى
جامعة بابل-كلية الهندسة
كجزء من متطلبات نيل درجة الماجستير
علوم في الهندسة الميكانيكية
(ميكانيك تطبيقي)

من قبل

أمير عبد المنعم كاظم عباس
(بكالوريوس هندسة ميكانيك 2004)

حزيران- 2009 جمادي الأخر- 1430

Abstract

In this research, the attitude motion of a torque free, axisymmetric dual-spin spacecraft containing double nutation ring dampers is analyzed. The dampers are mounted with equal offsets center from the spin axis, in the rotor section of the spacecraft, as a passive nutation damping system, where each one consists of a circular ring totally filled with a viscous fluid.

The equations of motion are developed using Newton-Lagrange approach resulting in equations of a nondimensionalized form, in terms of suitable dimensionless variables and parameters of the spacecraft and the nutation dampers.

The fluid motion inside the dampers is shown to occur in two distinct modes of motion, previously named the nutation-synchronous mode and spin-synchronous mode. The analytical expressions for the nutation angle and the time constant in both modes of motion are developed using zero-order approximation technique.

The analytical results are compared with those found numerically using computer simulation program, which is built by **Matlab 7/ program**. It is found that the proposed nutation damping system is an acceptable one. In addition, the comparison reveals that the time constant for nutation-synchronous mode is decreased by (50%) compare with using one viscous ring nutation damper as a damping system.

The effect of the various spacecraft and nutation dampers parameters on the dynamic characteristics and residual nutation angle is studied. It is found that the time constant in both modes of motion is of contrast requirements with respect to the increase in both the inertia ratio and the damping constant. Also, it is found that the time constant in the spin-synchronous mode is greatly affected by the offset distance. Finally, it is concluded that the residual nutation angle increases with increasing the ring radius and the ring mean radius, while it decreases with increasing the inertia ratio.

الخلاصة

في هذا البحث، تم تحليل الحركة الترنحية للمركبة الفضائية ذات البرم المزدوج والخالية من تأثير العزوم الخارجية والمحتواة على زوج من المخمدات الترنحية. تم تثبيت المخمدين بمركزين مزاحين عن محور الدوران, داخل الجسم الدوار للمركبة الفضائية, كمنظومة اخمادة سلبية, حيث إن كل مخمد يتألف من حلقة دائرية مملوءة كليا بسائل لزج.

تم اشتقاق معادلات الحركة باستخدام طريقة نيوتن-لاكرانج (Newton-Lagrange) والتي تنتج عنها معادلات لابعدية بدلالة متغيرات ومقادير لابعدية خاصة بمنظومة المركبة الفضائية والمخمدين.

تكون حركة المائع داخل المخمدين على طورين منفصلين من الحركة تدعى طور التزامن الترنحي (nutation-synchronous mode) وطور التزامن التدويمي (spin-synchronous mode). وقد وجدت التعابير التحليلية الخاصة بزاوية الترنح وثابت الزمن لكلا الطورين باستخدام طريقة الرتبة الصفرية التقريبية (zero-order approximation technique).

تمت مقارنة النتائج التحليلية مع تلك التي حصل عليها بواسطة برامج محاكاة حاسوبية بنيت باستخدام برنامج الماتلاب(**Matlab/7**). وقد وجد إن المنظومة المقترحة تعتبر مقبولة ويمكن استخدامها كمنظومة إخماد سلبي داخل المركبات الفضائية ذات البرم المزدوج. بالإضافة إلى ذلك فقد كشفت المقارنة على إن ثابت الزمن الخاص بطور التزامن الترنحي قد قل بنسبة (50%) بالمقارنة مع استخدام مخمد حلقي مفرد كمنظومة إخماد سلبي.

تمت دراسة تأثير المقادير المختلفة والخاصة بالقمر الصناعي والمخمدين على الخصائص الديناميكية وزاوية الترنح المتبقية. وقد وجد إن ثابت الزمن في كلا الطورين هو ذات متطلبات متضاربة بالنسبة لنسبة عزم القصور الذاتي وثابت التخميد. كما وجد إن ثابت الزمن الخاص بطور التزامن التدويمي قد تأثر وبصورة كبيرة بمقدار إزاحة كل مخمد عن محور الدوران. وأخيرا, تم الاستنتاج على إن زاوية الترنح المتبقية تزداد بزيادة نصف القطر الرئيسي للحلقة ونصف قطر الأنبوب وتقل بزيادة نسبة عزم القصور الذاتي.

Acknowledgement

*“**In The Name of Allah, The Gracious, The Merciful**”*

*Praise be to Allah for providing me the willingness and strength to accomplish this work. Sincere gratitude and appreciation are devoted to my supervisor **Asst. Prof. Dr. Ahmed A. Al-Ragihy** for his guidance, patience, valuable advises, continuous encouragement and efforts during the work of this study.*

*I wish to express my cordial thanks and deepest gratitude to my co-supervisor **Asst. Prof. Dr. Alaa M. Hussein Al-Jussani** for his generous guidance, valuable suggestions and active interest in this work.*

*Special thanks to **Dr. Hameed D. Lafta**, the Head of the Mechanical Engineering Department, University of Kufa for his support, guidance, and his appreciated assistance.*

Finally, I would like to thanks my friends and all persons who spent any effort in helping me in this work.

Ameer

June - 2009

Certification

*We certify that the preparation of this thesis titled "**The Dynamics of Dual-Spin Spacecraft Using Two Ring Dampers**" was made by **Ameer Abdul mona'm Kadhem Abbas** under our supervision at the Department of Mechanical Engineering in the University of Babylon in partial fulfillment of the requirements for the Degree of Master of Science in Mechanical Engineering.*

Signature:
Name: **Asst. Prof. Dr. Ahmed A. Al-Ragihy**
Date: / /

Signature:
Name: **Asst. Prof. Dr. Alaa M. Hussein Al-Jussani**
Date: / /

In view of the available recommendation, I forward this thesis for discussion by the Examining Committee.

Signature:
Name: **Prof. Dr. Adil A. Alwan Al-Moosawy**
Head of the Mechanical Engineering Department
Date: / /

Committee Certification

*We certify, as an examining committee, that we have read this thesis titled "**The Dynamics of Dual-Spin Spacecraft Using Two Ring Dampers**", and examined the student **Ameer Abdul mona'm Kadhem Abbas** in its content and in what is connected with it, and that in our opinion it meets the standard of thesis for the Degree of Master of Science in Mechanical Engineering.*

Signature:
Name: **Asst. Prof. Dr. Nabil Hassan Hadi**
Date: / /
(*Chairman*)

Signature:
Name: **Asst. Prof. Dr. Ahmed Abdul Hussain Ali**
Date: / /
(*Member*)

Signature:
Name: **Asst. Prof. Dr. Hatem Hadi Obeid**
Date: / /
(*Member*)

Signature:
Name: **Asst. Prof. Dr. Ahmed A. Al-Ragihy**
Date: / /
(*Supervisor*)

Signature:
Name: **Asst. Prof. Dr. Alaa M. Hussein Al-Jussani**
Date: / /
(*Supervisor*)

Approved by the Dean of the College of Engineering

Signature:
Name: **Asst. Prof. Dr. Salah Tawfeek Al-Bazzaz**
Date: / /

Contents

CHAPTER THREE: Attitude Dynamics & Stability of Dual-Spin Spacecraft

CHAPTER FOUR: Dynamics of Dual-Spin Spacecraft Containing Nutation Dampers

CHAPTER FIVE: Results & Discussion

List of Figures

Nomenclature

Vector Notations

$\vec{\mathbf{a}}$	Euler axes	
$\vec{h}$	Angular momentum vector of the spacecraft	
$\vec{h}_P$	Angular momentum vector of the platform along the spin axis	
$\vec{M}$	Applied torque vector	
$\vec{r}$	The position vector of point G with respect to O	
$\dot{T}_P$, $\dot{T}_R$	Energy dissipation rate of the platform and the rotor respectively	

List of Symbols

A	Principal transverse moment of inertia of the spacecraft	kg m^2
A_R	Principal transverse moment of inertia of the rotor	kg m^2
A_x, A_y	Moments of inertia of the spacecraft measured along xy axes	kg m^2
b_1, b_2	Ratio of the ring height to the ring mean radius of first and second ring respectively	
B_P	Principal transverse moment of inertia of the platform	kg m^2
C	Moment of inertia of principal spin axis of the spacecraft	kg m^2
C_f	Coefficient viscous friction between the liquid and the ring damper	N s/m
C_P, C_R	Moments of inertia of the platform and the rotor along z-axis	kg m^2
C_s	Specular reflection	
d	Ring center offset	mm
e_x, e_y, e_z	Unit vectors	
F_v	Damping force	N
G	Ratio of the ring center offset to the ring mean radius	

h_1, h_2	Heights of the first and the second ring dampers	mm
I	Rigid body inertia matrix	
$[I]_1$, $[I]_2$	Inertia matrices of the first and the second ring dampers respectively	
$[I_P]$, $[I_R]$	Inertia matrices of the platform and the rotor respectively	
$[I]_s$	Spacecraft inertia matrix	
I_s	Moment of inertia of the spacecraft about the spin axis	kg m^2
I_T	Transverse moment of inertia of the spacecraft	kg m^2
I_u, I_v, I_z	Moments of inertia of the first ring damper about uvz axes	kg m^2
$I_{u'}$, $I_{v'}$, $I_{z'}$	Moments of inertia of the second ring damper about $u'v'z'$ axes	kg m^2
I_{uz}, $I_{u'z'}$	Products moment of inertia of the ring dampers	kg m^2
I_x, I_y, I_z	Principal moments of inertia of the spacecraft	kg m^2
I_{xx}, I_{yy}, I_{zz}	Moments of inertia of the rigid body about xyz axes	kg m^2
I_{xy}, I_{yz}, I_{xz}	Products moment of inertia of the rigid body about xyz axes	kg m^2
L	Distance between the center of each surface and the center of mass of the spacecraft	m
m	Mass of the viscous fluid	kg
m_b	Mass of the rigid body	kg
M_P, M_R	Mass of the platform section and the rotor section respectively	kg
M_x, M_y, M_z	Components of the applied torques	N m
$ouvz$, $ou'v'z'$	Coordinate systems of the ring dampers	
$OXYZ$	Fixed reference frame	
OXYZ	Inertial reference frame at the spacecraft center of mass	
oxyz	Spacecraft reference frame	
$O_P\,x_P\,y_P\,z_P$	Coordinate system located at the platform center of mass	
O_p, O_R, O_s	Mass center of the platform, rotor, and the spacecraft respectively	
$O_R\,x_R\,y_R\,z_R$	Coordinate system located at the rotor center of mass	
P	Platform of the dual-spin spacecraft	
p, q, r	Dimensionless angular velocity components of the spacecraft	
P_a	Amplitude	
p_e, q_e, r_e	Steady state angular velocity components of the spacecraft	
$\bar{q}$	Quaternion	
q_1, q_2, q_3	Quaternions components	
q_4	Scalar component of Quaternion vector	
$\{Q\}$	Column matrix of the moment component of the non-conservative forces	N m
Q_α	Generalized moment associated with the generalized coordinate α	N m
R	Ring mean radius	m

r	Ring radius	mm
r_c	Distance between the centers of masses of the rotor and the platform	m
r_i	Distance from the center of the tube	mm
R_r	Rotor of the dual-spin spacecraft	
T	Total kinetic energy of the spacecraft equipped with double ring dampers	N m
t	Time	sec
T_b	Total torque about the bearing axis	N m
T_f	Torque produce by bearing friction	N m
T_i	Kinetic energy of the particle	N m
T_k	Kinetic energy of the rigid body	N m
T_m	Torque produce by DC motor	N m
T_{rot}	Rotational kinetic energy of the spacecraft	N m
V_f	Linear velocity of the fluid relative to the ring	m/s
$\mathbf{X_O, Y_O, Z_0}$	Inertial reference frame at the earth center of mass	

Greek Symbols

α	Relative angular displacement between the fluid and the spacecraft	rad
α_e	Steady state relative angular displacement of the damping fluid	rad
$\alpha_\circ$	Initial value of α in the spin-synchronous mode	rad
$\tilde{\alpha}$	Small variation in α in the spin-synchronous mode	rad
α_r	Relative rotation between the platform and the rotor	rad
δ	Fullness of the ring	
ε	Inertia ratio of the fluid to the transverse moment of inertia of the spacecraft	
ε_d	Small perturbed motion	
η	Damping constant of the damping fluid	
η_n	Damping constant of the damping fluid in nutation-synchronous mode	
η_s	Damping constant of the damping fluid in spin-synchronous mode	
θ	Nutation angle of the spacecraft	rad
θ_n	Spacecraft nutation angle in nutation-synchronous mode	rad
θ_r	Residual nutation angle of the spacecraft	rad
θ_s	Spacecraft nutation angle in spin-synchronous mode	rad
θ_t	Transition nutation angle	
λ_P, λ_R	Nutation frequencies of the platform and the rotor respectively	rad/s
ρ_f	Density of the damping fluid	kg/m^3
σ	Inertia ratio	
σ_P	Ratio of the platform spin axis moment of inertia to the transverse moment of inertia of the spacecraft	
τ	Dimensionless time variable	
τ_n	Dimensionless time constant in the nutation-synchronous mode	
τ_{cs}	Dimensionless time constant in the spin-synchronous mode	
Φ	Rotation angle about Euler axis	rad
Ψ	Angle between the total angular velocity vector and the angular Velocity vector about the spin axis	rad
ω_P, ω_R	Angular velocity of the platform and the rotor	rad/s
ω_t	Transverse angular velocity component of the spacecraft	rad/s
ω_u, ω_v, ω_z	Angular velocity components of the spacecraft along u, v, and z axes	rad/s
ω_x, ω_y, ω_z	Angular velocity components of the spacecraft along xyz axes	rad/s
Ω	Initial spin rate of the spacecraft along z-axis	rad/s
Ω_n	Nutation frequency of the spacecraft about the angular momentum vector	rad/s
Ω_P, ω_{Pz}	Inertial spin rate of the platform along z-axis	rad/s

References

[1] Agrawell, B.N., “**Design of Geosynchronous Spacecraft**,” Printice-Hall 1986.

[2] Alfriend, K. T., “**Partially Filled Viscous Ring Nutation Damper**,” Journal of Spacecraft and Rockets, Vol. 11, No. 7, 1974, pp. 456-462.

[3] Ali, M. H., “**Dynamics of Spinning Spacecraft Containing a Nutation Damper**,” M.Sc. Thesis, University of Babylon, 2007.

[4] Annett, R., Shackcloth, W. J. and Tonkin, S. W., "**Theory, Simulation, and Practical Tests of a Counter Spun Nutation Damper for Prolate Spinners**," AIAA Journal, Vol. 3, No. 4, August 1980.

[5] AD and AC, "**Attitude determination and attitude control**," internet web site.

[6] Bhuta, P. G. and Koval, L. R., “**A Viscous Ring Damper for a Freely Precessing Satellite**,”International Journal of Mechanical Sciences, Vol. 8, 1966, pp. 383-395.

[7] Bretl, T., “**More About Quaternions**,” February 11, 2008.

[8] Carrier, G. F. and Miles, J.W., “**On the Annular Damper for a Freely Precessing Gyroscope**,” Journal of Applied Mechanics, Vol. 27, 1960, pp. 237-240.

[9] Cartwright, W. F., Massingill, E. C., and Trueblood, R. D., “**Circular Constraint Nutation Damper**,” AIAA Journal, Vol. 1, No. 6, 1963, pp. 1375-1380.

[10] Cloutier, G. J., “**Nutation Damper Instability on Spin-Stabilized Spacecraft**,” AIAA Journal, Vol. 7, No. 11, 1969, pp. 2110-2115.

[11] Cochran, J. E. and Shu, P. H., “**Effects of Energy Addition and Dissipation on Dual-Spin Spacecraft Attitude Motion**,” Journal of Guidance, Control, and Dynamics, Vol. 6, No. 5, 1983, pp. 368-373.

[12] Cochran, J. E., Jr. and Thompson, J. A., “**Nutation Dampers vs Precession Dampers for Asymmetric Spacecraft**,” Journal of Guidance and Control, Vol. 3, No. 1, 1980, pp. 22-28.

[13] Dachwald, B., “**Spacecraft Attitude Determination and Control**,” Spacecraft Design II, Internet Web Site, 2007.

[14] Doebelin, E.O., "**Control System Principles and Design**," John Wiley & Sons, 1985.

[15] Engineering Mechanics Laboratory, " **Feasibility Study and Design of Passive Dampers for a Manned Rotating Space Station**", NASA Contractor Report, NASA CR-163, MARCH 1965.

[16] Fonseca, I. M., Santos, M. C., and Neri, J. A. C. F., “**On the Attitude Dynamics of the Second Brazilian Scientific Satellite SACI-2**,” National Institute for Space Research- INPE, S. J., Campos, S. P., Brazil, 1999.

[17] Hall, C. D., “**Momentum Transfer Dynamics of a Gyrostat with a Discrete Damper**,” Journal of Guidance, Control, and Dynamics, Vol. 20, No. 6, 1997, pp. 1072–1075.

[18] Hall, C. D., ”**Spacecraft Attitude Dynamics and Control**,” e-book, January 12, 2003.

[19] Hameed, D. L., ”**Analysis & Design of Passive Nutation Damping for Dual-Spin Spacecraft**,” Ph.D. Thesis, University of Baghdad, 2003.

[20] Hong, J. Z., "**Residual nutation angle of satellites with viscous nutation dampers**," Acta Astronautica J. Vol. 15, No. 1, 1987, pp. 1-7.

[21] Hubert, C., and Swanson, D., “**Surface Tension Lockup in the Image Nutation Damper-Anomaly and Recovery**,” internet web site.

[22] Likins, P.W., "**Spacecraft Attitude Dynamics and Control-A Personal Perspective on Early Developments**," Journal of Guidance, Control, and Dynamics, Vol. 9, No. 2, 1986,pp. 129–134.

[23] Makovec, K. L., "**A Nonlinear Magnetic Controller For Three Axis Stability of Nanosatellite**," M.Sc. Thesis, Virginia Polytehnical Institute and State University, July, 2001.

[24] Meirovitch, L ., "**Methods of Analytical Dynamics**," McGraw-Hill Book Company, New York, 1970.

[25] Meriam, J. L., "**Dynamics**," John Wiley & Sons, Second Edition, 1975.

[26] Miles, J. W., "**On the Annular Damper for a Freely Precessing Gyroscope-II**," Journal of Applied Mechanics, Vol. 30, 1963, pp. 189–192.

[27] Mingori, D. L., "**Effects of Energy Dissipation on the Attitude Stability of Dual-Spin Satellites**," AIAA Journal, Vol. 7, No. 1, 1969, pp. 20–27.

[28] NASA Space Vehicle Design Criteria, "**Spacecraft Attitude Control During Thrusting Maneuvers**," National Aeronautics and Space Administration, Feb. 1971.

[28] Sandfry, R. A., "**Equilibria of a Gyrostat with a Discrete Damper**," Ph. D Thesis, Virginia Polytechnic Institute and State University, July 9, 2001.

[30] Schrodenger, C., "**Guidance, Navigation, and Control**," Second Edition, Internet Web Site, 1994.

[31] Sen, A. K., "**Stability of a Dual-Spin Satellite with a four Nutation Damper**," AIAA Journal, Vol. 8, No. 4, July 1972, pp. 822-823.

[32] Sen, A. K., " A **Nutation Damper for a Dual-Spin Spacecraft**," IEEE Transactions on Aerospace and Electric Systems, Vol. AES-6, No. 6, 1970.

[33] Sen, A. K., "**On the Existence of a Trap State for OSO- Type Satellite**," IEEE Transactions on Aerospace and Electric Systems, Vol. AC-17, No. 4, August 1972.

[34] Sen, A. K., "**The Use of a Spinning Dissipator for Attitude Stabilization of Earth-Orbiting Satellite**," IEEE Transactions on Aerospace and Electric Systems, Vol. AES-9, No. 2, March 1973.

[35] Takaichi, A., Nishimura, J., and Hinada, M., "**Effect of Void Gas Lying between Fluid Slugs in Nutation Dampers**," The Proceeding of The Symposium on mechanic for spaceflight , Tokyo university, March 1987.

[36] Tokin, S. W., "**Non-Active Nutation Damping for Single-Spin Spacecraft of all mass Distributions**," Aeronautical Journal, 1976, pp. 394-401.

[37] Tseng, G. T., "**Nutational Stability of an Asymmetric Dual-spin spacecraft**", AIAA Journal, Vol. 13, No. 8, August 1976, pp. 488-493.

[38] Winfree, P. W. and Jr., J. E. C., "**Nonlinear Attitude Motion of a Dual-Spin Spacecraft Containing Spherical Dampers,**" Journal of Guidance, Control, and Dynamics, Vol. 9, No. 6, 1986, pp. 681–690.

[39] Yang, W.Y., Cao, W., Chang, T., and Morris, J., " **Applied Numerical Methods using Matlab**", JohnWily & Sons, 2005.

[40] Yu, E. Y., "**Spin Decay, Spin-Precession Damping, and Spin-Axis Drift of the Telstar Satellite,**" The Bell system technical Journal, Sep. 1963, pp. 2169-2193.

Bibliography

[1] Beer, F. P., and Jr, E. R. J.," **Vector Mechanics for Engineers Dynamic**", McGRAW-Hill, Third Edition, 1977.

[2] Flatley, T. W., "**Equilibrium State for a Class of Dual-Spin Spacecraft**", NASA Technical Report, NASA TR, R-362, MARCH 1971.

[3] Fowles, G. R., "**Analytical Mechanics**", Holt, Rinehart, and Winston, Inc, Second Edition , 1970.

[4] Lopes, R. V. D. F., Ricci, M. G., and Guedes, U. T. V.," **Partially Filled Viscous Ring Nutation Damper: Brief Description and Preliminary design**", June 25, 1986.

[5] Mathworks, "**Simulink**", The Mothworks, Inc, 1999.

[6] Rao, S. S., "**Mechanical Vibrations**", Addison-Wesley, Third Edition, 1995.

[7] Shibly, A. H., "**Sliding Mode Controller for a Three-Axis Gas Jet Satellite Attitude control System**", M.Sc thesis, University of Baghdad, December 1995.

[8] عبد الكريم البيكو ,"**البرمجة باستخدام الماتلاب**" , 2006

Appendix-B

B.1 Solution of the Equation of Nutation Angle Rate

The differentiation of the nutation angle rate θ' may be given by:

$$\theta' = \frac{ph_v - qh_u}{h_t} \tag{B.1}$$

where h_u, h_v and h_t are given by:

$$h_u = (A + I_u + I_{u'})\omega_u - (I_{uz} + I_{u'z'})(\omega_z + \dot{\alpha})$$
$$h_v = (A + I_v + I_{v'})\omega_v$$
$$h_t = \sqrt{h_u^2 + h_v^2}$$

Substituting for h_u, h_v and h_t in Eq. (B.1) then

$$\theta' = \frac{\left[(A + I_v + I_{v'})\omega_v\right]p - \left[(A + I_u + I_{u'})\omega_u - (I_{uz} + I_{u'z'})(\omega_z + \dot{\alpha})\right]q}{\sqrt{\left[(A + I_u + I_{u'})\omega_u - (I_{uz} + I_{u'z'})(\omega_z + \dot{\alpha})\right]^2 + \left[(A + I_v + I_{v'})\omega_v\right]^2}} \tag{B.2}$$

or in terms of dimensionless variables:

$$\theta' = \frac{\left[\frac{I_v + I_{v'}}{A} - \left(\frac{I_u + I_{u'}}{A}\right)\right]pq + \frac{(I_{uz} + I_{u'z'})}{A}(r + \alpha')q}{\sqrt{\left(1 + \frac{I_u + I_{u'}}{A}\right)^2 p^2 - 2\left(1 + \frac{I_u + I_{u'}}{A}\right)\frac{(I_{uz} + I_{u'z'})}{A}(r + \alpha')p + \left(\frac{(I_{uz} + I_{u'z'})}{A}\right)^2 (r + \alpha')^2 + \left[\left(1 + \frac{I_v + I_{v'}}{A}\right)q\right]^2}} \tag{B.3}$$

Eq. (B.3) can be given in terms of dimensionless parameters by:

$$\theta' = \frac{\left[\frac{I_v + I_{v'}}{A} - \left(\frac{I_u + I_{u'}}{A}\right)\right]pq + \frac{(I_{uz} + I_{u'z'})}{A}(r + \alpha')q}{\sqrt{(1 + f(\varepsilon))^2 p^2 - 2(1 + f(\varepsilon))f(\varepsilon)(r + \alpha')p + f(\varepsilon)^2 (r + \alpha')^2 + (1 + f(\varepsilon))^2 q^2}} \tag{B.4}$$

where $f(\varepsilon)$ represents the term containing the parameter ε.

Substituting for I_u, $I_{u'}$, $I_{v'}$, I_v, I_{uz} and $I_{u'z'}$ and taken into account that $\varepsilon \ll 1$, so that, Eq. (B.4) may be given by:

$$\theta' = \frac{(2G^2 p + G(b_1 + b_2)(r + \alpha'))\varepsilon q}{\sqrt{p^2 + q^2}} \tag{B.5}$$

In the following section, the expression of $\tan\theta$ in terms of dimensionless parameters is developed. It is known that

$$\tan\theta = \frac{h_t}{h_z} \tag{B.6}$$

Form above, the expression of the transverse angular momentum vector h_t, in terms of dimensionless quantities is given by:

$$h_t = A\sqrt{p^2 + q^2 + f(\varepsilon, \varepsilon^2)} \tag{B.7}$$

The spin axis angular momentum components in terms of dimensionless quantities is given by:

$$h_z = (C + 2I_z)r + 2I_z\alpha' - (I_{uz} + I_{u'z'})p + C_p\frac{\Omega_p}{\Omega} \tag{B.8}$$

Substituting of Eqs. (B.7) and (B.8) into Eq. (B.6), results in:

$$\tan\theta = \frac{A\sqrt{p^2 + q^2 + f(\varepsilon, \varepsilon^2)}}{(C + 2I_z)r + 2I_z\alpha' - (I_{uz} + I_{u'z'})p + C_p\frac{\Omega_p}{\Omega}} \tag{B.9}$$

or

$$\tan\theta = \frac{\sqrt{p^2 + q^2}}{\left(\frac{C + 2I_z}{A}\right)r + \frac{2I_z}{A}\alpha' - \frac{(I_{uz} + I_{u'z'})}{A}p + \frac{C_p}{A}\frac{\Omega_p}{\Omega}} \tag{B.10}$$

Eq.(B.10) can be given in terms of ε and σ by:

$$\tan\theta = \frac{\sqrt{p^2 + q^2}}{(\sigma + f(\varepsilon))r + f(\varepsilon)\alpha' - f(\varepsilon)p + \lambda_s} \tag{B.11}$$

where $f(\varepsilon)$ represents the term containing the parameter ε.

Using zero order approximation, then Eq. (B.11) is given by:

$$\tan\theta = \frac{\omega_t}{(\sigma r + \lambda_s)} \tag{B.12}$$

where ω_t is the transverse angular velocity component, and given by:

$$\omega_t = \sqrt{p^2 + q^2} \tag{B.13}$$

***Appendix*-C**

C.1 Solution of the Equation of the Fluid Motion in Spin Synchronous Mode

In this mode the spacecraft is being close to the nominal state and the fluid goes to the stationary state. Since the change in the rotational speed of the fluid is small compared with the change in relative spin of the spinning rotor $\lambda_n \tau$.

So, the fluid motion α can be expressed as:

$$\alpha = \alpha_0 + \tilde{\alpha} \tag{C.1}$$

such that $\alpha_0 >> \tilde{\alpha}$.

where α_0 is the initial value of the α and $\tilde{\alpha}$ represents small changes occurs in α, such that

$$\begin{aligned} &\sin(\alpha - \alpha_0) = \sin\tilde{\alpha} = \tilde{\alpha} \\ &\cos(\alpha - \alpha_0) = \cos\tilde{\alpha} = 1 \end{aligned} \tag{C.2}$$

The following relations also can be established:

$$\begin{aligned} &\sin(\alpha - \lambda_n \tau) \approx \sin(\alpha_0 - \lambda_n \tau) \\ &\cos(\alpha - \lambda_n \tau) \approx \cos(\alpha_0 - \lambda_n \tau) \end{aligned} \tag{C.3}$$

The basis of the above assumptions is that the change in α is small compared with $\lambda_n \tau$.

Using the above assumption, then Eq. (4.69) (section 4.2.4.2) becomes:

$$\alpha'' + \frac{\eta}{\zeta}\alpha' - \left[\frac{G(b_1 + b_2)}{2\zeta}(1 + \lambda_n)\right]\omega_t \sin(\alpha_0 - \lambda_n \tau) = 0 \tag{C.4}$$

Assume the forced oscillating solution of Eq. (C.4) is given by:

$$\tilde{\alpha} = \alpha - \alpha_0 = A\sin(\alpha_0 - \lambda_n \tau) + B\cos(\alpha_0 - \lambda_n \tau) \tag{C.5}$$

To find the constants *A* and *B*, substituting Eq. (C.5) into Eq. (C.4), then

$$-\lambda_n^{\,2}\left[A\sin(\alpha_0-\lambda_n\tau)+B\cos(\alpha_0-\lambda_n\tau)\right]$$
$$+\frac{\eta}{2\zeta}\left[-A\cos(\alpha_0-\lambda_n\tau)+B\sin(\alpha_0-\lambda_n\tau)\right]=\left[\frac{G(b_1+b_2)}{2\zeta}(1+\lambda_n)\right]\omega_t\sin(\alpha_0-\lambda_n\tau) \qquad \text{(C.6)}$$

Collecting the terms multiplied by $\cos(\alpha_0-\lambda_n\tau)$ and $\sin(\alpha_0-\lambda_n\tau)$, then the constants *A* and *B* are given by:

$$A=-\left[\frac{G(b_2+b_1)(1+\lambda_n)}{2\zeta\left(\lambda_n^{\,2}+\dfrac{\eta^2}{\zeta^2}\right)}\right]\omega_t, \qquad B=\left[\frac{G\eta(b_2+b_1)(1+\lambda_n)}{2\zeta^2\lambda_n\left(\lambda_n^{\,2}+\dfrac{\eta^2}{\zeta^2}\right)}\right]\omega_t$$

Substitute *A* and *B* values in Eq. (C.5), then the expression of $\tilde{\alpha}$ becomes:

$$\tilde{\alpha}=-\left[\frac{G(b_2+b_1)(1+\lambda_n)}{2\zeta\left(\lambda_n^{\,2}+\dfrac{\eta^2}{\zeta^2}\right)}\right]\omega\sin(\alpha_0-\lambda_n\tau)+\left[\frac{G\eta(b_2+b_1)(1+\lambda_n)}{2\zeta^2\lambda_n\left(\lambda_n^{\,2}+\dfrac{\eta^2}{\zeta^2}\right)}\right]\omega_t\cos(\alpha_0-\lambda_n\tau) \qquad \text{(C.7)}$$

re-arranging Eq. (C.7) and substitute for ω_t, then Eq. (C.7) becomes:

$$\tilde{\alpha}=K\tan\theta_s\left[\eta\cos(\alpha_0-\lambda_n\tau)-\lambda_n\zeta\sin(\alpha_0-\lambda_n\tau)\right] \qquad \text{(C.8)}$$

where θ_s referred to the nutation angle in the spin-synchronous mode and the constant *K* is given by:

$$K=\frac{\sigma_n}{\lambda_n^{\,2}}\left[\frac{G(b_1+b_2)(1+\lambda_n)}{2\varsigma^2\left(\lambda_n+\dfrac{\eta^2}{\varsigma^2\lambda_n}\right)}\right]$$

C.2 Solution of the Nutation Angle (θ_s) in the Spin Synchronous Mode

The differential equation of the nutation angle rate Eq. (4.50) is given by:

$$\theta' = -\left[2G^2\omega_t\cos(\alpha-\lambda_n\tau) + G(b_1+b_2)(1+\alpha')\right]\varepsilon\sin(\alpha-\lambda_n\tau) \tag{C.9}$$

It was mentioned that $\tilde{\alpha}$ represent small variation in α such that

$\alpha = \alpha_0 + \tilde{\alpha}$, where $\alpha_0 >> \tilde{\alpha}$.

Using the approximation of small angle, then:

$$\sin(\alpha-\alpha_0) = \sin\tilde{\alpha} = \tilde{\alpha}$$

$$\cos(\alpha-\alpha_0) = \cos\tilde{\alpha} = 1$$

$$\sin(\alpha+\tilde{\alpha}) \approx \sin\alpha_0 \tag{C.10}$$

$$\sin(\alpha+\alpha_0) = \sin(2\alpha_0+\tilde{\alpha}) \approx \sin(2\alpha_0)$$

$$\cos(\alpha+\alpha_0) = \cos(2\alpha_0+\tilde{\alpha}) \approx \cos(2\alpha_0)$$

Using the above relations, then the expression of $\sin(\alpha-\lambda_n\tau)$ may be given by:

$$\begin{aligned}\sin(\alpha-\lambda_n\tau) &= \sin(\alpha_0+\tilde{\alpha}-\lambda_n\tau) = (\sin\alpha_0+\tilde{\alpha}\cos\alpha_0)\cos\lambda_n\tau - (\cos\alpha_0-\tilde{\alpha}\sin\alpha_0)\sin\lambda_n\tau \\ &= (\sin\alpha_0\cos\lambda_n\tau - \cos\alpha_0\sin\lambda_n\tau) + (\cos\alpha_0\cos\lambda_n\tau - \sin\alpha_0\sin\lambda_n\tau)\tilde{\alpha} \\ &= \sin(\alpha_0-\lambda_n\tau) + \tilde{\alpha}\cos(\alpha_0-\lambda_n\tau)\end{aligned} \tag{C.11}$$

Since, that in the spin-synchronous mode, the nutation angle θ_s is small enough such that $\tan\theta_s \approx \theta_s$.

Using the above mentioned assumption and Eq. (C.11), then Eq. (C.9) becomes:

$$\theta' = -\varepsilon\begin{bmatrix}2G^2\theta_s\sigma_n\cos(\alpha-\lambda_n\tau)\left(\sin(\alpha_0-\lambda_n\tau)+\tilde{\alpha}\cos(\alpha_0-\lambda_n\tau)\right) \\ +G(b_1+b_2)(1+\alpha')\left(\sin(\alpha_0-\lambda_n\tau)+\tilde{\alpha}\cos(\alpha_0-\lambda_n\tau)\right)\end{bmatrix} \tag{C.12}$$

Substituting for $\tilde{\alpha}$ from Eq. (C.8), the differentiation of $(\tilde{\alpha}')$ term from Eq. (C.8), and expanding the trigonometric terms, then Eq. (C.12) becomes:

$$\theta_s' = -\varepsilon\left\{\begin{array}{l} 2G^2\sigma_n\theta_s\left[\cos\alpha\sin\alpha_\circ\cos^2\lambda_n\tau + \sin\lambda_n\tau\cos\lambda_n\tau\left(\sin\alpha\sin\alpha_\circ - \cos\alpha\cos_\circ\right) - \sin\alpha\cos\alpha_\circ\sin^2\lambda_n\tau\right] \\ + G(b_1+b_2)\left[\sin\left(\alpha_\circ - \lambda_n\tau\right) + K\theta_s\left[\begin{array}{l} -\lambda_n\zeta\left[\begin{array}{l}\sin\alpha_\circ\cos\alpha_\circ\cos^2\lambda_n\tau + \sin^2\alpha_\circ\cos\lambda_n\tau\sin\lambda_n\tau \\ -\cos^2\alpha_\circ\cos\lambda_n\tau\sin\lambda_n\tau - \sin\alpha_\circ\cos\alpha_\circ\sin^2\lambda_n\tau\end{array}\right] \\ +\eta\left[\begin{array}{l}\cos^2\alpha_\circ\cos^2\lambda_n\tau + 2\sin\alpha_\circ\cos\alpha_\circ\cos\lambda_n\tau\sin\lambda_n\tau \\ +\sin^2\alpha_\circ\sin^2\lambda_n\tau\end{array}\right] \\ +\lambda_n{}^2\zeta\left[\begin{array}{l}\sin\alpha_\circ\cos\alpha_\circ\cos^2\lambda_n\tau - \cos^2\alpha_\circ\cos\lambda_n\tau\sin\lambda_n\tau \\ +\sin^2\alpha_\circ\cos\lambda_n\tau\sin\lambda_n\tau - \sin\alpha_\circ\cos\alpha_\circ\sin^2\lambda_n\tau\end{array}\right] \\ +\eta\lambda_n\left[\begin{array}{l}\sin^2\alpha_\circ\cos^2\lambda_n\tau - 2\sin\alpha_\circ\cos\alpha_\circ\cos\lambda_n\tau\sin\lambda_n\tau \\ \cos^2\alpha_\circ\sin^2\lambda_n\tau\end{array}\right]\end{array}\right]\right]\end{array}\right\} \tag{C.13}$$

Since that the nutation angle θ_s is small, then the terms of $\theta_s{}^2$ can be neglected, and using the following relationships:

$$\sin^2 x + \cos^2 x = 1, \quad \cos^2 x = \frac{1+\cos 2x}{2}, \quad \sin^2 x = \frac{1-\cos x}{2}, \quad \sin x\cos x = \frac{1}{2}\sin 2x$$

Then Eq. (C.13) reduces to:

$$\theta_s' = -\theta_s\left[E_1\cos 2\lambda_n\tau + E_2\sin 2\lambda_n\tau + \frac{G(b_1+b_2)\varepsilon\eta K}{2}(1+\lambda_n)\right] - G\varepsilon(b_1+b_2)\sin(\alpha_0 - \lambda_n\tau) \tag{C.14}$$

where

$$E_1 = \varepsilon G^2\sigma_n\sin 2\alpha_0 + G(b_1+b_2)K\varepsilon\left[\frac{-\zeta\lambda_n}{2}\sin 2\alpha_0 + \frac{\eta}{2}\cos 2\alpha_0 + \frac{\zeta\lambda_n{}^2}{2}\sin 2\alpha_0 - \frac{\eta\lambda_n}{2}\cos 2\alpha_0\right]$$

$$E_2 = -\varepsilon G^2\sigma_n\cos 2\alpha_0 + G(b_1+b_2)K\varepsilon\left[\frac{\zeta\lambda_n}{2}\cos 2\alpha_0 + \frac{\eta}{2}\sin 2\alpha_0 - \frac{\zeta\lambda_n{}^2}{2}\cos 2\alpha_0 - \frac{\eta\lambda_n}{2}\sin 2\alpha_0\right]$$

Eq. (C.14) can be written in term of the spin-synchronous time constant as:

$$\theta_s' + \theta_s\left[E_1\cos 2\lambda_n\tau + E_2\sin 2\lambda_n\tau + \frac{1}{\tau_{cs}}\right] = -G\varepsilon(b_1+b_2)\sin(\alpha_0 - \lambda_n\tau) \tag{C.15}$$

Where

$$\tau_{cs} = \frac{2}{G(b_1+b_2)\varepsilon\eta K(1+\lambda_n)} = \frac{4\zeta^2\lambda_n\left[\lambda_n{}^2+\dfrac{\eta^2}{\zeta^2}\right]}{G^2\varepsilon(b_1+b_2)^2(1+\lambda_n)^2\eta\sigma_n} \tag{C.16}$$

The typical time history curve (figure (5.1)) of the nutation angle time history shows that the decay of the nutation angle consists of dominant exponential decay with on it an oscillation of small amplitude represents the effect of the trigonometric terms. Accordingly, the trigonometric terms contribute nothing to the decay of the nutation angle, which is caused mainly by the exponential decay term, so that the trigonometric terms can be neglected. Then, the general solution of Eq. (C.15) may be given by:

$$\theta_s = \theta_{sc} + \theta_{s.P.I} \tag{C.17}$$

where θ_{sc} represents the complementary part of the solution and $\theta_{s.P.I}$ is the particular integral part of the solution.

These solutions may be given by:

$$\theta_{sc} = ce^{-\frac{\tau}{\tau_{cs}}} \tag{C.18a}$$

$$\theta_{s.P.I} = A'\sin(\alpha_0 - \lambda_n\tau) + B'\cos(\alpha_0 - \lambda_n\tau) \tag{C.18b}$$

Substituting Eq. (C.18b) into Eq. (C.15), then the constants A' and B' are given by:

$$A' = -\frac{(b_1+b_2)G\varepsilon}{\tau_{cs}\left(\lambda_n{}^2+\dfrac{1}{\tau_{cs}{}^2}\right)}\ , \qquad B' = -\frac{(b_1+b_2)G\varepsilon\lambda_n}{\left(\lambda_n{}^2+\dfrac{1}{\tau_{cs}{}^2}\right)}$$

Substituting the solution $\theta_{s.P.I}$ of Eq.(C.18b) in Eq.(C.17) and using the initial condition for the value of θ_s as $\theta_s = \theta_{s0}$ at time $\tau = \tau_0$, then the constant c is given by:

$$c = \left[\theta_{s0} + \left(\frac{\frac{1}{\tau_{cs}} \sin(\alpha_0 - \lambda_n \tau_0) + \lambda_n \cos(\alpha_0 - \lambda_n \tau_0)}{\left(\lambda_n{}^2 + \frac{1}{\tau_{cs}{}^2} \right)} \right) G\varepsilon (b_1 + b_2) \right] e^{\frac{\tau_0}{\tau_{cs}}}$$

Finally, the complete solution of the nutation angle θ_s is given by:

$$\theta_s = \left[\theta_{s0} + \left(\frac{\frac{1}{\tau_{cs}} \sin(\alpha_0 - \lambda_n \tau_0) + \lambda_n \cos(\alpha_0 - \lambda_n \tau_0)}{\left(\lambda_n{}^2 + \frac{1}{\tau_{cs}{}^2} \right)} \right) G\varepsilon (b_1 + b_2) \right] e^{\frac{-(\tau - \tau_0)}{\tau_{cs}}} - \left(\frac{\frac{1}{\tau_{cs}} \sin(\alpha_0 - \lambda_n \tau) + \lambda_n \cos(\alpha_0 - \lambda_n \tau)}{\left(\lambda_n{}^2 + \frac{1}{\tau_{cs}{}^2} \right)} \right) G\varepsilon (b_1 + b_2) \qquad \text{(C.19)}$$

***Appendix*-D**

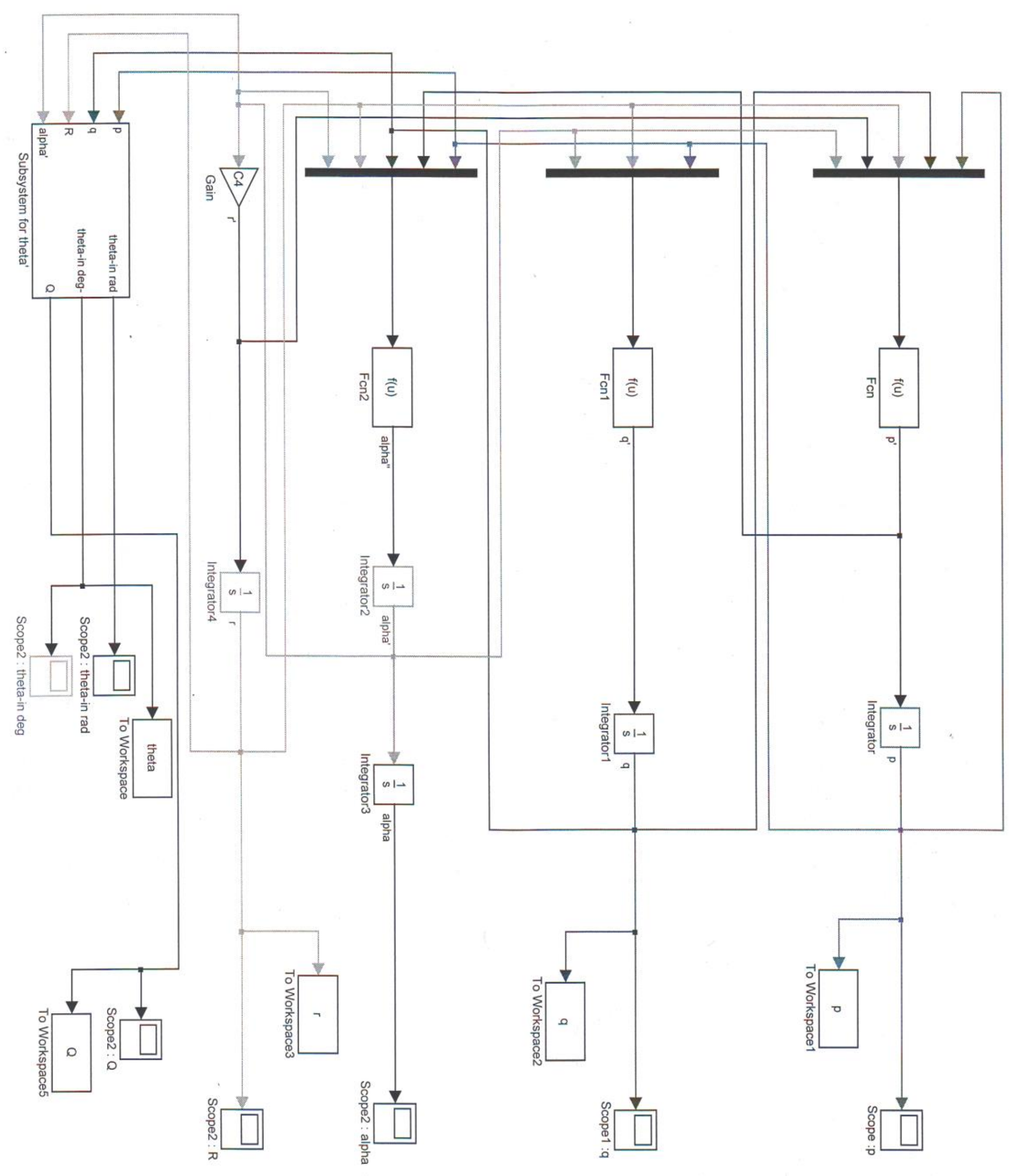

Figure (D.1) Simulik program for calculation of the p , q , r , α , and nutation angle time history.

Appendix-A

A.1 Equations of motion

It is advantageous in solving the problem to introduce the dimensionless form for the variables and to express the parameters of the system in terms of suitable dimensionless parameters.

Let the dimensionless time variable τ be defined as:

$$\tau = \Omega t \tag{A.1}$$

so that, the time derivative with respect to τ is given by:

$$\frac{d}{dt}(\ ) = \Omega \frac{d}{d\tau}(\ ) = \Omega(\ )', \quad d\tau = \Omega dt \tag{A.2}$$

where Ω is the initial spin rate of the rotor, and $(\ )'$ denotes the differentiation with respect to the dimensionless time variable τ. Also, let the dimensionless angular velocity components p , q and r are defined as:

$$p = \frac{\omega_u}{\Omega} \ , \quad q = \frac{\omega_v}{\Omega} \ , \quad r = \frac{\omega_z}{\Omega} \tag{A.3}$$

Let the following dimensionless parameters be defined as:

$\sigma = \dfrac{C}{A}$: ratio of the rotor spin axis principal moment of inertia to the total transverse principal moment of inertia of the spacecraft.

$b_1 = \dfrac{h_1}{R}$: ratio of the first ring height above the spacecraft center of mass to the ring mean radius.

$b_2 = \dfrac{h_2}{R}$: ratio of the second ring height above the spacecraft center of mass to the ring mean radius.

$\eta = \dfrac{C_f}{m\Omega}$: dimensionless damping constant.

$\varepsilon = \dfrac{mR^2}{A}$: ratio of the inertia of the fluid to the total transverse principal moment of inertia of the spacecraft.

$G = \dfrac{d}{R}$: ratio of the ring center offset to the ring mean radius.

$$\zeta = 1 + \frac{d^2}{R^2}$$

The moments of inertia of the fluid are given by:

$$\begin{aligned}
I_u &= \frac{1}{2}mR^2 + mh_1^{\,2} & \qquad I_{u'} &= \frac{1}{2}mR^2 + mh_2^{\,2} \\
I_v &= \frac{1}{2}mR^2 + m(h_1^{\,2} + d^2) & \qquad I_{v'} &= \frac{1}{2}mR^2 + m(h_2^{\,2} + d^2) \\
I_z &= mR^2 + md^2 & \qquad I_{z'} &= mR^2 + md^2 \\
I_{uz} &= mdh_1 & \qquad I_{u'z'} &= mdh_2
\end{aligned} \tag{A.4}$$

The equations of motion, as derived in chapter four in section (4.2.1), are:

$$\begin{aligned}
&(A + I_u + I_{u'})\dot{\omega}_u - (I_{uz} + I_{u'z'})(\dot{\omega}_z + \ddot{\alpha}) - (\omega_z + \dot{\alpha})\left[(A + I_v + I_{v'})\right]\omega_v \\
&\qquad + \left[C\omega_z + 2I_z(\omega_z + \dot{\alpha}) - (I_{uz} + I_{u'z'})\omega_u + C_p\omega_p\right]\omega_v = 0
\end{aligned} \tag{A.5}$$

$$\begin{aligned}
&(A + I_v + I_{v'})\dot{\omega}_v + (\omega_z + \dot{\alpha})\left[(A + I_u + I_{u'})\omega_u - (I_{uz} + I_{u'z'})(\omega_z + \dot{\alpha})\right] \\
&\qquad - \left[C\omega_z + 2I_z(\omega_z + \dot{\alpha}) - (I_{uz} + I_{u'z'})\omega_u + C_p\omega_{pz}\right]\omega_u = 0
\end{aligned} \tag{A.6}$$

$$\begin{aligned}
&C\dot{\omega}_z + 2I_z(\dot{\omega}_z + \ddot{\alpha}) - (I_{uz} + I_{u'z'})\dot{\omega}_u - \omega_v\left[(A + I_u + I_{u'})\omega_u - (I_{uz} + I_{u'z'})(\omega_z + \dot{\alpha})\right] \\
&\qquad + \omega_u\left[(A + I_v + I_{v'})\omega_v\right] = 0
\end{aligned} \tag{A.7}$$

$$\begin{aligned}
&2I_z(\dot{\omega}_z + \ddot{\alpha}) - (I_{uz} + I_{u'z'})\dot{\omega}_u - [(A + I_u + I_{u'})\omega_u - (I_{uz} + I_{u'z'})(\omega_z + \dot{\alpha})]\omega_v \\
&\qquad + [(A + I_v + I_{v'})\omega_v]\omega_u = -2C_f R^2\dot{\alpha}
\end{aligned} \tag{A.8}$$

Subtracting Eq. (A.8) from Eq. (A.7), to give:

$$C\dot{\omega}_z = 2C_f R^2\dot{\alpha} \tag{A.9}$$

Re-arrenging Eq. (A.9) to obtian

$$\dot{\omega}_z = \frac{2C_f R^2 \dot{\alpha}}{C} \tag{A.10}$$

Substituting Eq. (A.10) into Eq. (A.8), and results in:

$$2I_z\left(\frac{2C_f R^2\dot{\alpha}}{C} + \ddot{\alpha}\right) - [I_{uz} + I_{u'z'}]\dot{\omega}_u - [(A + I_u + I_{u'})\omega_u - (I_{uz} + I_{u'z'})(\omega_z + \dot{\alpha})]\omega_v$$
$$+ (A + I_v + I_{v'})\omega_u\omega_v = -2C_f R^2 \dot{\alpha} \tag{A.11}$$

divided Eq. (A.11) by the factor ($2I_z$), gets:

$$\ddot{\alpha} + \frac{2C_f R^2\dot{\alpha}}{C} - \left(\frac{I_{uz} + I_{u'z'}}{2I_z}\right)\dot{\omega}_u + \left(\frac{I_v - I_u}{2I_z}\right)\omega_u\omega_v + \left(\frac{I_{v'} - I_{u'}}{2I_z}\right)\omega_u\omega_v$$
$$+ \left(\frac{I_{uz} + I_{u'z'}}{2I_z}\right)(\omega_z + \dot{\alpha})\omega_v + \frac{C_f R^2\dot{\alpha}}{I_z} = 0 \tag{A.12}$$

Substituting of Eqs. (A.2), (A.3), and (A.4) and using the definition of the dimensionless parameters σ, b_1, b_2, ε and ζ then Eq. (A.12) becomes:

$$\alpha'' + C_1\alpha' + C_2 pq + C_3((r + \alpha')q - p') = 0 \tag{A.13}$$

The constants values in the non dimensional form:-

$$C_1 = \frac{\eta}{\zeta}\left(1 + \frac{2\varepsilon\zeta}{\sigma}\right), \qquad C_2 = \frac{G^2}{\zeta}, \qquad C_3 = \frac{G(b_1 + b_2)}{2\zeta}$$

Substituting of Eqs. (A.2) and (A.3) into Eq. (A.5) and using α'' from Eq. (A.13), then Eq. (A.5) becomes:

$$\left[1 + \left(\frac{I_u + I_{u'}}{A}\right) - \left(\frac{I_{uz} + I_{u'z'}}{A}\right)C_3\right]p' + \left[\left(\frac{C}{A} - 1\right)r - \alpha' + \frac{C_p}{A}\frac{\Omega_p}{\Omega}\right]q$$
$$+ \left[\begin{array}{l} \left[\left(\frac{I_{uz} + I_{u'z'}}{A}\right)C_3 + \frac{2I_z}{A} - \left(\frac{I_v + I_{v'}}{A}\right)\right]r + \left[\left(\frac{I_{uz} + I_{u'z'}}{A}\right)C_3 + \frac{2I_z}{A} - \left(\frac{I_v + I_{v'}}{A}\right)\right]\alpha' \\ + \left[\left(\frac{I_{uz} + I_{u'z'}}{A}\right)C_2 - \left(\frac{I_{uz} + I_{u'z'}}{A}\right)\right]p \end{array}\right]q$$
$$- \left(\frac{I_{uz} + I_{u'z'}}{A}\right)r' + \left(\frac{I_{uz} + I_{u'z'}}{A}\right)C_1\alpha' = 0 \tag{A.14}$$

Dividing Eq. (A.14) by the factor of p' and using the definition of the dimensionless parameters σ, b_1, b_2, ε and ζ then Eq. (A.14) becomes:

$$p' + \frac{(\lambda r - \alpha' + \lambda_S)}{D_1} q + \frac{(A_1 r + A_2 \alpha' + A_3 p)}{D_1} q - \frac{A_4}{D_1} r' + \frac{A_5}{D_1} \alpha' = 0 \tag{A.15}$$

where

$$D_1 = 1 + \varepsilon \left(1 + b_1^2 + b_2^2 - \frac{G^2 (b_1 + b_2)^2}{2\zeta} \right)$$

$$A_1 = \varepsilon \left(1 - (b_1^2 + b_2^2) + \frac{G^2 (b_1 + b_2)^2}{2\zeta} \right)$$

$$A_2 = \varepsilon \left(1 - (b_1^2 + b_2^2) + \frac{G^2 (b_1 + b_2)^2}{2\zeta} \right) = A_1$$

$$A_3 = \varepsilon G (b_1 + b_2) \left(\frac{G^2}{\zeta} - 1 \right)$$

$$A_4 = \varepsilon G (b_1 + b_2), \qquad A_5 = \varepsilon G (b_1 + b_2) C_1$$

Note that $\lambda = \sigma - 1$, $\quad \lambda_s = \dfrac{C_P \Omega_P}{A\Omega}$, $\quad \lambda_n = \lambda + \lambda_s$

Rearranging Eq. (A.6) and substituting Eqs. (A.2), (A.3), then Eq. (A.6) becomes:

$$\left(1 + \frac{I_v + I_{v'}}{A}\right) q' - \left(\frac{I_{uz} + I_{u'z'}}{A}\right)(r + \alpha')^2 - \left[\left(\frac{C}{A} - 1\right) r - \alpha' + \frac{C_p}{A}\frac{\Omega_p}{\Omega}\right] p$$
$$+ \left[\left(\left(\frac{I_u + I_{u'}}{A}\right) - \frac{2I_z}{A}\right) r + \left(\left(\frac{I_u + I_{u'}}{A}\right) - \frac{2I_z}{A}\right)\alpha' + \left(\frac{I_{uz} + I_{u'z'}}{A}\right) p\right] p = 0 \tag{A.16}$$

Dividing Eq. (A.16) by the factor of q', using Eq.(A.4) and the definition of dimensionless parameters σ, b_1, b_2, ε and ζ then Eq. (A.16) becomes:

$$q' - \frac{(\lambda r - \alpha' + \lambda_s)}{D_2} p + \frac{(B_1 r + B_2 \alpha' + B_3 p)}{D_2} p - \frac{B_4}{D_2}(r + \alpha')^2 = 0 \tag{A.17}$$

where

$$D_2 = 1 + \varepsilon\left(1 + b_1^2 + b_2^2 + 2G^2\right)$$

$$B_1 = \varepsilon\left(b_1^2 + b_2^2 - 2G^2 - 1\right)$$

$$B_2 = \varepsilon\left(b_1^2 + b_2^2 - 2G^2 - 1\right) = B_1$$

$$B_3 = \varepsilon(b_1 + b_2)G$$

$$B_4 = \varepsilon(b_1 + b_2)G = B_3$$

By the same way Eq. (A.10) will be:

$$r' - C_4\alpha' = 0 \tag{A.18}$$

where

$$C_4 = \frac{2\eta\varepsilon}{\sigma}$$

Thus, the equations of motion of the spacecraft provided with double ring nutation dampers are

$$\alpha'' + C_1\alpha' + C_2 pq + C_3((r + \alpha')q - p') = 0 \tag{A.19}$$

$$p' + \frac{(\lambda r - \alpha' + \lambda_S)}{D_1} q + \frac{(A_1 r + A_2\alpha' + A_3 p)}{D_1} q - \frac{A_4}{D_1} r' + \frac{A_5}{D_1}\alpha' = 0 \tag{A.20}$$

$$q' - \frac{(\lambda r - \alpha' + \lambda_s)}{D_2} p + \frac{(B_1 r + B_2\alpha' + B_3 p)}{D_2} p - \frac{B_4}{D_2}(r + \alpha')^2 = 0 \tag{A.21}$$

$$r' - C_4\alpha' = 0 \tag{A.22}$$

CHAPTER ONE

Introduction

1.1 Foreword

Artificial satellites offer a significant capability improvement to terrestrial techniques in many fields. The fundamental advantage of a satellite is its ability to obtain a global look at a large portion of earth's surface.

Placing the satellite in orbit is not the end of the story but it is necessary to point the satellite toward the selected targets, or to scan the selected sky area with satellite. Therefore, the satellite attitude needs to be measured and controlled.

The motion of the spacecraft is specified by its position, velocity, attitude, and attitude motion. The first two quantities describe the translational motion of the center of mass of the spacecraft and are subject of what is variously called celestial mechanics, orbit determination or space navigation. The last quantities describe the rotational motion of the spacecraft about the center of mass. The spacecraft's orbit and attitude are coupled. For example, the velocity and altitude of a satellite determine the drag and aerodynamic torque applied, thus affecting its attitude and rotation rate [30].

1.2 Spacecraft Attitude Determination and Control

A high pointing accuracies for various satellite missions is required. This requirement is achieved through an attitude control system that maintains the spacecraft attitude (its orientation in space) within the allowable limits. The attitude control system consists of sensors for attitude determination and actuators to provide corrective torques. Therefore, the spacecraft must be contain an attitude determination and control systems (ADCS).

1.2.1 Attitude Determination

A basic requirement associated with attitude control system of a spacecraft is the determination of its attitude before and after execution of such maneuvers. This is usually done with respect to a set of inertial reference to some object of interest such as the earth. The attitude of a spacecraft is its orientation in space with respect to some reference system where it describes how the spacecraft body axes are oriented relative to an inertial or rotating coordinate system.

Many types of sensors such as sun sensor, earth sensor, magnetometers, gyroscopes, and others are used to sense angles in the inertial space. The selection of sensors for attitude determination depends on several factors such as the type of the spacecraft stabilization, operational procedure and the required accuracy [1].

1.2.2 Attitude control

The attitude control is the process of orienting and moving of the spacecraft in the desired direction. In other wards, its control of the angular position and rotation of the spacecraft, either relative to the object that it is orbiting (Earth, Moon ...) , or relative to the celestial sphere. It consist of two areas: attitude stabilization and attitude maneuver control. For engineering purposes, attitude control is needed for functions such as pointing the antennas and/or instruments in a desired directions, pointing solar panels (arrays) toward the sun, keeping sensors and sensitive equipment away from the sun's light and heat, and pointing the control jets (thrusters) in the desired direction to accomplish efficient thrust maneuvers.

Attitude stabilization is the process of maintaining an existing orientation. It is classified into two broad categories: spin-stabilization and three-axes stabilization. Spin-stabilization is based on gyroscopic stiffness due to the rotation of all or part of the spacecraft body, while, in the case of three-axes stabilization, the entire spacecraft, except the solar arrays, which are sun oriented, is oriented toward the earth [1]. Attitude maneuver control is the process of controlling the orientation of the spacecraft from one attitude to another. For a spin-stabilized spacecraft, control action is applied to adjust the angular momentum vector in inertial space (for a torque-free situation, the energy dissipation is used to adjust the angular momentum vector, active maneuver control system is used here only). For three-axes stabilization spacecraft, control action is applied either simultaneously or as a sequence, to change the orientation of the spacecraft from one attitude to another.

A spacecraft is said to be spin-stabilized if its angular momentum is much greater in magnitude than the effect of disturbance torque impulses during the time interest. A spinning body is defined as one in which the angular velocity component on one body axis (spin axis) remains much greater in magnitude than the angular velocity component on any axis orthogonal to it [28] .

There are two major types of the spin-stabilized spacecraft. The first is a single rigid or quasi-rigid body (single-spin satellite) spinning with respect to inertial space. The other is a multibody system in which various bodies have various states of rotation, but at least one is spinning. The latter type is sometimes called a “dual-spin“ satellite, if it is a two-body system with at least one body rigid and symmetric about the axis of relative rotation (spin axis), it is called a “gyrostat”. In both cases there is a dominant component of angular momentum in body axes which is large with respect to the disturbance torque impulse [28].

In the single-spin stabilized spacecraft, the whole body rotates about the axis of maximum or minimum principal moment of inertia. Early communication satellites, such Syncom I, intelsat I, and ATS I, II [1], figure (1.1), were single-spin stabilized. The primary limitations of these satellites were that they could not use earth-oriented antenna, thus resulting in the requirement for an omnidirectional antenna with a consequential very low antenna gain toward the earth.

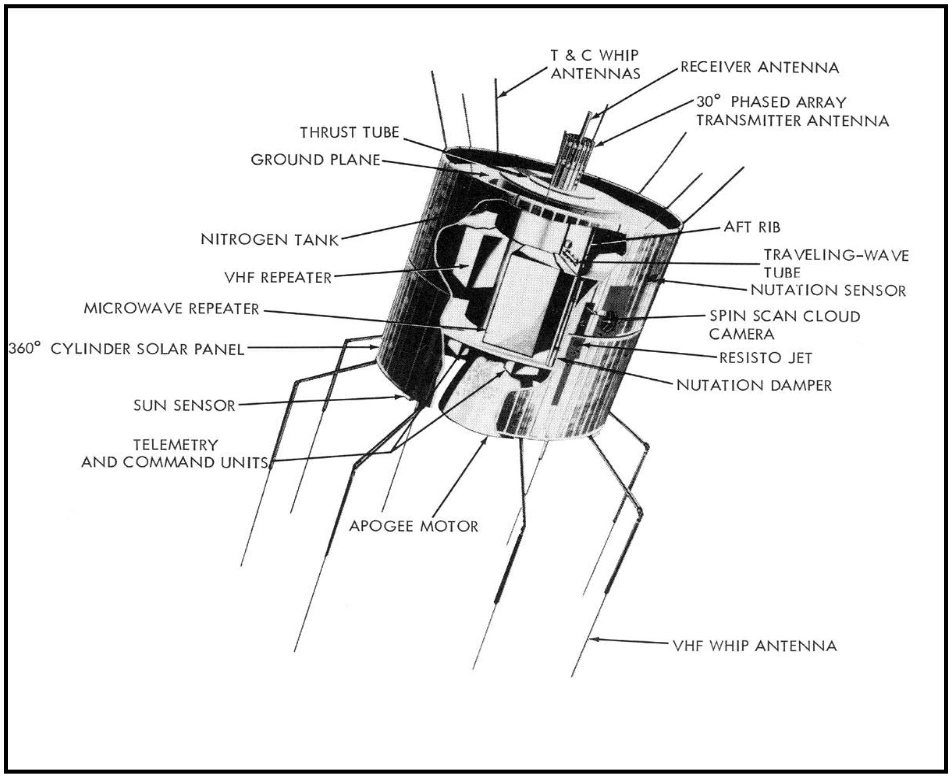

Figure (1.1) Application Technology Satellite (ATS-I).

The limitations of single-spin satellites are overcome with dual-spin satellites. In spacecraft with dual-spin stabilized, a major portion of the spacecraft is spun (the bus or rotor), while the payload section (the platform) is despun at a different rate about the same axis, figure (1.2). This technique is favorable because fixed inertial orientation is possible on the despun portion (allows Earth pointing payload) which provides both scanning and pointing capability and can gave spin about minimum moment of inertia axis [29].

The bus or the spinning rotor rotates at a higher spin rate to provide gyroscopic stiffness and the platform rotating at a much slower rate in accordance the desired orientation, (orients toward the earth by rotating one revolution per day). There are two types which are commonly known as the external rotor and the body stabilized spacecraft, each type employs a different method of attitude stabilization [19]. The external rotor type or "Gyrostat" uses spin stabilization where the rotor of relatively large moment of inertia rotates to provide gyroscopic stiffness (spin relatively slowly ≈50 rpm), while the platform usually containing communication equipment and antenna are despun. A typical example of an external rotor dual spin spacecraft is the intelsat IV, figure (1.2).

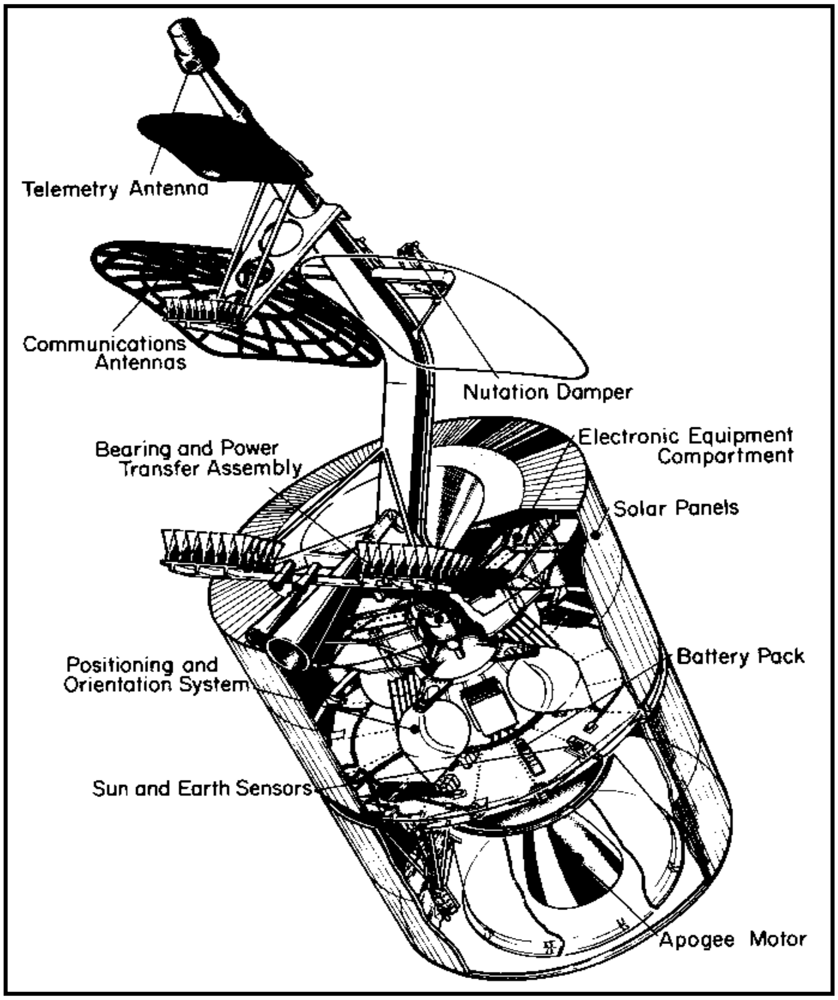

Figure (1.2) External rotor spacecraft: intelsat IV.

In the case of the body stabilized spacecraft, gyroscopic stiffness is achieved via spinning momentum wheel contained within a despun body (high spin rate ≈3000 rpm). These are also referred to as momentum bias satellite. A typical example of this type of dual spin spacecraft is shown in figure (1.3).

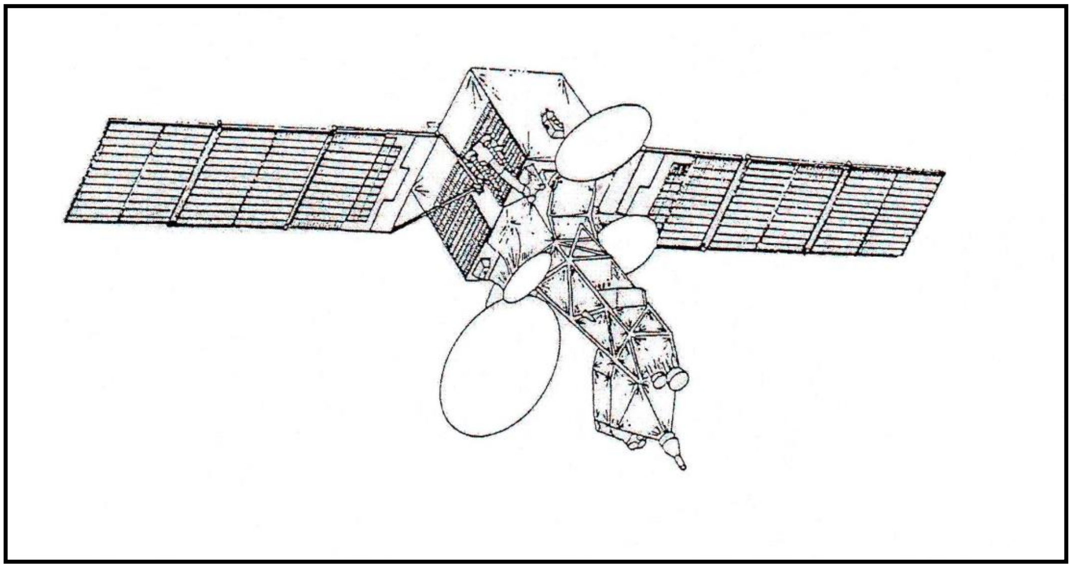

Figure (1.3) Body stabilized spacecraft: Intelsat V.

The techniques that provide attitude stabilization and control of a spacecraft are passive, semi passive, and active, control systems [5] (table 1.1).

Table (1.1) Attitude control system types [5]

Passive	*Semi-passive*	*Active*
Gravity gradient	Momentum bias with magnetics	Propellant
Spinner with nutation damper	Reaction wheels with magnetics for momentum dumping	Reaction wheels with propellant for momentum dumping
Dual spinner with nutation damper	Control moment gyros with magnetics for momentum dumping	Control moment gyros with propellant for momentum dumping

Table (1.1), the passive control system is adopted in the present study. Passive system does not require any external power sources, once they are in place, they use gravity or momentum to create the necessary control forces and moments. They also tend to be somewhat inflexible in operation and are less accurate than active control system. The passive attitude control using [13]:-

- Spin-stabilization.
- Gravity-gradient stabilization.
- Aerodynamic stabilization.
- Magnetic stabilization.
- Solar radiation pressure stabilization.

The spacecraft separation from the booster, reorientation maneuvers, and/or environmental disturbing torques, such as aerodynamic torques and solar radiation pressure can produce transverse angular rates with a resulting conical motion, is termed “free precession”, of the spin axis about the total momentum vector of the spacecraft (which is constant in magnitude and direction in the absence of external moments).

In other words, if the spinning body has mass symmetry about the spin axis then the spin axis describes a right circular cone with the total momentum vector aligned with the cone centerline. If the body is asymmetrical about spin axis then the spin axis describes a more complex figure which revolves about the fixed angular momentum vector. For this case the angle of the spin axis relative to the angular momentum vector is not constant as it was in the symmetrical case but various periodically at twice the body precession frequency. This periodic variation in the half cone angle is termed nutation and corresponding the half cone angle is termed the nutation angle. This typical motion of combined precession and nutation has at times been loosely but descriptively termed “wobble” and the nutation angle described as the wobble angle [15]. The wobble motion will continue indefinitely in the absence of energy dissipation, unless it is corrected. Although nutation can in principle be controlled by thruster firing, it is normally controlled passively [6].

For a real spacecraft the oscillating acceleration forces associated with free precession induce small elastic deformations and relative motions among the spacecraft members thereby causing energy to be dissipated. Energy dissipation implies a change in the total kinetic energy level of the spacecraft and hence a change in the nutation angle (half-cone angle of the free precession). The kinetic energy cannot be completely dissipated since angular momentum must be conserved so there must be a minimum energy state which will be approaches asymptotically. The final motion associated with this minimum energy states must not produce further energy dissipating forces and therefore must consist of a pure spin about a principal axis of inertia [15].

Several methods of reducing the wobble motion have been proposed and implemented. Of these, passive devices are appealing in that they eliminate the need for a sensor and a power source and provide a high degree of reliability. Of the various schemes which have been proposed and analyzed the ones containing fluids in a closed tube (nutation dampers) are especially desirable since they do not involve any moving parts, other than the fluid, and hence eliminate the possibility of stiction or cold welding that occurs in the space environmental. Nutation dampers dissipate energy actively by providing friction (simple device: fluid-in-tube device) where in this type of device, kinetic energy is dissipated by convert into heat when nutational motion causes the fluid to move through the tube.

1.3 Objective and Approach of the Project

The attitude motion of a torque free, axisymmetric dual-spin spacecraft is investigated in this research. The rotor section of the spacecraft contained double nutation ring dampers which are used as a passive nutation damping system to eliminate the attitude motion. Each damper consists of a circular ring of circular cross section totally filled with a viscous fluid and fixed with offset center from the spin axis, in a plane perpendicular to the spin axis, above the center of mass of the spacecraft.

The equations of motion are developed using Newton-Lagrange approach. The approximate analytical expressions for the nutation angle time history are developed, in terms of suitable dimensionless variables and parameters, using zero-order approximation technique. The time constant of the nutation damping system are obtained in terms of suitable dimensionless parameters. The analytical results are compared with those obtained numerically using computer simulation program, which is called **MATLAB 7** / simulink program, to verify the reliability of the proposed nutation damping system.

CHAPTER TWO

Review of literature

2.1 Introduction

A considerable amount of the significant works related to the dynamics and stability of spinning satellite with energy dissipation has been undertaken. Two methods of analyzing energy dissipation are considered; a non-specific energy sink and a discrete damper. Then the developments for spin stabilized spacecraft with specific damping systems are discussed.

2.2 Spin-Stabilized Spacecraft with Energy Dissipation

A classical rigid body analysis of the attitude stability of a spinning single-body spacecraft indicates that a state of steady spin of the spacecraft is stable if the rotation is about its principal axis of either minor or major moment of inertia. After that, it is fairly well known that a spinning oblate, or flywheel shaped, spacecraft having energy dissipating components on board will spin with contracting nutation until it is spinning about the principal axis of maximum moment of inertia. Also, it is well known that a spinning prolate, or rod shaped, spacecraft is unstable under similar conditions and tend to go into a flat spin. These facts were demonstrated most inconveniently by Explorer I motion, the very first US artificial satellite [22].

In the early 1960’s little consideration was given to possible stable minor-axis spin concepts. According to Likins [22], Vernon Landon was aware that storing enough angular momentum in a rotor could overcome the minor axis instability.

The idea of designing satellites with a spinning section and a despun, or slowly spinning section originated from the desire to use spin-stabilization on an earth-pointing satellite, where the high spin rate section is referred to as the rotor, while the slowly spinning section is called the platform. This concept, later named “dual-spin”, was successfully demonstrated in 1962 by Ball Brothers with the orbit of their (Orbiting Solar Observatory) OSO I satellite. However, OSO I spins about a principal axis of maximum inertia [29].

The main attraction of this stabilization scheme (dual-spin stabilization) rests on the fact that a rod-shaped satellite can be rendered asymptotically stable about its axis of least inertia by using a passive dissipators. From a design point of view, a rod-shaped satellite is always preferable to the disk-shaped one because the dimensional limitation of the booster fairing can be overcome by using the former design [36].

Satellite designers did not have rigorous methods of analyzing the stability and energy dissipation of generic satellite models, so analysts developed a class of approximate methods, known as “energy-sink” methods. Fundamental to these methods is the energy sink hypothesis which states that the kinetic energy of any real body is slowly dissipated into heat energy. Also included in the hypothesis the assumption that the dissipation motion is sufficiently small so that the spacecraft has an essentially constant inertia ellipsoid [29]. This technique was used extensively to design the internal energy dissipators (nutation dampers) on Syncom and later satellites [22], where, in this method the damper is considered as an energy removal device or “sink” and the change in the kinetic energy level of the spacecraft in the absence of external torques is computed.

According to Sandfry [29], in 1964, Vernon Landon along with Brian Stewart, he published a paper showing instability criteria for two co-axial axisymmetric bodies with energy dissipation with one of the bodies. The model was rather restrictive, but the energy-sink approximation yielded an important result: the system could be stable in a minor-spin axis with energy dissipation on the platform. London's analysis did not allow for energy dissipation on both the platform and rotor simultaneously. London note that with a motor, a torque could be applied to the rotor to keep the relative angular rate constant. He identified the motor as an energy source or sink, which must be accounted for in the analysis.

Also, Sandfry [29] cited that, independent of London and Strewart, Tony Iorillo in 1965 also discovered that the energy dissipation on the platform, a dual-spin spacecraft could be stable in spin about the minor axis. Iorillo also used an energy-sink analysis to study a dual-spin configuration, but he included energy dissipation on both the platform and rotor. He concluded that the spin axis could be stable provided the energy dissipation of the platform was large enough relative to that of the rotor. Iorillo's work led to the development of TACSAT I, the first on-orbit demonstration in 1969 of Hughes "Gyrostat" satellite concept, what is usually referred to as a dual-spin satellite.

In 1969, Mingori [27] extended the work achieved by Iorillo by including the effect of internal moving parts as well as dissipation. He was concluded that dual-spin spacecraft with a prolate rotor, spin about its axis of minimum moment of inertia, will be asymptotically stable if the energy dissipation in the platform is dominant over that in the rotor.

2.2.1 Dynamics of Spin-Stabilized Spacecraft with a Specific Nutation Damping System

Generally, there are two purposes for spacecraft to be equipped with nutation damping device. The first one is to stabilize the spacecraft whose attitude motion is unstable with removing the damping system [4,36]. The other is to consider the nutation damper as a passive positioning control device, since it can dissipate the energy of the coning motion of the spacecraft and convert its transverse angular momentum into the spin axis angular momentum so as to confine the spacecraft to be close to the state of pure spin [2,38].

The damping device may be generally named according to their mounting in the spacecraft with respect to the spin axis. Whereas, the damper mounted parallel to the spin axis, sometimes called an axial damper, is excited by the precession, or coning motion of the symmetric axis about the inertially fixed angular momentum vector, and was therefore referred to as a precession damper. While the damper aligned normal to the spin axis, often referred to as circumferential damper, is excited by nutation, or the nodding oscillation of the spin axis about its conical path, and was called a nutation damper. For stable, spinning, asymmetric bodies either a precession or nutation damper attenuates both precession and nutation [29].

Researches have studied the performance of different damper devices and configuration with rigid bodies. Two major types of damping mechanisms that where modeled and analyzed including spring-mass-dashpot or (ball-in-tube) dampers, and viscous ring nutation dampers.

2.2.1.1 Spin-Stabilized Spacecraft with Spring-Mass-Dashpot Dampers

Spring-mass damper in the form of ball-in curved tube damper has found an application as a passive nutation damping devices. In 1963, Yu [40] studied the dynamics of spinning satellite equipped with a ball in curved tube precession damper filled with neon gas. The analyses were based on the energy sink approach and the study included an experimental measurement to determine the rolling resistance moment and the coefficient of the viscous friction between the ball and the damping fluid. He estimated that the energy dissipation due to rolling resistance moment could be neglected compare to that due to the viscous friction force and the analysis restricted for small nutation angle approximation only.

Nonlinear phenomenon known as “Trap states” can arise in spin-stabilized spacecraft because of the nonlinear effects of the energy dissipating mechanism (spring-mass-dashpot) normally presented in the spacecraft. In 1969, Cloutier [10], and in 1972, Sen [33] examined the instabilities or “trap states” in a spinning satellites. They explained that instability or trap state is referred to the situation which damper mass moves to an extreme position and remains there, hence, it would not perform its intended function of dissipation energy in order to damp out nutation. They found that this unstable behavior is quite possible for a damper mounted in a single-spin spacecraft or on the spinning section of a dual-spin spacecraft where the other member is essentially despun. On the other hand, the unstable behavior of a damper mounted on the despun member of a dual-spin configuration is found to be extremely unlikely.

Sandfry [29] mentioned that, in 1973, Shneider and Likins, studied the effectiveness of spring-mass-dashpot dampers in passively damping the coning motion of spinning rigid bodies. They studied the dampers mounted parallel and normal to the desired satellite spin axis. Shneider and Likins used an energy sink method and numerical simulation to support the conclusion that for any physically feasible spacecraft, the precession damper dissipates more energy per unit mass than the nutation damper for small coning angles. For larger coning angles and certain rigid body asymmetries, nutation dampers have superior average energy dissipation rates.

In 1980, Cochran and Thompson [12] re-examined the same problem as Shneider and Likins. Using a different method for approximating the elliptic functions in the energy sink method, they validated the superiority of precession damper for small coning angles. Also, they achieved better agreement with numerical simulation than Shneider and Likins for larger angles, where nutation dampers had larger average dissipation rates.

In 1983, Cochran and Shu [11] examined an axisymmetric dual-spin spacecraft with energy addition due to constant-speed rotor and energy dissipation provided by a spring-mass-dashpot damper. They applied the generalized method of averaging, assuming a small damper mass, as well as an energy sink method. By accounting for the contribution of the rotor torque to rotational kinetic energy, the energy sink method produce an average time rate of change of nutation angle which agreed well with the generalized method of averaging and numerical simulation .

Much works focused on the stability of the nominal spin in the presence of energy dissipation for either a single or dual-spin satellites. However, when nominal spin is destabilized, Other stable equilibria exist. These equilibria represent “trap states” that could capture the free-spinning satellite until a correcting maneuver is preformed.

In 1997, Hall [17] studied the motion of a torque free, rigid gyrostat with a spring-mass-dashpot damper. He considered the case of a single-rotor gyrostat with rotor axis parallel to an undeformed system principal axis (damper axis parallel to the rotor axis). He used a liner analysis to derive stability criteria for the nominal spin and concluded that for the specific case of a single rotor gyrostat with rotor and damper aligned with the major principal axis, it is possible to obtain an explicit stability criteria that can be used in damper design. And for multi rotor gyrostat, explicit stability criteria are not available.

In 2001, Sandfry [29] studied the dynamics and relative equilibira states of a gyrostat with energy dissipation provided by a spring-mass-dashpot damper. The equation of motion are developed using Newton-Euler approach, resulting in equations in terms of system momenta and damper variables. He used analytical and numerical methods to explore system equilibria, including the bifurcations that occur for various system parameters for varying rotor momentum and damper parameters. It was shown that for systems with tuned dampers, where the natural frequency of the spring-mass-damper matches the gyrostat precession frequency, the existence of certain equilibria are related to the damper tuning Condition. Also, the global equilibria and bifurcations for varying rotor momentum provide a unique perspective on the dynamics of simple rotor spinup maneuvers.

2.2.1.2 Spin-Stabilized Spacecraft with Nutation Ring Dampers

Ring partially filled with viscous fluid has been used on satellites as nutation dampers. In 1960, Carrier and Miles [8,26] were the first to examine a partially filled viscous ring damper. They approached the problem from a fluid mechanics standpoint and found that for small nutation angles the fluid spreads out around the outer part of the ring. But for larger angles, gaps begin to appear in the fluid and somewhere between (0.5-1)°, the fluid behave as a rigid slug.

In 1963, Cartwright et al. [9] treated the fluid as a rigid slug in their analysis of a spinning rigid body with a ring damper. For spins about a body axis of symmetry, they identified two distinct motions which they named the nutation-synchronous and spin-synchronous modes. For larger nutation angles the slug moves within the ring roughly synchronous with the satellite precession. As damping continues, nutation angle decreases until the spin-synchronous mode begins. This mode is roughly synchronous with the satellite spin rate and continues damping the nutation angle, although in an oscillatory manner.

In 1966, Bhuta and Koval [6] investigated a completely filled viscous ring damper with a spinning rigid body. The damping rate was not as high as for partially filled ring dampers, but a completely filled ring does not appreciably change the inertia properties of the spacecraft. They treated the problem from fluid mechanics standpoint, and found an optimum design for the damper analytically in terms of a dimensionless number, which is called wobble Reynolds number, and experimentally in terms of energy dissipation achieved by the damper. Agreement between the results was excellent.

In 1973, Alfriend [2] re-examined the behavior of the fluid as a rigid slug in a partially filled ring damper and generated an approximate solution for nutation angle time history and the time constants for nutation-synchronous mode and spin-synchronous mode. He explained that in the mode for very small nutation angle (smaller than 5°) which was analyzed by [8], the fluid spreads out over the outer wall of the tube. Also, he found that the spin-synchronous mode may be entirely not exist if the ring is not offset from the spin axis.

In 1986, Winfree and Jr [38] investigated the nonlinear attitude motion of a symmetric dual-spin spacecraft containing two spherical dampers located on the rotor and platform (one damper on each). The spherical dampers are extended to represent fully filled fuel tanks. They used a perturbation method that treats the effects of the motion of the dampers as perturbating torques in conjunction with the generalized method of averaging. They illustrated that for the case of free rotor, averaged equations for the nutation angle and the symmetry axis component of the rotor angular momentum are used to show that “stability reversal” may occur due to varying relative spin rate of the rotor, and unfortunately there no explicit stability criterion was obtained for this case.

In 1986, Hong [20] discussed the reasons why the viscous dampers make the residual angle occur. He studied tube with endpots dampers in two mounted types (meridionally and equatorially mounted respectively) in the spacecraft. The relationship of the maximum residual nutation angle to the structural parameters of the system and the properties of the medium in the damper was developed. The relationship as used to obtain some effective measures to decrease the residual angle. It was found that, the resistance acting on the fluid in the viscous damper at three phase line (air, liquid, and solid meet) is the reason why the residual nutation angle of satellite is induced when the viscous ring dampers are used.

In 1987, Takaichi et al. [35] investigated the effect of separating the damping fluid slug into several slugs in nutation damper of a partially filled type, due to the existence of temperature gradient, on the damping characteristics as well as the effect of the offset center of the damper on the dynamic characteristics. They found, as the offset grows greater, the damping time becomes shorter and concluded that the increase in kinematic viscosity of working fluid is advantageous, but there is little merit in having a large size of inner radius of the ring. It is also shown better to mount the damper in an equatorial plane that is as far from the center of gravity of the satellite as possible. This phenomenon has occurred, a drastic increase in the damping time is inevitable, so it is most important for the whole damper to be kept uniform in temperature.

In 1999, Fonseca et al.[16] studied the effects of the critical rates of inertia on the nutation of the second Micro Brazilian Scientific Satellite which comes from a partially filled viscous ring nutation damper mounted with offset center on the satellite. The satellite provided with four mechanical arms which after deploying, the satellite spins about its major axis. The nutation damper will contribute for the satellite to enter in a flat-spin motion if the spacecraft inertia rate in non-deploying arms configuration does not satisfy the major axis rule. They recommended that, the rate of inertia must be avoided if very closed to unity and it must be greater than one and the critical time for deploying must be less than four minuets to guarantee the major axis rule.

In 2003, Hameed [19] proposed a completely filled viscous ring damper provided with ball for dual-spin spacecraft with axisymmetric rotors. The ball motion was experienced to occur in two modes of motion, as [9]. The analysis was based on the Newton-Lagrange approach and the study included an experimental measurement to determine the coefficient of friction of the viscous fluid. It was found that, the proposed nutation damping system is an acceptable one. Also, the comparison revealed that the dynamic characteristic is better for nutation damper filled with viscous liquid than that filled with viscous gas. It was found that the residual nutation angle increase with increasing the ring mean radius, the ball radius, and the ratio of the ring height to ring mean radius.

In 2007 , Ali [3] examined by the same approach above the effect of the ring damper offset on the decay of the attitude motion and stability of the spacecraft. The used damper was totally filled and without ball. He was found that the time constant in spin synchronous mode will decrease in increasing of the damper offset. Also it is concluded that, the time constants in both modes of motion will decrease in using a fluid with high damping coefficient and it will increase with increasing of the spin rate.

2.2.2 Other Damping Devices for Spin-Stabilized Spacecraft

Other damping devices proposed for dual-spin spacecraft included a four mass structure pivoted on a torsional system which offers dissipative torque in addition to the restoring torque as nutation damper in 1969 by Sen [31]. The damper is of symmetrical configuration about the mass center. Thus, the damper motion did not vary the inertia properties of the spacecraft. It is found that a circular disk or wheel of uniform mass distribution can be used to replace the four-mass structure in the proposed design.

Spinning dissipaters as rotor dampers are another form of passive nutation damping system that have been on spacecraft. In 1970, Sen [32] examined a high performance nutation damper for use in a dual spin spacecraft. The damper consists of a wheel of uniform mass distribution. Torsional arrangement mounted around the center of the wheel used to provide the damping and restoring (spring) torque. He pointed out that the performance of the damper can be improved by increasing the mass and the dimensions of the damper, but it should be noted that the ultimate performance will be limited by such factors as restrictions on the payload dimensions or the allowable weight of the damping system.

In 1973, Sen [34] presented a novel stabilizing system, which act both as a passive nutation damper and a momentum source for an earth pointing satellite. The system designed to use four identical wheels mounted co-axially with and at the ends of the arms of a cruciform structure. The results obtained for a specific design of the stabilizer indicated that the global stability of the desired attitude motion of the spacecraft could be guaranteed with associated damping time constant as low as one second.

In 1976, Tseng [37] examined a dual-spin spacecraft with a wheel damper on the platform and a two-degrees of freedom tilting ring damper (rotor damper) on the rotor. He employed an energy sink method to establish the close form nutational stability criterion and the time constant. It was demonstrated that through the analysis and several numerical examples the energy sink predictions correlate extremely well with the system simulation results.

In 1976, Tonkin [36] and, in 1979, Annett et al. [4] described a counterspun flywheel nutation damper consists of a flywheel attached by dissipative tilting mounting on the axle of a motor parallel to the spacecraft spin axis, but spinning in the opposite direction to the spacecraft. It is treated by theory using differential equations applied to a quasi-steady state showing that it stabilizes oblate and prolate spinners and that it fits into a comparatively unexplored corner of the field that is greatly understood. As a result of the theory, some optimization is done. The equations of motion were simulated on analog computer in an attempt to study the performance of spacecrafts that are inertially more difficult to treat by theoretical means.

As it is obvious from the literature review, there is no one (as far as researcher knowledge goes) has used more than one partially or completely filled nutation ring damper in an dual-spin spacecraft as a passive nutation damping system.

The present work investigate adding an additional viscous ring damper, as that used by [3], in the rotor section of the spacecraft as an attempt to reduce or eliminate the undesirable nutational motion of an axisymmetric dual-spin spacecraft.

CHAPTER THREE

Attitude Dynamics & Stability of Dual-Spin Spacecraft

3.1 Introduction

The attitude dynamic and stability of a specific dual-spin spacecraft are studied in this chapter. The mathematical model of a spacecraft is developed which is important to the understanding of the attitude behavior of the spacecraft system. The derivation of the attitude motion equations are presented for this model, and a linearization technique is adopted to obtain the solution for these equations. Attitude stability of spinning spacecraft without and with energy dissipation are explained.

3.2 Attitude Dynamics of Spinning Spacecraft

Attitude dynamics describe the orientation of a body in an orbit and can be explained using rotations. When examining attitude dynamics, it is important to describe the reference frames being used to give a basis for the rotations.

3.2.1 Reference Frames

Three main reference frames are used to describe the orientation, or attitude, of a spacecraft in orbit. These are the inertial, orbital, and body frames [23]:-

1- Earth-Centered Inertial Frame.

2- Orbital Frame.

3- Body Frame.

3.2.1.1 Earth-Centered Inertial Frame

To define the position of a satellite in space, it is necessary to define the orbit of the satellite relative to an inertial frame and the location of the satellite in the orbit. Also called "celestial coordinates", the Earth centered inertial (ECI) coordinate system is centered in the middle of the earth. As shown in figure (3.1), the $\mathbf{Z_0}$ axis points through the geographic North pole, or the axis of rotation which is perpendicular to equatorial plane. The $\mathbf{X_O}$ axis is in the direction of the vernal equinox, which is the interaction of the earth equatorial plane and the earth orbital plane about the sun axis, where the latter is known as the ecliptic plane. The $\mathbf{Y_O}$ axis is in the equatorial plane and finishes the "triad" of the vectors [18,23].

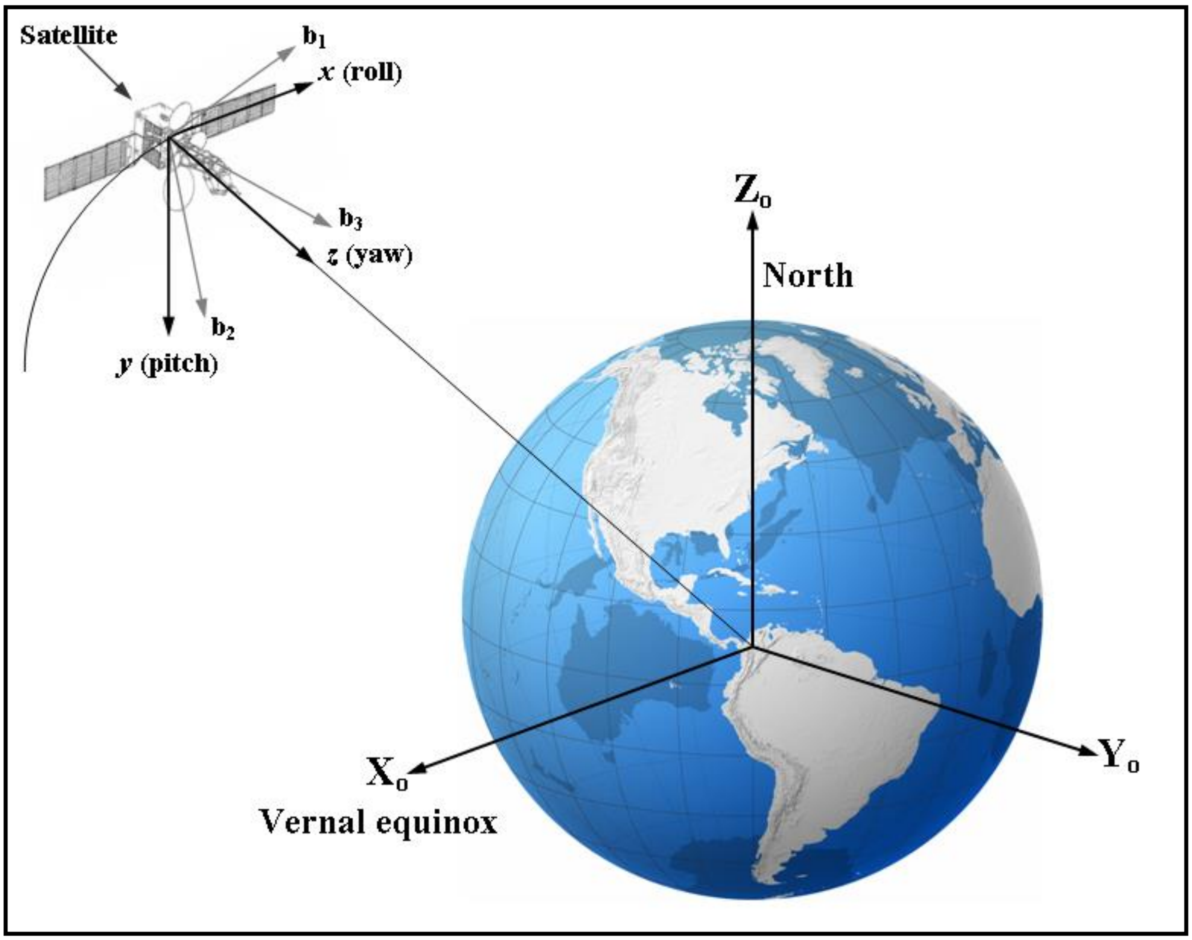

Figure(3.1) Reference Frames.

3.2.1.2 Orbital Frame

It is similar to an "airplane" three-axis coordinate system, where the attitude motion of the spacecraft is most commonly described in terms of it, namely roll, pitch, and yaw. The orbital frame is located at the mass center of the spacecraft, and the motion of the frame depends on the orbit. This frame is non-inertial because of orbital acceleration and the rotation of the frame. Referring to figure (3.1), the nominal yaw axis, $\boldsymbol{z}$ axis is along the vector from the center of mass of the spacecraft to the center of mass of the earth (nadir direction). The nominal pitch axis, $\boldsymbol{y}$ is in the negative orbit normal direction and the nominal roll axis, $\boldsymbol{x}$ completes the triad, and is in the velocity vector direction for circular orbits [1,18,23].

3.2.1.3 Body-Fixed Frame

Like the orbital frame, the body frame is originated at the spacecraft's mass center. This frame is fixed in the body of the spacecraft, and therefore is non-inertial. The relative orientation between the orbital and body frames is the basis of attitude dynamics and control. Referring to figure (3.1), the $\mathbf{b}_3$ axis is in the nadir direction, the $\mathbf{b}_2$ axis is in the negative orbit normal direction , and $\mathbf{b}_1$ axis completes the triad. It can be seen that the satellite coordinates $\mathbf{b}_1\mathbf{b}_2\mathbf{b}_3$ is not aligned with $\boldsymbol{xyz}$ coordinate system, hence the attitude control goal is to matching these axes (coordinates) to achieve stabilization [18,23].

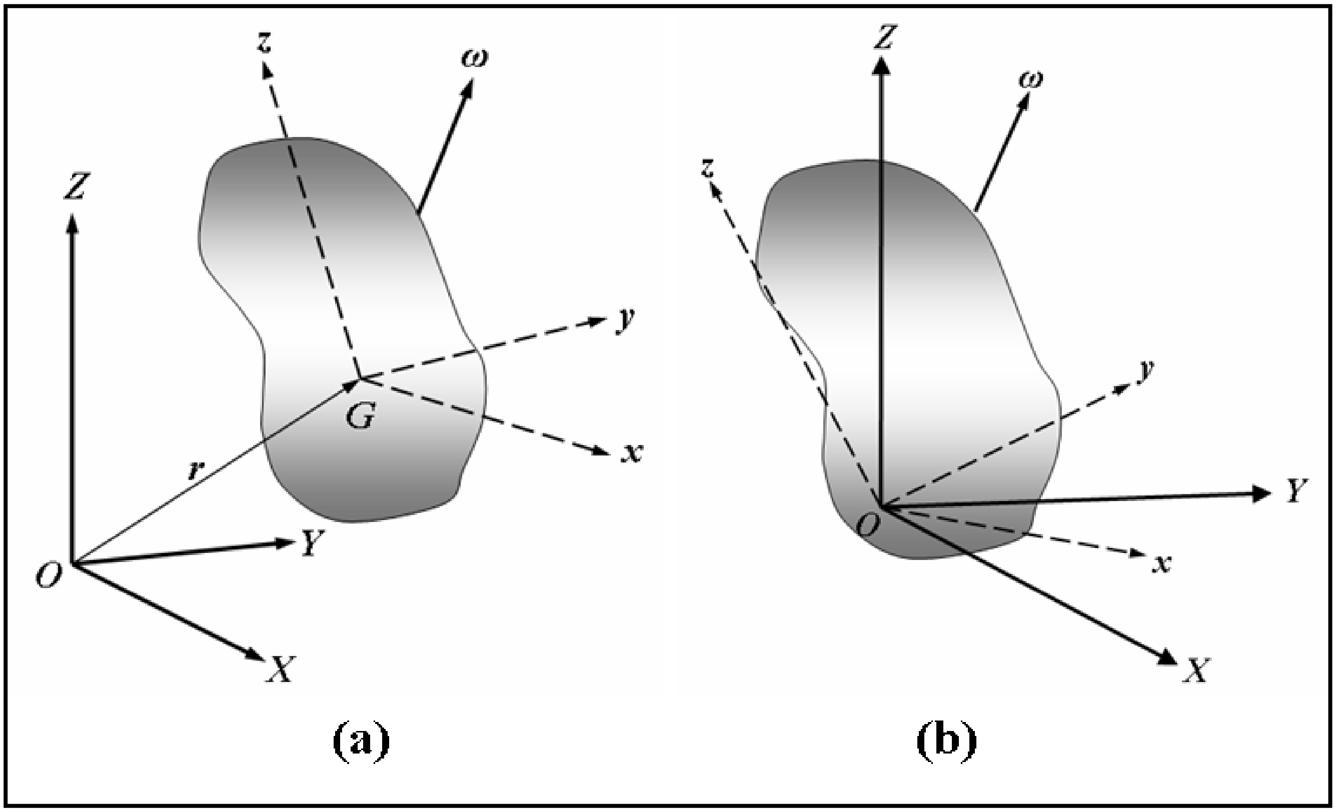

Figure(3.2) Rigid Body Motion.

3.2.2 Dynamic Equations of Motion

The basic problem of attitude dynamics is the determination of a spacecraft's motion about a given set of axes. This motion can be derived from the angular momentum of a general rigid body.

Consider now a rigid body moving with any general motion in space relative to the fixed reference axes with origin *O*, figure (3.2a), or rotating about a fixed point *O*, figure (3.2b). Axes *xyz* are attached to the body with origin at the mass center *G*. The angular velocity $\bar{\omega}$ of the body becomes the angular velocity of the *xyz* frame as observed from the fixed reference axes *XYZ*.

The general expression for the angular momentum, $\vec{h}$, about either the mass center G or about a fixed point O for a rigid body rotating with an instantaneous angular velocity $\vec{\omega}$ can given as [25]:

$$\begin{aligned}\vec{h} &= i(I_{xx}\omega_x - I_{xy}\omega_y - I_{xz}\omega_z) \\ &\quad + j(-I_{yx}\omega_x + I_{yy}\omega_y - I_{yz}\omega_z) \\ &\quad + k(-I_{zx}\omega_x - I_{zy}\omega_y + I_{zz}\omega_z)\end{aligned} \tag{3.1}$$

and the components of $\vec{h}$ are clearly

$$\begin{aligned}h_x &= I_{xx}\omega_x - I_{xy}\omega_y - I_{xz}\omega_z \\ h_y &= -I_{yx}\omega_x + I_{yy}\omega_y - I_{yz}\omega_z \\ h_z &= -I_{zx}\omega_x - I_{zy}\omega_y + I_{zz}\omega_z\end{aligned} \tag{3.2 a, b, c}$$

The above expressions of the angular momentum components can be written in matrix form as:

$$\vec{h} = \begin{Bmatrix} h_x \\ h_y \\ h_z \end{Bmatrix} = \begin{bmatrix} I_{xx} & -I_{xy} & -I_{xz} \\ -I_{yx} & I_{yy} & -I_{yz} \\ -I_{zx} & -I_{zy} & I_{zz} \end{bmatrix} \begin{Bmatrix} \omega_x \\ \omega_y \\ \omega_z \end{Bmatrix} \tag{3.3}$$

The equations of motion are based on Newton's second law, which states that the rate of change of linear momentum of a particle is equal to the force acting on the particle. It should be noted that, in applying this law one must measure motion relative to an inertial coordinate system.

The above definition of the linear momentum can be extended to define the rotational motion of a rigid body about its center of mass (figure (3.2)), which becomes that the rate of change of the angular momentum is equal to the sum of the applied moments, or in vector form as [25]:

$$\sum \vec{M} = \dot{\vec{h}} = \left[\frac{d\vec{h}}{dt}\right]_{XYZ} \tag{3.4}$$

where the terms are taken about either a fixed point *O* or about the mass center *G*. In the derivative of the moment principle the derivative of $\vec{h}$ was taken with respect to an absolute coordinate system. When $\vec{h}$ is expressed in terms of components measured relative to a moving coordinate system *x-y-z* which has an angular velocity $\vec{\omega}$, then the moment relation becomes:

$$\sum \vec{M} = \left[\frac{d\vec{h}}{dt}\right]_{xyz} + \vec{\omega} \times \vec{h}$$

$$= (i\dot{h}_x + j\dot{h}_y + k\dot{h}_z) + \vec{\omega} \times \vec{h} \tag{3.5}$$

The terms in parentheses represent that part of $\dot{\vec{h}}$ due to the change in magnitude of the components of $\vec{h}$, and the cross product terms represents that part due to the changes in direction of the components of $\vec{h}$. Expansion of the cross product and rearrangement of terms give:

$$\sum M_x = \dot{h}_x - h_y \omega_z + h_z \omega_y$$

$$\sum M_y = \dot{h}_y - h_z \omega_x + h_x \omega_z \tag{3.6a, b, c}$$

$$\sum M_z = \dot{h}_z - h_x \omega_y + h_y \omega_x$$

These three differential equations are relating applied moment components to angular momentum changes. Thus the general attitude motion of a rigid body and/or a satellite is given by these three simply written equations. It is interesting to note that set of equations appear to be three first order in terms of angular momentum vector. These differential equations can be converted into second order differential equations when it is required to measure the orientation of a rigid body in inertial space through the Euler angles and rates.

3.2.3 Mathematical Modeling of Dual-Spinning Spacecraft

It was mentioned previously that, the spacecraft attitude control system of spin stabilization type is consisting of single-spin stabilization and dual-spin stabilization, and it is also mentioned that, the dual-spin stabilization class is the type of the attitude control system adopted in the present study.

Generally, dual-spin spacecraft is consisting of two rigid bodies, which are connected by means of a bearing axis (spin axis). One of the bodies, the rotor, is spun at high rate to stabilize the spacecraft via gyroscopic stiffness. The second body, the platform, is nearly despun so that its payload instrument can be inertially pointed toward the earth or other point in the space. The relative motion between two bodies is restricted to rotation about the bearing axis. The mass centers of the two bodies must lie in the axis of rotation and the axis of rotation is a common principal axis of the two bodies.

3.2.3.1 Description of The Present Model

The above description represents a general description of dual-spin spacecraft, because each model being under investigation must have its own characteristics. The characteristics are greatly related to the dynamic imbalance problem, the problem of symmetry, and asymmetry which appear in the rotor or the platform or both of them.

The dual-spin spacecraft chosen in the present study is shown schematically in figure (3.3). The system is composed of a rigid symmetric rotor R_r and a rigid platform P whose respective mass centers, C_R and C_P, lie on the common axis (bearing axis), and are separated by distance (r_c). Two sets of reference axes ($O_P x_P y_P z_P$) and ($O_R x_R y_R z_R$) are introduced at the mass centers C_P and C_R respectively, and, the x, y, and, z coordinates are located at the system center of mass and are fixed relative to the rotor. The axes z_P, z_R, and z are coincided with the axis of rotation and the relative rotation of body P with respect to the body R_r about the z-axis is denoted by the angle α_r.

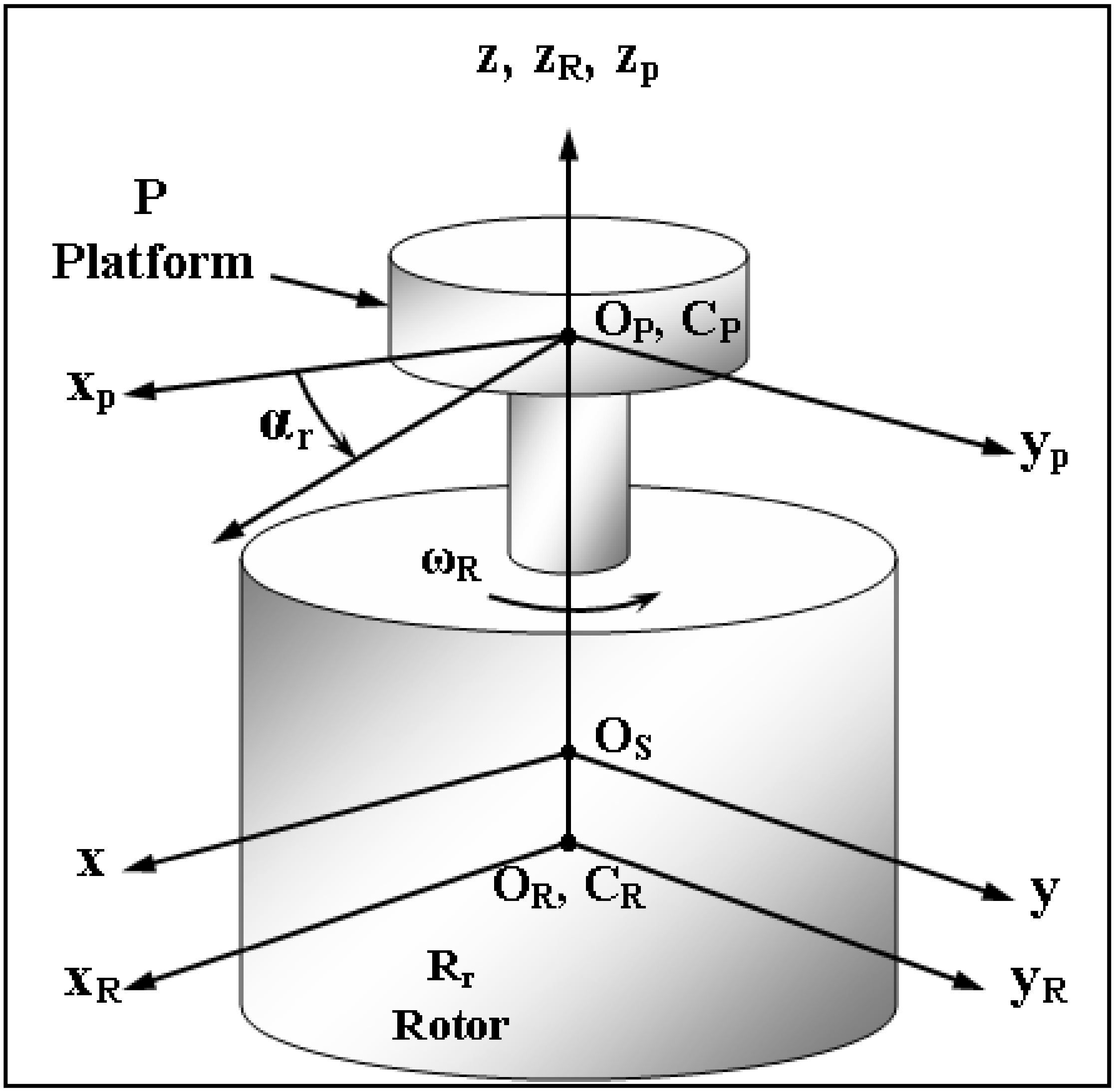

Figure (3.3) Dual-Spin Spacecraft Model.

The platform P and the rotor R_r have masses of M_P and M_R respectively. The individual centroidal inertia tensors, $[I_P]$ and $[I_R]$ referred to their respective axes sets ($O_P x_P y_P z_P$) and ($O_R x_R y_R z_R$) take the following form:

$$[I_P]=\begin{bmatrix} B_P & 0 & 0 \\ 0 & B_P & 0 \\ 0 & 0 & C_P \end{bmatrix}, \quad [I_R]=\begin{bmatrix} A_R & 0 & 0 \\ 0 & A_R & 0 \\ 0 & 0 & C \end{bmatrix} \tag{3.7}$$

In the present study, both bodies are statically balanced, since their mass centers lie on the bearing axis, and are also dynamically balanced, since their common axis (bearing axis) is one of their principal axes. The bearing axis, is the axis of symmetric as evidence from the double entry of B_P , and A_R in their inertia tensors.

3.2.3.2 Equations of Motion of Dual-Spin Spacecraft

The essential dynamic properties of the model, which is adopted in the present study, are described in the previous section. Therefore, the basic components of the satellite (the rotor and platform), that are shown in figure (3.3), are two symmetrical rigid bodies with system center of mass O_s, and the relative motion between the two bodies is restricted to rotation about common axis (bearing axis).

The angular velocity components of the platform and the rotor, referred to their reference axes are:

$$\vec{\omega}_P = \omega_x e_x + \omega_y e_y + \Omega_P e_z$$

and

$$\vec{\omega}_R = \omega_x e_x + \omega_y e_y + \omega_z e_z \tag{3.8 a, b}$$

where Ω_P is the inertial spin rate of the platform about the spin axis.

The system angular momentum can be obtained by using expression of Eq.(3.3), after omitting the inertia products due to the symmetry, then

$$\vec{h} = [I]_s \cdot \vec{\omega}_R + \vec{h}_P \tag{3.9}$$

where $[I]_s$ is the matrix of the moment of inertia of the dual-spin spacecraft not including the symmetric principal moment of inertia of the platform, which given by:

$$[I]_s = \begin{bmatrix} A_x & 0 & 0 \\ 0 & A_y & 0 \\ 0 & 0 & C \end{bmatrix}$$

It is evidenced that, the two principal moments of inertia about x and y axes are equal, because the platform and the rotor are assumed to be symmetrical, and $\vec{h}_P$ is the angular momentum vector of the platform about the bearing axis and it is given by;

$$\vec{h}_P = \begin{bmatrix} 0 & 0 & C_p\Omega_p \end{bmatrix}^T \tag{3.10}$$

Substituting for the angular momenta and their time derivatives in Eqs.(3.6), then, the attitude equations of motion of symmetric spacecraft are given by:

$$\begin{aligned}
&A\dot{\omega}_x + (C-A)\omega_z\omega_y + C_P\Omega_P\omega_y = \sum M_x \\
&A\dot{\omega}_y - (C-A)\omega_z\omega_x - C_P\Omega_P\omega_x = \sum M_y \\
&C\dot{\omega}_z + C_P\dot{\Omega}_P = \sum M_z \\
&C_P\dot{\Omega}_P = T_b \\
&\dot{\alpha}_r = \Omega_P - \omega_z
\end{aligned} \tag{3.11 a, b, c, d, e}$$

where

$A = A_x = A_y$: transverse principal moments of inertia along x , and y axes.

C: spin axis principal moment of inertia of the rotor.

C_P: spin axis principal moment of inertia of the platform.

$T_b = T_m + T_f$: total torque.

T_m: torque produce by DC motor on the platform.

T_f : torque produce by bearing friction.

$\dot{\alpha}_r$: relative rotation rate of the platform with respect to the rotor.

3.2.3.3 Torque-Free Motion of Rigid Axisymmetric Spacecraft

In the study of attitude motion dynamics the motion of axisymmetric spacecraft is the most common situation. An axisymmetric body is a body, which contains two planes of symmetry. A general condition of axisymmetric bodies is that moments of inertia about two of the axes are equal (e.g A_x = A_y). The phrase "torque-free" simply referred to the condition that no external moments act on the body.

The equations of motion for torque-free axisymmetric bodies with moments of inertia ($A_x = A_y = A$), were given in the previous section. Using a body fixed frame of reference coincide with the principal axes, the torque components are assumed to be zero, and by noting that the inertial spin rate of the platform is maintained constant during its normal operating mode by suitable control loop (i.e. $\dot{\Omega}_P = 0$), then Eqs. (3.11) reduced to:

$$A\dot{\omega}_x + (C-A)\omega_z\omega_y + C_P\Omega_P\omega_y = 0$$
$$A\dot{\omega}_y - (C-A)\omega_z\omega_x - C_P\Omega_P\omega_x = 0 \qquad \text{(3.12 a , b ,c)}$$
$$C\dot{\omega}_z = 0$$

Although the above equations are still nonlinear and coupled, a solution of motion can be obtained on the basis of perturbation analysis. It is known that, the common axis (z-axis) is spin axis of the spacecraft, then the initial motion can be described by $\omega_x = \omega_y = 0$, and $\omega_z = \Omega$, where Ω is the initial spin rate of the spacecraft, and the perturbed motion is given by $\omega_z = \Omega + \varepsilon_d$, and $\omega_x \neq 0$, $\omega_y \neq 0$, where ω_x and ω_y are small.

Substituting these conditions in Eqs. (3.12), and neglecting the product of small quantities, then the resulting linearized equations are:

$$\dot{\omega}_x + \lambda_n\Omega\omega_y = 0$$
$$\dot{\omega}_y - \lambda_n\Omega\omega_x = 0 \qquad \text{(3.13 a, b, c)}$$
$$\dot{\varepsilon}_d = 0$$

where

$$\lambda_n = \lambda + \lambda_s$$
$$\lambda = \sigma - 1$$
$$\lambda_s = \frac{\Omega_P}{\Omega}\frac{C_P}{A}$$

$\sigma = \frac{C}{A}$: inertia ratio of the principal moment of inertia of the spin axis to the transverse principal moment of inertia of the spacecraft.

From Eq.(3.13 c), it can be concluded that ε_d remains constant. Differentiating Eq. (3.13 a) and substituting ω_x and ω_y from Eq. (3.13 b) respectively, then

$$\ddot{\omega}_x + \lambda_n{}^2\Omega^2\omega_x = 0$$

$$\ddot{\omega}_y + \lambda_n{}^2\Omega^2\omega_y = 0 \qquad (3.14\text{ a, b})$$

From Eqs. (2.14 a, b), it can be obtained that:

$$\omega_x = P_a \sin(\lambda_n \tau - \gamma) \qquad (3.15)$$

where

P_a : the amplitude.

γ : the phase angle.

τ: the dimensionless time and it is given by $\tau = t\Omega$.

Inserting Eq.(3.15) into Eq.(3.13 a), gives:

$$\omega_y = P_a \cos(\lambda_n \tau - \gamma) \qquad (3.16)$$

The resultant transverse angular velocity ω_t is the sum of velocity ω_x and ω_y, and introducing complex variable notation, then ω_t is given by:

$$\omega_t = \omega_y + i\omega_x$$

$$\omega_t = P_a \ e^{i(\lambda_n \tau - \gamma)} \qquad (3.17)$$

The resultant transverse angular velocity of the spacecraft ω_t is a vector in the xy plane, rotating with the angular velocity ($\lambda_n\Omega$).

3.3 Attitude Stability of Spinning Spacecraft

The term stability here is used to describe the motion of a torque free rigid body after being disturbed from steady spin. Thus motion is stable if amplitudes of disturbed quantities are bounded by initial values.

The stability of spinning spacecraft is investigated in the next sections for two cases, when spacecraft is without energy dissipation and with energy dissipation, then stability is obtained in terms of spacecraft inertia ratio.

3.3.1 Stability of Rotation about Principal Axes

Consider a rigid body that is rotating about one of its rotating principal axes. If there are external torques acting on the body and, for example, the rotating was initially about the *z*-axis (figure 3.3), then the body will continue to spin about the *z*-axis, i.e. $\omega_z = \Omega =$ constant, and $\omega_x = \omega_y = 0$. On the other hand, if a small impulsive disturbing torques is applied to the body, then the body will no longer rotate purely about the spin axis.

In the absence of external moments, Euler's equations of a rigid body (for general case, i.e. $I_x \neq I_y \neq I_z$) are given by [25]:

$$\begin{aligned} I_x\dot{\omega}_x - (I_y - I_z)\omega_y\omega_z &= 0 \\ I_y\dot{\omega}_y - (I_z - I_x)\omega_x\omega_z &= 0 \\ I_z\dot{\omega}_z - (I_x - I_y)\omega_x\omega_y &= 0 \end{aligned} \qquad (3.18\text{ a, b, c})$$

where I_x , I_y , I_z are the principal moments of inertia.

For linear stability analysis, it is assumed that the perturbation terms ω_x and ω_y, are much smaller in magnitude than ω_z. Neglecting, the products of the small perturbation terms and substituting for $\omega_z = \Omega$, then, the linearized rotational equations of motion become:

$$I_x\dot{\omega}_x + (I_z - I_y)\omega_y\Omega = 0$$
$$I_y\dot{\omega}_y - (I_z - I_x)\omega_x\Omega = 0 \qquad (3.19\text{ a, b, c})$$
$$I_z\dot{\Omega} = 0$$

where Ω is the spin rate about the z-axis, and it is constant as shown by Eq. (3.19 c). Differentiating Eqs. (3.19 a and b), and substituting $\dot{\omega}_x$ and $\dot{\omega}_y$ form Eqs. (3.19 a) and (3.19 b) respectively, it can be obtained that

$$\ddot{\omega}_x + \frac{(I_y - I_z)(I_x - I_z)}{I_y I_x}\Omega^2\omega_x = 0$$
$$\ddot{\omega}_y + \frac{(I_y - I_z)(I_x - I_z)}{I_y I_x}\Omega^2\omega_y = 0 \qquad (3.20\text{ a, b})$$

The characteristic equation is:

$$s^2 + \frac{(I_y - I_z)(I_x - I_z)}{I_y I_x}\Omega^2 s = 0 \qquad (3.21)$$

And the characteristic roots are:

$$s_{1,2} = \pm i\Omega\sqrt{\frac{(I_y - I_z)(I_x - I_z)}{I_y I_x}} \qquad (3.22)$$

If the spin axis (the z-axis) is either the major axis ($I_x < I_z$ and $I_y < I_z$) or minor axis ($I_x > I_z$ and $I_y > I_z$), then the characteristic roots become pure imaginary numbers and the rotational motion is said to be stable. If the spin axis is the intermediate axis then one of the characteristic roots is positive real number and the motion is said to be unstable [1,24,25].

In the case of axisymmetric spacecraft ($I_x = I_y = I_T$), two possible cases, $I_z > I_T$ and $I_z < I_T$, are shown in the figure (3.4), and the motion of the spacecraft can be represented in terms of the body cone and the space cone.

The body cone is fixed in the body and its axis coincides with the spin axis while the space cone is fixed in space and its axis is along the direction of the angular momentum vector $\vec{h}$. The total angular velocity is along the line of contact between the two cones. The plane containing the angular momentum $\vec{h}$, total angular velocity $\vec{\omega}$, and spin axis rotates about $\vec{h}$ at angular velocity of $\Omega_n = (I_z/I_T)\Omega$.

For a disk shaped body $(I_z/I_T)\rangle 1$, the inside surface of the body cone rolls on the outside surface of the space cone, as shown in figure (3.4 a). For a rod shaped body $(I_z/I_T)\langle 1$, the out side surface of the body cone rolls on the outside surface of the space cone as shown in figure (3.4 b).

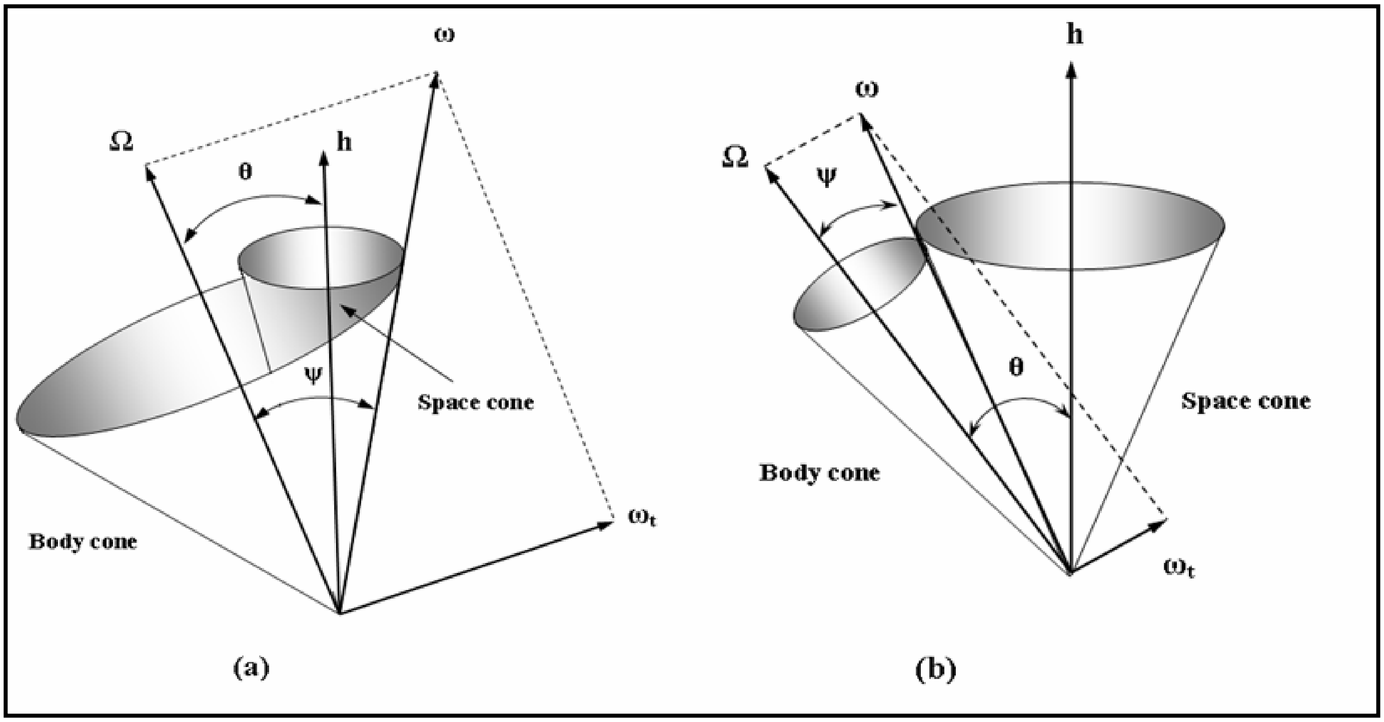

Figure (3.4) Spacecraft Motion For (a) A disk-shaped body, $I_z/I_T > 1$.

(b) A rod-shaped body, $I_z/I_T < 1$.

The nutation angle θ, which is the angle of inclination of the spin axis with respect to the vector of the angular momentum $\vec{h}$, is give by:

$$\sin\theta = \frac{I_T\omega_t}{H} \tag{3.23}$$

where H is the magnitude of the angular momentum vector $\vec{h}$.

The angle ψ, which is the angle between the total angular velocity vector and the angular velocity vector about the spin axis, is given by:

$$\tan\psi = \frac{\omega_t}{\Omega} \tag{3.24}$$

3.3.2 Dual-Spin Stabilization of an Energy Dissipation Spacecraft

In a dual-spin spacecraft, which consists of a rotor and platform, the rotor spins about the axis of principal moment of inertia providing gyroscopic stabilization and a despun platform provides a pointing towards the earth. As shown in the preceding section, for a rigid spacecraft, stable spin can take place about the axis of either the maximum or the minimum principal moment of inertia. However, satellite is likely to have several components experiencing relative motion, such as elastic structural deflection and liquid slosh due to acceleration about the center of mass, so that the satellite is not rigid.

Before considering, the stability criterion for dual-spin satellite, stability of spinning body in terms of the rotational kinetic energy and the angular momentum is considered. In the absence of external torques, the angular momentum of the spacecraft is conserved, but internal energy dissipation will cause the spacecraft to move toward a minimum energy state [1]. The kinetic energy, T_{rot}, of the spacecraft is related to the magnitude of the angular momentum *H*, and to the moment of inertia, I_s, about the spin axis by:

$$T_{rot} = \frac{1}{2}\frac{H^2}{I_s} \tag{3.25}$$

It can be seen that, for constant angular momentum, the kinetic energy is a minimum when the moment of inertia, I_s, is maximum. Hence, for a non-rigid spacecraft there is only one axis of stable spin, namely, the axis of the maximum moment of inertia [1].

In the case of dual-spin spacecraft, the stability criterion is given in terms of the moment of inertia ratio of the spin axis to the transverse axis and the amount of energy dissipation rate in the platform and the rotor. Iorillo presented stability criterion for dual-spin spacecraft in 1965 and a similar stability criterion was discovered independently by V.D Landon [1]. Accordingly, in a dual-spin stabilized spacecraft, the stable spin axis can be the axis of minimum moment of inertia if the rate of energy dissipation in the platform is higher than that in the rotor by a certain factor. The stability criterion of Iorillo, has been proved in a rigorous manner by many investigators [1]. In the following section, the stability criteria of dual-spin spacecraft are obtained by using energy sink arguments.

Consider an axisymmetric dual-spin spacecraft, which is shown in figure (3.3) of inertia properties defined previously, (see section 3.2.3.1), the expression of the kinetic energy, T_{rot}, the magnitude of the angular momentum $\vec{h}$, and the nutation frequency Ω_n are given by:

$$T_{rot} = \frac{1}{2}(A\omega_t^{\ 2} + C\Omega^2 + C_P\Omega_P^{\ 2}) \tag{3.26}$$

$$H^2 = (C\Omega + C_P\Omega_P)^2 + (A\omega_t)^2 \tag{3.27}$$

$$\Omega_n = \frac{C\Omega + C_P\Omega_P}{A} \tag{3.28}$$

Assuming that there is no external torque and that the shaft is frictionless. In real systems, a servo-loop-controlled motor acts to counterbalance any shift friction exactly. From the conservation of angular momentum principle, $\dot{H}$ is zero. Differentiating Eq. (3.27) with respect to time, and using $\dot{H} = 0$, then [1]:

$$A\omega_t\dot{\omega}_t = -\frac{(C\Omega + C_P\Omega_P)}{A}(C\dot{\Omega} + C_P\dot{\Omega}_P) = -\Omega_n(C\dot{\Omega} + C_P\dot{\Omega}_P) \tag{3.29}$$

Differentiating Eq. (3.26) with respect to time, then

$$\dot{T}_{rot} = \dot{T}_P + \dot{T}_R = A\omega_t\dot{\omega}_t + C\Omega\dot{\Omega} + C_P\Omega_P\dot{\Omega}_P \tag{3.30}$$

where $\dot{T}_P$ and $\dot{T}_R$ are the rate of energy dissipation of the platform and the rotor respectively. Combining Eqs. (3.29) and (3.30), so that

$$\dot{T}_{rot} = \dot{T}_P + \dot{T}_R = -\lambda_R C\dot{\Omega} - \lambda_P C_P\dot{\Omega}_P \tag{3.31}$$

where

$$\lambda_P = \Omega_n - \Omega_P$$
$$\lambda_R = \Omega_n - \Omega_R$$

in which λ_P and λ_R are the nutation frequencies of the platform and the rotor, respectively. In dual-spin spacecraft, it is known that the rotor and the platform are spinning about the spin axis independently, thus the reaction torques which tend to change the angular rates of the platform and the rotor can be obtained from Eq. (3.31) as [1]:

$$C_P \dot{\Omega}_P = -\frac{\dot{T}_P}{\lambda_P}$$

$$C\dot{\Omega}_R = -\frac{\dot{T}_R}{\lambda_R} \qquad (3.32\text{ a, b})$$

Combining Eqs. (3.29) and (3.32) then

$$A\omega_t \dot{\omega}_t = \Omega_n \left(\frac{\dot{T}_P}{\lambda_P} + \frac{\dot{T}_R}{\lambda_R} \right) \qquad (3.33)$$

Due to the presence of energy dissipation, the nutation angle θ is no longer constant. Differentiating Eq. (3.23) with respect to time, and using Eq. (3.33) then, the rate of change of nutation angle will be:

$$\dot{\theta} = \frac{2A}{\sin 2\theta} \frac{\Omega_n}{H^2} \left(\frac{\dot{T}_P}{\lambda_P} + \frac{\dot{T}_R}{\lambda_R} \right) \qquad (3.34)$$

For a stable spin of the spacecraft, the nutation angle must decay with the time (i.e. $\dot{\theta} < 0$), hence the stability condition is given by:

$$\left(\frac{\dot{T}_P}{\lambda_P} + \frac{\dot{T}_R}{\lambda_R} \right) \langle 0 \qquad (3.35)$$

Assuming that the rotor angular momentum is much larger than the platform angular momentum (i.e. $\Omega C >> \Omega_P C_P$) which is a reasonable assumption in view of the fact that Ω_P is approximately equal to the orbit rate, thus [1]:

$$\lambda_P = \Omega_n - \Omega_P = \frac{C\Omega + C_P\Omega_P}{A} - \Omega_P \approx \frac{C}{A}\Omega = \sigma\Omega$$

$$\lambda_R = \Omega_n - \Omega = \frac{C\Omega + C_P\Omega_P}{A} - \Omega \approx \left(\frac{C}{A} - 1\right)\Omega = (\sigma - 1)\Omega = \lambda\Omega \qquad (3.36\ \text{a, b})$$

Substituting Eqs. (3.36) into inequality (3.35), the stability condition becomes

$$\left(\frac{\dot{T}_P}{C/A} + \frac{\dot{T}_R}{C/A - 1}\right) \langle 0 \qquad (3.37)$$

These are two cases:

Case 1: C/A >1, the spacecraft is stable if the energy dissipations occur in either the platform or the rotor. This implies that a nutation damper can be placed on either the platform or the rotor.

Case 2: C/A<1, for this case the first term in Eq. (3.37), $\dot{T}_P/(C/A)$ is negative and the second term, $\dot{T}_R/[(C/A)-1]$, is positive. The stability condition becomes:

$$|\dot{T}_P| \rangle \left|\dot{T}_R \frac{C/A}{C/A - 1}\right| \qquad (3.38)$$

As an example, for a dual-spin stabilized spacecraft with C/A=2/3, substituting this value in Eq. (3.38), then the magnitude of energy dissipation rate of the platform should be at least twice the dissipation rate in the rotor, hence, the damper must be placed on the platform [1].

3.4 Environmental Disturbance Torques

Generally, two types of torques have been found to influence a spacecraft attitude, namely internal and external torques. It may be noted that, both types may affect the total rotational energy of a spacecraft, however, only an external torque will affect total angular momentum. External torques result from the interaction of the spacecraft with its environment. Important environmental torques affecting satellite attitude dynamics include gravity gradient, magnetic, aerodynamic, and solar radiation pressure torques [23].

Different environmental torques are also, more prevalent at different altitudes, and the relationship between altitude and disturbance torque strength is shown in figure (3.5). In low earth orbits (LEO), the largest environmental torques are gravity gradient, magnetic, and aerodynamic, whereas the most dominant torques at geosynchronous orbit (geostationary orbit) are solar radiation pressure and gravity gradient [23].

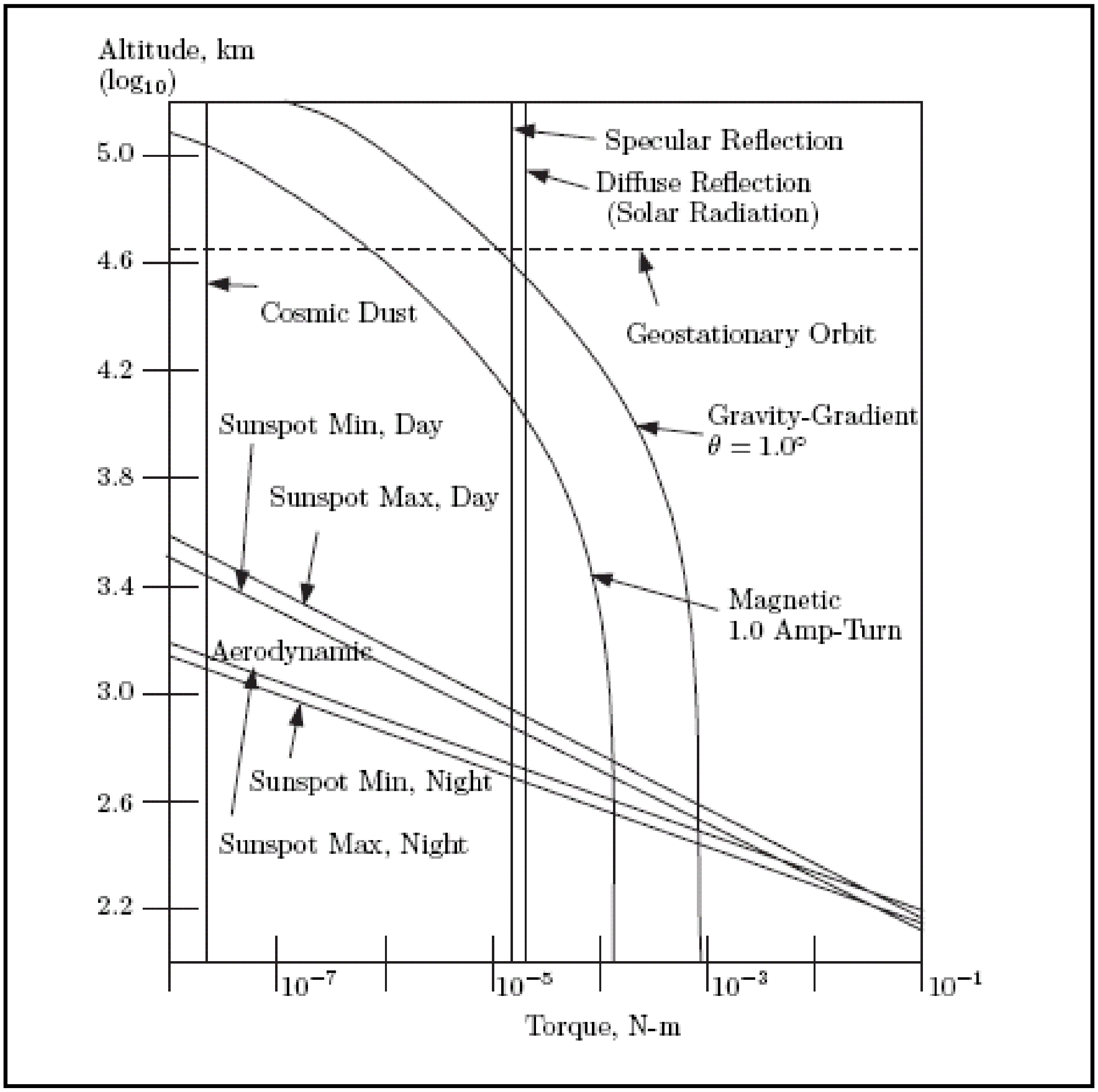

Figure (3.5) Comparison of Environmental Torques [23].

3.4.1 Gravity Gradient Torques

The gravity gradient torques is caused by the slight change in the gravitational pull between the top and the bottom of the satellite, i.e. the force of gravity is weaker on these parts of the spacecraft which are furthest away from the earth and stronger on those parts which closer. Because of this gravity gradient, the spacecraft tends to align its long axis with local vertical. If this is the desired orientation of the spacecraft, this torque acts to stabilize the satellite, otherwise, it is a perturbing torque and must be counteracted by other means. Gravity gradient torque is usually important only for spacecraft in low orbit. For nadir pointing spacecraft, this torque is nearly constant, while for inertial pointing vehicles it is periodic. Gravity gradient torques is generally ineffective in earth orbit altitudes of about 2000 Km [30].

3.4.2 Aerodynamic Drag Torques

Although there is obviously much less drag at orbital altitude than near the surface of the earth, aerodynamic drag can still cause large torque an a satellite, and often determines its lifetime.

It should be noted that symmetric areas of spacecraft cause no net aerodynamic torque. A spherical satellite, for example, would feel no aerodynamic at all, although the drag would eventually slow it down enough for re-entry. Torque due to aerodynamic is nearly constant for nadir pointing spacecraft [30].

3.4.3 Solar Radiation Torque

Solar radiation torque is caused by solar radiation pressure, which arises from transfer of linear momentum from solar radiation that is absorbed and/or reflected by satellite surface. It is a function of configuration and orientation of the spacecraft and on the surface reflectance of the vehicle. Solar radiation torque is cyclic for nadir pointing spacecraft and nearly constant for inertial pointing satellite [30].

3.4.4 Magnetic Field Torque

Magnetic coils, (or magnetic torques, or sometimes called torque rods), interact with the earth's magnetic field in order to produce torque. These devices are extremely simples and they consist of wire-wound ferrous rods on each axis. When current is passed through the wire coil, the device become an electromagnet which exerts a torque against the local magnetic field.

Magnetic torques have the advantage of simplicity and reliability. They also represent the only practical active method available to exert external torques on a spacecraft without expelling propellant. This makes them useful for momentum damping from wheels and control moment gyros [30].

Unfortunately, the magnetic field of the earth is not strong enough to permit these devices to exert much torque, and limits the usefulness for applications. Also, the magnetic torque can only act about two axes, since no torque can be produced in the direction of the local earth geomagnetic field vector. The fact that their performance is directly depending on the strength of the local magnetic field is also a serious drawback. Magnetic torques are useless for geosynchronous spacecraft, since the earth's magnetic field is very weak at such high altitudes[30].

3.5 Satellite Kinematics

The spacecraft attitude dynamic and control problem involve consideration of kinematics. Satellite kinematics is primarily interested describing the orientation of the satellite that is in rotational motion. Since the relative orientation of the satellite frame and the inertial frame is time dependent, so that, the time dependent relationship between the reference frames can be described by the called kinematic differential equations.

There is a number of schemes available for determining the kinematic differential equations. These schemes include: direction cosine matrix, Euler angles, Euler's eigen axis, and quaternion. Of these schemes, quaternions are commonly used for numerical attitude calculations, due to its easy use since it uses only multiplication and addition operation. Hence, it is very useful in digital computer to give faster computation compared with the equivalent direction cosine matrix solution [13]. The major disadvantage of the quaternion is no obvious physical meaning and it is almost impossible to visualize [13]. In this section the kinematic differential equations for the quaternions will be explained in details.

3.5.1 Quaternions

A quaternion is a four parameter set used to describe the orientation of one reference frame with respect to another. Mathematically quaternions are hyper complex numbers. Hamilton inverted quaternions as a result of searching for hyper complex numbers that could be represented by points in three dimensional space [18]. The quaternion is defined as either a complex number with three different "imaginary" parts:

$$\bar{q} = iq_1 + jq_2 + kq_3 + q_4 \tag{3.39}$$

or, by a four row-vector:

$$\bar{q} = \begin{bmatrix} q_1 \\ q_2 \\ q_3 \\ q_4 \end{bmatrix} = \begin{bmatrix} \mathbf{q} \\ q_4 \end{bmatrix} \tag{3.40}$$

where

$$\mathbf{q} = \begin{bmatrix} q_1 \\ q_2 \\ q_3 \end{bmatrix} = \sin(\Phi/2)\cdot\vec{\mathbf{a}}\,, \qquad \vec{\mathbf{a}} = \begin{bmatrix} a_1 \\ a_2 \\ a_3 \end{bmatrix}, \qquad q_4 = \cos(\Phi/2)$$

In Eq.(3.40), q_i (i = 1, 2, 3) are vectors and the fourth one is a scalar q_4. Kinematically quaternions define the rigid body attitude as Euler axis rotation. According to Euler's theorm of rotational motion, the attitude of a rigid body can be changed from any given orientation to any other orientation by rotating the body about an fixed axis called Euler axis or eigen axis. The rotation angle is defined as Φ and the axis of rotation is $\vec{\mathbf{a}}$. The direction of the Euler axis is indicated vector part of the quaternion (the first three components). The scalar part (the fourth component) is related to the rotation angle about Euler axis.

The relationship between the angular velocity component of the spacecraft, quaternion rates, and quaternions is given by [7]:

$$\begin{aligned} \omega_x &= 2(\dot{q}_1 q_4 + \dot{q}_2 q_3 - \dot{q}_3 q_2 - \dot{q}_4 q_1) \\ \omega_y &= 2(\dot{q}_2 q_4 + \dot{q}_3 q_1 - \dot{q}_1 q_3 - \dot{q}_4 q_2) \\ \omega_z &= 2(\dot{q}_3 q_4 + \dot{q}_1 q_2 - \dot{q}_2 q_1 - \dot{q}_4 q_3) \end{aligned} \tag{3.41 a, b, c}$$

where

ω_x, ω_y, ω_z: the angular velocity components of the spacecraft.

$\dot{q}_i$, q_i (i =1, 2, 3, 4): the quaternions rate and quaternions respectively.

It should be also noted that, the quaternions are not independent of each other, but constrained by the relationship:

$$q_1^{\ 2} + q_2^{\ 2} + q_3^{\ 2} + q_4^{\ 2} = 1 \tag{3.42}$$

Differentiating Eq.(3.41) with respect to time gives

$$2(q_1\dot{q}_1 + q_2\dot{q}_2 + q_3\dot{q}_3 + q_4\dot{q}_4) = 0 \tag{3.43}$$

These five equations (Eqs. 3.41, 3.42, and 3.43) can be combined into a matrix form, as follow:

$$\begin{bmatrix} \omega_x \\ \omega_y \\ \omega_z \\ 0 \end{bmatrix} = 2\begin{bmatrix} q_4 & q_3 & -q_2 & -q_1 \\ -q_3 & q_4 & q_1 & -q_2 \\ q_2 & q_1 & q_4 & -q_3 \\ q_1 & q_2 & q_3 & q_4 \end{bmatrix}\begin{bmatrix} \dot{q}_1 \\ \dot{q}_2 \\ \dot{q}_3 \\ \dot{q}_4 \end{bmatrix} \tag{3.44}$$

Because the 4x4 matrix in this equation orthonormal, this kinematic differential equations for quaternions can be simply obtained as follow:

$$\begin{bmatrix} \dot{q}_1 \\ \dot{q}_2 \\ \dot{q}_3 \\ \dot{q}_4 \end{bmatrix} = \frac{1}{2}\begin{bmatrix} q_4 & -q_3 & q_2 & q_1 \\ q_3 & q_4 & -q_1 & q_2 \\ -q_2 & q_1 & q_4 & q_3 \\ -q_z & -q_2 & -q_3 & q_4 \end{bmatrix}\begin{bmatrix} \omega_x \\ \omega_y \\ \omega_z \\ 0 \end{bmatrix} \tag{3.45}$$

which can be rewritten as:

$$\begin{bmatrix} \dot{q}_1 \\ \dot{q}_2 \\ \dot{q}_3 \\ \dot{q}_4 \end{bmatrix} = \frac{1}{2}\begin{bmatrix} 0 & \omega_z & -\omega_y & \omega_x \\ -\omega_z & 0 & \omega_x & \omega_y \\ \omega_y & -\omega_x & 0 & \omega_z \\ -\omega_x & -\omega_y & -\omega_z & 0 \end{bmatrix}\begin{bmatrix} q_1 \\ q_2 \\ q_3 \\ q_4 \end{bmatrix} \tag{3.46}$$

The kinematic differential equations (3.46) is integrated numerically using onboard flight computer to determine the orientation of spacecraft terms of quaternions. Quaternions have no inherent geometric singularity as do Euler angles. Moreover, quaternions are well suited for onboard real time computation because only products and no trigonometric relations exist in the quaternion kinematic differential equations. Thus, spacecraft orientation is now commonly described in terms of quaternions [13].

CHAPTER FOUR

Dynamics of Dual-Spin Spacecraft Containing Nutation Dampers

4.1 Introduction

In the present chapter, the dynamics of a spinning, torque free, axisymmetric dual-spin spacecraft equipped with two ring nutation dampers are investigated in terms of the proposed damper parameters, which appear in the equations for attitude of the spinning spacecraft. Approximate equations describing the attitude of the spacecraft are developed in terms of suitable dimensionless variables and time constants are obtained in terms of suitable set of dimensionless parameters.

4.2 Description of the Proposed Nutation Dampers

Each of the nutation dampers proposed in this study, consists of a circular ring of circular cross section completely filled with a viscous fluid. The nutation dampers are placed on the rotor section of the spacecraft and mounted with equal center offsets, in order to improve its damping performance, in parallel planes which are perpendicular to the spin axis of the spacecraft above the center of mass of the spacecraft, as shown in figure (4.1).

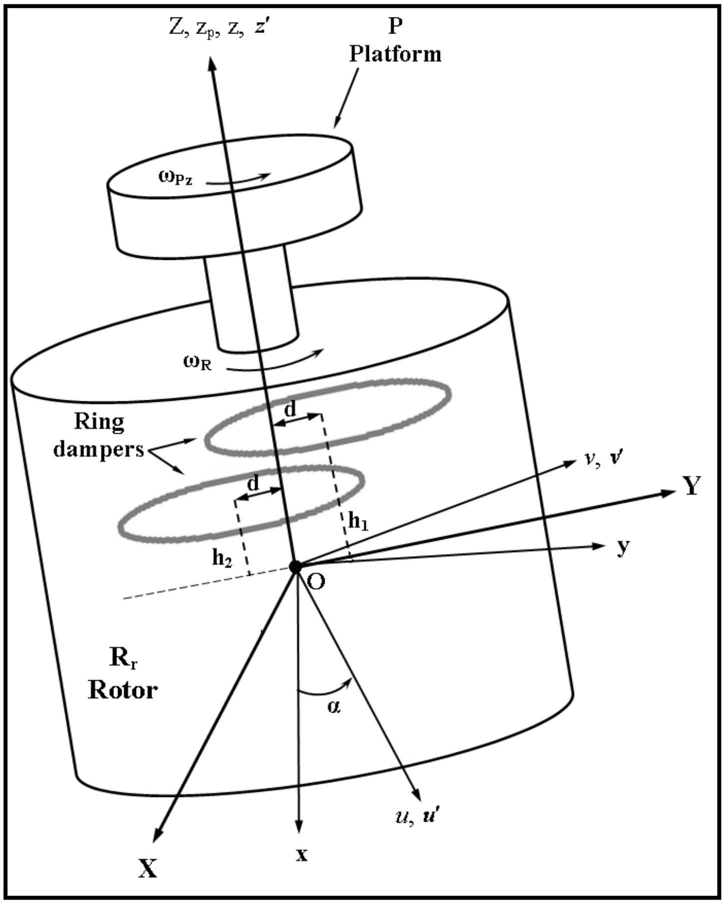

Figure (4.1) Dual-Spin Spacecraft Containing Nutation Dampers.

4.2.1 Equations of Motions

The model of dual-spin spacecraft adopted in this study is equipped with two nutation dampers filled with a viscous fluid and fixed with equal offsets in parallel planes, as shown figures (4.1) and (4.2). Referring to these figures, the coordinate system OXYZ is inertial reference frame with the origin O fixed in space coinciding with the center of mass of the inertially axisymmetric spacecraft. The local coordinate systems $ouvz$ and $ou'v'z'$ is fixed in the center of mass of the spacecraft such that the u and u' axes passing through the center of mass of a portion of the fluid and making an angle (α) counterclockwise with respect to the x-axis of the local coordinate system oxyz, which is fixed in the spacecraft center of mass (o).

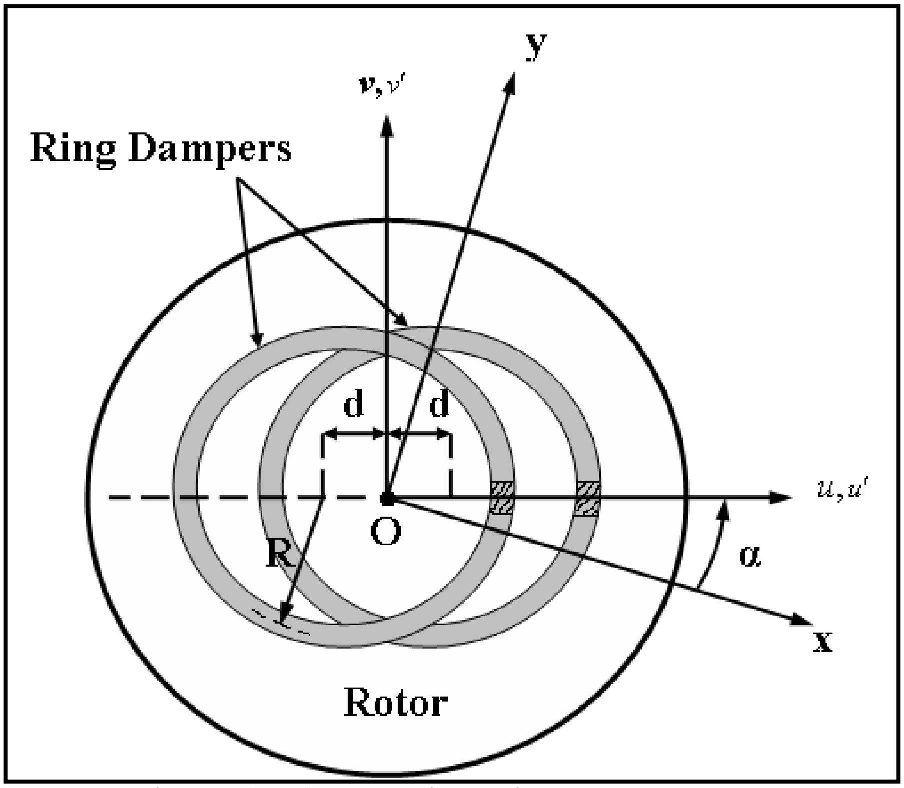

Figure (4.2) Nutation Ring Dampers.

The angular velocity components of the spacecraft measured in the local coordinate system oxyz, take into account that the transverse angular velocity components are the same for all the local coordinate systems which can be written as:

$$\vec{\omega}_s = \omega_u e_u + \omega_v e_v + \omega_z e_z \tag{4.1}$$

where

e_u, e_v, e_z are the unit vectors along *u*, *v* and *z* axes, and ω_u, ω_v and ω_z are the angular velocity components along the *uvz* coordinates.

The angular velocity of the fluid portion measured in the local coordinate system *ouvz* is given by:

$$\vec{\omega}_f = \omega_u e_u + \omega_v e_v + (\omega_z + \dot{\alpha}) e_z \tag{4.2}$$

where $\dot{\alpha}$ is the relative angular velocity of the fluid portion with respect to the x-axis.

The total angular momentum vector of the system may be given in the matrix form by:

$$\vec{h} = [I]_s\{\omega_s\} + [I]_1\{\omega_f\} + [I]_2\{\omega_f\} + \{h_p\} \tag{4.3}$$

where

$[I]_s$: is the moment of inertia matrix of the dual-spin system not including the symmetric principal moment of inertia of the platform, which given by:

$$[I]_s = \begin{bmatrix} A & 0 & 0 \\ 0 & A & 0 \\ 0 & 0 & C \end{bmatrix} \tag{4.4}$$

where A is the total transverse principal moment of inertia of the spacecraft and C is the rotor spin axis principal moment of inertia.

$[I]_1$ and $[I]_2$: are the moment of inertia matrices of the first damper and second damper respectively measured in the local coordinates uvz and $u'v'z'$, and given by:

$$[I]_1 = \begin{bmatrix} I_u & 0 & I_{uz} \\ 0 & I_v & 0 \\ I_{uz} & 0 & I_z \end{bmatrix}, \qquad [I]_2 = \begin{bmatrix} I_{u'} & 0 & I_{u'z'} \\ 0 & I_{v'} & 0 \\ I_{u'z'} & 0 & I_{z'} \end{bmatrix} \tag{4.5}$$

where

$$\begin{aligned} I_u &= \frac{1}{2}mR^2 + mh_1^2 & I_{u'} &= \frac{1}{2}mR^2 + mh_2^2 \\ I_v &= \frac{1}{2}mR^2 + m(h_1^2 + d^2) & I_{v'} &= \frac{1}{2}mR^2 + m(h_2^2 + d^2) \\ I_z &= mR^2 + md^2 & I_{z'} &= mR^2 + md^2 \\ I_{uz} &= mdh_1 & I_{u'z'} &= mdh_2 \end{aligned} \tag{4.6}$$

where

m : mass of the viscous fluid.

h_1, h_2 : heights of the first and second rings above the center of mass of the spacecraft.

R : ring mean radius.

d : offset of the ring dampers.

$\{h_P\} = [0 \quad 0 \quad C_P\omega_{Pz}]^T$: is the column vector, and C_P is the symmetric principal moment of inertia of the platform about the z-axis, and ω_{Pz} is the angular velocity component of the platform along the z-axis.

The total angular momentum can be written in terms of angular velocity components, so that Eq. (4.3) takes the following form:

$$\vec{h} = \begin{bmatrix} A & 0 & 0 \\ 0 & A & 0 \\ 0 & 0 & C \end{bmatrix}\begin{bmatrix} \omega_u \\ \omega_v \\ \omega_z \end{bmatrix} + \begin{bmatrix} I_u & 0 & -I_{uv} \\ 0 & I_v & 0 \\ -I_{uv} & 0 & I_z \end{bmatrix}\begin{bmatrix} \omega_u \\ \omega_v \\ \omega_z + \dot{\alpha} \end{bmatrix} + \begin{bmatrix} I_{u'} & 0 & -I_{u'z'} \\ 0 & I_{v'} & 0 \\ -I_{u'z'} & 0 & I_{z'} \end{bmatrix}\begin{bmatrix} \omega_u \\ \omega_v \\ \omega_z + \dot{\alpha} \end{bmatrix} + \begin{bmatrix} 0 \\ 0 \\ C_P\omega_{Pz} \end{bmatrix} \quad (4.7)$$

and after expansion the matrices, the above equation becomes

$$\vec{h} = \left(A\omega_u + I_u\,\omega_u - I_{uz}(\omega_z + \dot{\alpha}) + I_{u'}\omega_u - I_{u'z'}(\omega_z + \dot{\alpha})\right)e_u + (A\omega_v + I_v\omega_v + I_{v'}\omega_v)e_v$$
$$+\left(C\omega_z - I_{uz}\omega_u + I_z(\omega_z + \dot{\alpha}) - I_{u'z'}\omega_u + I_{z'}(\omega_z + \dot{\alpha}) + C_P\omega_{Pz}\right)e_z \quad (4.8)$$

In order to derive the equation of motion of the spacecraft, provided by two nutation dampers, the following assumptions are taken throughout the analysis

1- Gravity effects are neglected [2].

2- The total mass of the fluid in the dampers is only a few percent of the mass of the Spacecraft.

It is important to note that the inertial spin rate of the platform of the satellite adopted in the present study will be maintained at a rate of ($\omega_{Pz} = \Omega_P =$ constant) during its normal operating mode by use of a suitable despin control loop, so that the time derivative of the platform spin rate ($\dot{\omega}_{Pz}$) will be zero.

The governing differential equation of the system is given by:

$$\vec{M} = \left[\frac{d\vec{h}}{dt}\right]_{XYZ} \quad (4.9)$$

where $\vec{M}$ is the vector sum of the external disturbance torques.

When the external torque components are zero, the system referred to as a freely precessing system, then the principle of conservation of angular momentum can be applied, such that:

$$\left[\frac{d\vec{h}}{dt}\right]_{XYZ} = 0 \tag{4.10}$$

The time derivative of the angular momentum in an inertial reference frame may be given by:

$$\left[\frac{d\vec{h}}{dt}\right]_{XYZ} = \left[\frac{d\vec{h}}{dt}\right]_{uvz} + \vec{\omega}_f \times \vec{h} = 0 \tag{4.11}$$

and can be written in a matrix form as:

$$\left[\frac{d\vec{h}}{dt}\right]_{uvz} + \lfloor \omega_f \rfloor \{h\} = 0 \tag{4.12}$$

where

$\lfloor \omega_f \rfloor$: skew symmetric matrix of the angular velocity components of the fluid, and given by:

$$\lfloor \omega_f \rfloor = \omega_f^{\times} = \begin{bmatrix} 0 & -(\omega_z + \dot{\alpha}) & \omega_v \\ (\omega_z + \dot{\alpha}) & 0 & -\omega_u \\ -\omega_v & \omega_u & 0 \end{bmatrix}$$

$\{h\} = \lfloor h_u \quad h_v \quad h_z \rfloor^T$: is the column matrix of the angular momentum vector of the system.

Rewriting Eq. (4.12) in terms of angular velocity and rearranges to get the following three equations of motion which describe the dynamic of dual-spin spacecraft containing nutation dampers:

$$\begin{aligned}(A + I_u + I_{u'})\dot{\omega}_u - (I_{uz} + I_{u'z'})(\dot{\omega}_z + \ddot{\alpha}) - (\omega_z + \dot{\alpha})\left[(A + I_v + I_{v'})\right]\omega_v \\ + \lfloor C\omega_z + 2I_z(\omega_z + \dot{\alpha}) - (I_{uz} + I_{u'z'})\omega_u + C_p\omega_p \rfloor \omega_v = 0\end{aligned} \tag{4.13}$$

$$\begin{aligned}(A + I_v + I_{v'})\dot{\omega}_v + (\omega_z + \dot{\alpha})\left[(A + I_u + I_{u'})\omega_u - (I_{uz} + I_{u'z'})(\omega_z + \dot{\alpha})\right] \\ - \lfloor C\omega_z + 2I_z(\omega_z + \dot{\alpha}) - (I_{uz} + I_{u'z'})\omega_u + C_p\omega_{pz} \rfloor \omega_u = 0\end{aligned} \tag{4.14}$$

$$C\dot{\omega}_z + 2I_z(\dot{\omega}_z + \ddot{\alpha}) - (I_{uz} + I_{u'z'})\dot{\omega}_u - \omega_v\left[(A + I_u + I_{u'})\omega_u - (I_{uz} + I_{u'z'})(\omega_z + \dot{\alpha})\right]$$
$$+ \omega_u\left[(A + I_v + I_{v'})\omega_v\right] = 0 \qquad (4.15)$$

The other equation of motion that describes the rotational motion of the fluid inside the rings about the spin axis (z-axis) can be obtained by using Lagrange's equation expressed in terms of quasi-coordinates [24]:

$$\frac{d}{dt}\left\{\frac{\partial T}{\partial \omega}\right\} + [\omega]\left\{\frac{\partial T}{\partial \omega}\right\} = \{Q\} \qquad (4.16)$$

where

T: kinetic energy of the system.

$[\omega]$: skew symmetric matrix of the angular velocity components and it is given by

$$[\omega] = \begin{bmatrix} 0 & -\dot{\alpha} & \omega_v \\ \dot{\alpha} & 0 & -\omega_u \\ -\omega_v & \omega_u & 0 \end{bmatrix}$$

$\{Q\}$: column matrix of the moment components of the non-conservative forces (dissipative forces):

$$\{Q\} = \begin{bmatrix} 0 & 0 & Q_\alpha \end{bmatrix}^T$$

Using Eq. (4.16), the equation of motion corresponding to the quasi-coordinate α is given by:

$$\frac{d}{dt}\left\{\frac{\partial T}{\partial \dot{\alpha}}\right\} - \omega_v \frac{\partial T}{\partial \omega_u} + \omega_u \frac{\partial T}{\partial \omega_v} = Q_\alpha \qquad (4.17)$$

where Q_α is the generalized moment associated with the generalized coordinate α, and it is given by:

$$Q_\alpha = 2C_f R^2 \dot{\alpha}$$

C_f : coefficient of the viscous friction between the viscous fluid and the ring wall.

The kinetic energy, T, of the system is:

$$T = \frac{1}{2}\Big[A\omega_u{}^2 + A\omega_v{}^2 + C\omega_z{}^2 + C_p\Omega_p{}^2 + I_u\omega_u{}^2 + (I_u + I_{u'})\omega_u{}^2 + (I_v + I_{v'})\omega_v{}^2 + I_z(\omega_z + \dot{\alpha})^2\Big]$$

$$- I_{uz}\omega_u(\omega_z + \dot{\alpha}) - I_{u'z'}(\omega_z + \dot{\alpha})\omega_u \tag{4.18}$$

The derivative terms of the kinetic energy according to Eq. (4.17) are:

$$\frac{\partial T}{\partial \dot{\alpha}} = 2I_z(\omega_z + \dot{\alpha}) - (I_{uz} + I_{u'z'})\omega_u)$$

$$\frac{d}{dt}\left\{\frac{\partial T}{\partial \dot{\alpha}}\right\} = 2I_z(\dot{\omega}_z + \ddot{\alpha}) - (I_{uz} + I_{u'z'})\dot{\omega}_u$$

$$\frac{\partial T}{\partial \omega_u} = (A + I_u + I_{u'}) - (I_{uz} + I_{u'z'})(\omega_z + \dot{\alpha})$$

$$\frac{\partial T}{\partial \omega_v} = (A + I_v + I_{v'})$$

Substitute the above derivative terms into Eq. (4.17) gives the following equation:

$$2I_z(\dot{\omega}_z + \ddot{\alpha}) - (I_{uz} + I_{u'z'})\dot{\omega}_u - [(A + I_u + I_{u'})\omega_u - (I_{uz} + I_{u'z'})(\omega_z + \dot{\alpha})]\omega_v$$

$$+ [(A + I_v + I_{v'})\omega_v]\omega_u = -2C_f R^2\dot{\alpha} \tag{4.19}$$

In order to carry out the analysis of the problem, it is interesting to introduce the dimensionless form for the equations of motion (4.13), (4.14),(4.15) and (4.19), thus, the dimensionless form for the equations of motion are given by (details are given in appendix A):

$$p' + \frac{(\lambda r - \alpha' + \lambda_s)}{D_1}q + \frac{(A_1 r + A_2\alpha' + A_3 p)}{D_1}q - \frac{A_4}{D_1}r' + \frac{A_5}{D_1}\alpha' = 0 \tag{4.20}$$

$$q' - \frac{(\lambda r - \alpha' + \lambda_s)}{D_2}p + \frac{(B_1 r + B_2\alpha' - B_3 p)}{D_2}p - \frac{B_4}{D_2}(r + \alpha')^2 = 0 \tag{4.21}$$

$$\alpha'' + C_1\alpha' + C_2 pq + C_3((r + \alpha')q - p') = 0 \tag{4.22}$$

$$r' - C_4\alpha' = 0 \tag{4.23}$$

4.2.2 Approximate Analyses (Zero-Order Approximation)

The equations of motion of the spacecraft which are developed in the previous section, are complicated in their nature. These equations are strongly coupled nonlinear differential equations. An approximate solution for the equations of motion must be developed. Different methods of approximate analysis adopted by many investigators to obtain closed form solution for the equations of motion, where, the references [6] and [30] adopted the energy sink approach in their analyses, while the references [2,3,19,36,38] their analyses based on the zero order approximation method.

In the present study zero order approximation method is adopted, in order to obtain an approximate solution for the attitude equations of motion of the system. Zero order approximation method is based on the fact that the mass of the fluid is much smaller than that of the spacecraft, or in other wards, the moment of inertia of the fluid is very small compared with that of the spacecraft. The ratio of the fluid moment of inertia (mR^2) to the transverse moment of inertia of the spacecraft is called (ε). Therefore, dependent on the basis of zero order approximation method any term containing the inertia ratio (ε), it is neglected.

4.2.3 Approximate Solution of the Problem

Before developing the solution for the attitude equations of the spacecraft, the equation, which describes the nutation angle in terms of the dimensionless parameters and variables, will be developed.

The cosine and sine terms of the nutation angle (θ) are given by:

$$\cos\theta = \frac{h_z}{h} \tag{4.24}$$

$$\sin\theta = \frac{h_t}{h} \tag{4.25}$$

where h_t is the transverse angular momentum and h is the total angular momentum of the system and it is given by:

$$h^2 = h_z^2 + h_t^2 = \text{constant} \tag{4.26}$$

where h_t is given by:

$$h_t^2 = h_u^2 + h_v^2 \tag{4.27}$$

Differentiating Eq. (4.24) with respect to the dimensionless time τ, gives

$$-\sin\theta \cdot \theta' = \frac{h_z'}{h} \tag{4.28}$$

Substituting Eq. (4.25) in Eq. (4.28) gives:

$$-\frac{h_t}{h}\theta' = \frac{h_z'}{h} \tag{4.29}$$

$$\therefore \ \theta' = -\frac{h_z'}{h_t} \tag{4.30}$$

The time derivative of the spin angular momentum vector h_z may be given by:

$$\frac{dh_z}{dt} = \omega_v h_u - \omega_u h_v \tag{4.31}$$

or, with respect to the dimensionless time τ and in terms of dimensionless angular velocity variables (p and q) is given by:

$$h_z' = qh_u - ph_v \tag{4.32}$$

Substituting Eq. (4.32) into Eq. (4.30), yields the following equation:

$$\theta' = \frac{ph_v - qh_u}{h_t} \tag{4.33}$$

In terms of dimensionless variables and parameters, Eq. (4.33), can be written in the following form (details are given in appendix B):

$$\theta' = \frac{\left[2G^2 p + G(b_1 + b_2)(r + \alpha')\right]\varepsilon q}{\sqrt{p^2 + q^2}} \tag{4.34}$$

Referring to Eqs. (4.20), (4.21), (4.22), and (4.23) apply the zero order approximation procedure (neglecting the terms multiplying by ε), so that, the constants are given by (appendix A):

$A_1=A_2=A_3=A_4=A_5=0$

$B_1=B_2=B_3=B_4=0$

$D_1=D_2=1$

$C_4=0$

Using the above values of the constants, the equations of motion become:

$$p' + (\lambda r - \alpha' + \lambda_s) q = 0 \tag{4.35}$$

$$q' - (\lambda r - \alpha' + \lambda_s) p = 0 \tag{4.36}$$

$$r' = 0 \tag{4.37}$$

$$\alpha'' + \frac{\eta}{\zeta}\alpha' + \frac{G^2}{\zeta} pq + \frac{G}{2\zeta}(b_1 + b_2)\big((r + \alpha')q - p'\big) = 0 \tag{4.38}$$

The solution of the angular velocity component r is obtained from Eq. (4.37), with the fact that the initial value of the r component equal to 1, then the solution of Eq. (4.37) is:

$$r = 1 \tag{4.39}$$

Substituting the solution of the r component in Eq. (4.39) into Eqs. (4.35) and (4.36), the following equations are obtained:

$$p' + (\lambda_n - \alpha') q = 0 \tag{4.40}$$

$$q' - (\lambda_n - \alpha') p = 0 \tag{4.41}$$

where

$$\lambda_n = \lambda + \lambda_s$$

Differentiating Eq. (4.41) and substituting the result into Eq. (4.40) and using the following initial conditions, $q(\tau = 0) = q_\circ \neq 0$ and $q'(\tau = 0) = 0$, then, the solution of p and q are given by:

$$p = q_\circ \cos(\lambda_n \tau - \alpha) \tag{4.42}$$

$$q = q_\circ \sin(\lambda_n \tau - \alpha) \tag{4.43}$$

The total transverse angular velocity component ω_t is given by:

$$\omega_t = p + iq \tag{4.44}$$

or

$$\omega_t = q_\circ \left[\cos(\lambda_n \tau - \alpha) + i \sin(\lambda_n \tau - \alpha)\right] \tag{4.45}$$

this also expressed in exponential notation as:

$$\omega_t = q_\circ e^{i(\lambda_n \tau - \alpha)} \tag{4.46}$$

Using the initial conditions, $\alpha(t=0) = 0$, Eq. (4.46) becomes:

$$q_\circ = \omega_t \tag{4.47}$$

Substituting for $q_\circ$ in Eqs. (4.42) and (4.43), then

$$p = \omega_t \cos(\lambda_n \tau - \alpha) \tag{4.48}$$

$$q = \omega_t \sin(\lambda_n \tau - \alpha) \tag{4.49}$$

Substituting Eqs. (4.48) and (4.49) into Eq. (4.34), then Eq.(4.34) becomes:

$$\theta' = \left[2G^2 \omega_t \cos(\lambda_n \tau - \alpha) + G(b_1 + b_2)(1 + \alpha')\right] \varepsilon \sin(\lambda_n \tau - \alpha) \tag{4.50}$$

Now, it is required to express for ω_t in terms of the nutation angle θ, (details are given in appendix B), which is given by:

$$\tan\theta = \frac{\omega_t}{(\sigma r + \lambda_s)} = \frac{\omega_t}{(\sigma + \lambda_s)} \tag{4.51 a}$$

Then

$$\tan\theta = \frac{\omega_t}{\sigma_n} \tag{4.51 b}$$

where: $\sigma_n = \sigma + \lambda_s$

Substituting for p' from Eq. (4.35), and using Eq. (4.39), then Eq. (4.38) becomes:

$$\alpha'' + \frac{\eta}{\zeta}\alpha' + \left[\frac{G(b_1 + b_2)}{2\zeta}(1 + \alpha') + \frac{G^2}{\varsigma} p - \frac{G(b_1 + b_2)}{2\zeta}(\alpha' - \lambda_n)\right] q = 0 \tag{4.52}$$

To find the solution of the nutation angle θ, it is necessary to obtain the solution for the fluid motion in both modes of motion of the spacecraft inside the dampers.

4.2.4 Damper motion

A symmetric dual-spin spacecraft, which is spinning about its axis of symmetry has a constant nutation angle when no damping is present. The transverse angular velocity ω_t rotates at a rate of $(\sigma\Omega + \sigma_p \Omega_p)\cos\theta$ and the spacecraft rotates relative to ω_t at a rate of $((1-\sigma)\Omega + \sigma_p \Omega_p)$. When no damping is present, a plane containing the angular momentum vector $\vec{h}$ or ω_t and the z-axis, called the nutation plane, is formed. The fluid then moves at a constant rate of $((1-\sigma)\Omega + \sigma_p \Omega_p)$, (relative spin), with respect to the spacecraft. At the same time, the fluid is subjected to centrifugal force due to the relative rotation (spin) about the z-axis. This type of motion is called “nutation synchronous” motion. In this mode the fluid moves at a constant rate with respect to the spacecraft or ring. Hence, the energy dissipation rate is a constant.

If σ > 1, the nutation angle decreases which cause a decreases in the centrifugal force. Eventually the component of the centrifugal force is not large enough to balance the damping force and the fluid begins to decelerated and oscillated until becomes at rest. This type of motion is called “spin-synchronous” motion. The terms of nutation-synchronous and spin-synchronous were first introduced by Cartwright et al. [9].

The purpose now is to determine the fluid motion α and consequently θ in these two modes of motion as a function of dimensionless parameters.

4.2.4.1 Nutation Synchronous Mode

Let ϕ measure the position of the center of a portion of the fluid with respect to the nutation plane. Assuming that at τ =0, α =0, then

$$\phi = \alpha - \lambda_n \tau \tag{4.53}$$

Substituting for ϕ in Eq. (4.52) and using Eqs. (4.48) and (4.49), then Eq. (4.52) becomes:

$$\phi'' + \frac{\eta}{\zeta}(\phi' + \lambda_n) + \left[\frac{G^2}{\zeta}\omega_t \cos(\phi) - \frac{G(b_1+b_2)}{2\zeta}\phi' + \frac{G(b_1+b_2)}{2\zeta}(1+\phi'+\lambda_n)\right]\omega_t \sin(-\phi) = 0 \tag{4.54}$$

Rearrange this equation gives:

$$\phi'' + \frac{\eta}{\zeta}\phi' - \left[\frac{G^2}{\zeta}\omega_t \cos(\phi) + \frac{G(b_1+b_2)}{2\zeta}(1+\lambda_n)\right]\omega_t \sin(\phi) = -\frac{\eta}{\zeta}\lambda_n \tag{4.55}$$

As mentioned in pervious section, that in the nutation synchronous mode the fluid moves at a constant rate with respect to the spacecraft, the relative position ϕ is constant. Accordingly, the particular solution (steady state solution) of Eq. (4.55), is $\phi = \phi_s$. Therefore, substitution of ϕ into Eq. (4.55), and taking into account that $\phi' = \phi'' = 0$, $\lambda_n = \lambda + \lambda_s$, $\lambda = \sigma - 1$, then:

$$-\left[\frac{G^2}{\varsigma}\omega_t \cos(\phi_s) + \frac{G}{2\varsigma}(b_1+b_2)(1+\lambda_n)\right]\omega_t \sin(\phi_s) = -\frac{\eta}{\varsigma}\lambda_n \tag{4.56}$$

Rearranging this equation is to give:

$$\left[2G^2\omega_t \cos(\phi_s) + G(b_1+b_2)(1+\lambda_n)\right]\omega_t \sin(\phi_s) = 2\eta\lambda_n \tag{4.57}$$

Using Eq. (4.53) and substituting $\phi = \phi_s$ and $\phi' = 0$, then, the nutation angle rate Eq. (4.50), becomes:

$$\theta_n' = -\left[2G^2\omega_t \cos\phi_s + G(b_1+b_2)(1+\lambda_n)\right]\varepsilon \sin(\phi_s) \tag{4.58}$$

where θ_n referred to the nutation angle in the nutation-synchronous mode.

Substituting the left hand side of Eq. (4.58) into Eq. (4.57), get:

$$\theta_n{}' = \frac{-2\eta\lambda_n\varepsilon}{\omega_t} \tag{4.59}$$

after substituting ω_t from Eq. (4.51 b) into above equation, becomes:

$$\tan\theta_n\theta_n' = \frac{-2\eta\lambda_n\varepsilon}{\sigma_n} \tag{4.60}$$

Carrying out the integration, then Eq. (4.60) will take the following form:

$$\cos\theta_n = \cos\theta_{n0}e^{\frac{\tau}{\tau_n}} \tag{4.61}$$

where θ_{n0} is the initial value of θ_n and τ_n is the dimensionless time constant of the system in nutation-synchronous mode, and it is given by:

$$\tau_n = \frac{\sigma_n}{2\eta_n\lambda_n\varepsilon} = \frac{\sigma+\lambda_s}{2\eta_n(\lambda+\lambda_s)\varepsilon} \tag{4.62}$$

where η_n is the damping constant in nutation-synchronous mode.

It is clear in this mode, that the cosine of the nutation angle, not the nutation angle, exhibits exponential behavior, hence, Eq. (4.61) is valid for $0<\theta<\frac{\pi}{2}$.

If small angle approximation has been used (i.e. $\tan\theta \approx \theta$), then Eq. (4.60) becomes:

$$\theta_n\theta_n' = \frac{-2\eta\lambda_n\varepsilon}{\sigma_n} \tag{4.63}$$

Carrying out the integration, then Eq. (4.63) becomes:

$$\theta_n = \sqrt{\theta_{n\circ}^{\ 2} - \frac{2\eta\lambda_n\varepsilon}{\sigma_n}\tau} \tag{4.64}$$

At the end of the nutation-synchronous mode, the system goes into the spin-synchronous mode and the nutation angle θ_n has minimum value in this mode. Using Eq. (4.51 b), then Eq. (4.57) will be:

$$\left[2G^2\sigma_n\tan\theta_n\cos(\phi_s) + G(b_1+b_2)(1+\lambda_n)\right]\sigma_n\tan\theta_n\sin(\phi_s) = 2\eta\lambda_n \tag{4.65}$$

to satisfy the condition of minimum value of the nutation angle, the angle ϕ_s should be equal to $\pm\frac{\pi}{2}$, substitute this value into Eq. (4.65), then:

$$\tan\theta_t = \frac{2\eta_n\lambda_n}{G(b_1+b_2)\sigma_n^{\ 2}} \tag{4.66}$$

where θ_t is the transition angle of the nutation angle from the nutation-synchronous mode to spin-synchronous mode.

4.2.4.2 Spin Synchronous Mode

In spin synchronous mode, the spacecraft becomes more closely to the state of pure spin about the spin axis (z-axis). Accordingly, the relative rotation speed of the fluid, about the spin axis with respect to the rings, will decrease. Eventually, the relative rotational speed between the fluid and the rings becomes zero, then, the spacecraft spin axis aligned with the initial direction of the total angular momentum vector. In the spin-synchronous mode, it can be shown that the fluid moves with a small variation in its speed with respect to the damper ring [3,48], and it is necessary to find the solution for the motion of the fluid (α) as a function of dimensionless variable time (τ).

Substituting for p and q from Eqs. (4.48) and (4.49) into Eq. (4.52) and take into account that $\lambda_n = \lambda + \lambda_s$, then Eq. (4.52) becomes:

$$\alpha'' + \frac{\eta}{\zeta}\alpha' + \left[\frac{G(b_1+b_2)}{2\zeta}(1+\alpha') + \frac{G^2}{\varsigma}\omega_t\cos(\lambda_n\tau-\alpha) - \frac{G(b_1+b_2)}{2\zeta}(\alpha'-\lambda_n)\right]\omega_t\sin(\lambda_n\tau-\alpha) = 0 \tag{4.67}$$

Rearranging

$$\alpha'' + \frac{\eta}{\zeta}\alpha' - \left[\frac{G(b_1+b_2)}{2\zeta}(1+\lambda_n) + \frac{G^2}{\varsigma}\omega_t\cos(\alpha-\lambda_n\tau)\right]\omega_t\sin(\alpha-\lambda_n\tau) = 0 \tag{4.68}$$

Since the spin-synchronous mode occurs for the smaller nutation angles, then from Eq. (4.51 b) it can be concluded that $\omega_t << 1$, thus the last term within the brackets in Eq. (4.68) will be dropped, and Eq. (4.68) becomes:

$$\alpha'' + \frac{\eta}{\zeta}\alpha' - \left[\frac{G(b_1+b_2)}{2\zeta}(1+\lambda_n)\right]\omega_t\sin(\alpha-\lambda_n\tau) = 0 \tag{4.69}$$

As it is mentioned above that the fluid moves with a small variation in its speed, then:

$$\alpha = \alpha_{\circ} + \tilde{\alpha} \tag{4.70}$$

where $\alpha_{\circ}$ is the initial value of α and $\tilde{\alpha}$ represent the small change occurs in α such that $\alpha_{\circ} >> \tilde{\alpha}$. The basis of this assumption is that the change in α is small compared with $\lambda_n \tau$. An approximate steady state solution of Eq. (4.69), may be given by (details are given in Appendix C):

$$\tilde{\alpha} = K \tan\theta_s \left[\eta \cos(\alpha_0 - \lambda_n \tau) - \lambda_n \zeta \sin(\alpha_0 - \lambda_n \tau)\right] \tag{4.71}$$

where θ_s referred to the nutation angle in the spin-synchronous mode, and the constant K is given by:

$$K = \frac{\sigma_n}{\lambda_n{}^2} \left[\frac{G(b_1 + b_2)(1 + \lambda_n)}{2\varsigma^2 \left(\lambda_n + \dfrac{\eta^2}{\varsigma^2 \lambda_n} \right)} \right]$$

The differential equation of the nutation angle rate (Eq. (4.50)) may be given by:

$$\theta' = -\left[2G^2 \omega_t \cos(\alpha - \lambda_n \tau) + G(b_1 + b_2)(1 + \alpha')\right] \varepsilon \sin(\alpha - \lambda_n \tau) \tag{4.72}$$

Assuming that θ_s is small enough, then, the terms of ($\theta_s{}^2$) can be neglected and as mentioned above that the change in α is small, then Eq. (4.72) can be reduced to (details are given in Appendix C):

$$\theta_s' + \theta_s \left[E_1 \cos 2\lambda_n \tau + E_2 \sin 2\lambda_n \tau + \frac{1}{\tau_{cs}} \right] = -G\varepsilon(b_1 + b_2)\sin(\alpha_0 - \lambda_n \tau) \tag{4.73}$$

where E_1 and E_2 are constants and the time constant in spin-synchronous mode τ_{cs} is given by:

$$\tau_{cs} = \frac{4\varsigma^2 \lambda_n \left[\lambda_n{}^2 + \dfrac{\eta_s{}^2}{\varsigma^2} \right]}{G^2 \varepsilon (b_1 + b_2)^2 (1 + \lambda_n)^2 \eta_s \sigma_n} \tag{4.74}$$

where η_s is the damping constant in the spin-synchronous mode.

The solution of Eq. (4.73) (detail in Appendix C) is:

$$\theta_s = \left[\theta_{s0} + \left(\frac{\frac{1}{\tau_{cs}} \sin(\alpha_0 - \lambda_n \tau_0) + \lambda_n \cos(\alpha_0 - \lambda_n \tau_0)}{\left(\lambda_n{}^2 + \frac{1}{\tau_{cs}{}^2} \right)} \right) G\varepsilon(b_1 + b_2) \right] e^{\frac{-(\tau-\tau_0)}{\tau_{cs}}} - \left(\frac{\frac{1}{\tau_{cs}} \sin(\alpha_0 - \lambda_n \tau) + \lambda_n \cos(\alpha_0 - \lambda_n \tau)}{\left(\lambda_n{}^2 + \frac{1}{\tau_{cs}{}^2} \right)} \right) G\varepsilon(b_1 + b_2) \qquad (4.75)$$

4.3 The Residual Nutation Angle & The Relative Equilibria States

At the end of the spin-synchronous mode, the nutation angle decreases to a certain level where the nutation motion cannot excite the relative motion of the viscous fluid inside the damper, and the system kinetic energy is no longer dissipated. Thus the threshold of the nutation dampers over which the relative motion can be caused by the nutation motion is just the residual nutation angle.

The dynamic behavior of the spacecraft as close as pure spin is in the steady state condition which reflects the relative state of equilibrium of the spacecraft. In the steady state condition, it is known that all derivatives (primes) with the time are vanished. In order to obtain the equations of the relative equilibria states, let p_e, q_e, r_e, and α_e denote the state of relative equilibria, and by setting $p' = 0$, $q' = 0$, $r' = 0$, and $\alpha'' = \alpha' = 0$ in Eqs. (4.20), (4.21), (4.22), and (4.23), then these equations are given by:

$$[(\lambda + A_1) r_e + A_3 p_e + \lambda_s] q_e = 0 \qquad (4.76)$$

$$B_3 p_e{}^2 + (B_1 - \lambda) r_e p_e - B_3 r_e{}^2 - \lambda_s p_e = 0 \qquad (4.77)$$

$$(C_2 p_e - C_3 r_e) q_e = 0 \qquad (4.78)$$

Assuming that the rotor angular momentum is much larger than the platform angular momentum (i.e. $C\Omega >> C_p\Omega_p$, or $\lambda >> \lambda_s$) which is a reasonable assumption in viewing the fact that Ω_p is approximately equal to the orbital rate, so that the above equations can be reduced to:

$$[(\lambda + A_1)r_e + A_3 p_e]q_e = 0 \tag{4.79}$$

$$B_3 p_e^{\,2} + (B_1 - \lambda)r_e p_e - B_3 r_e^{\,2} = 0 \tag{4.80}$$

$$(C_2 p_e - C_3 r_e)q_e = 0 \tag{4.81}$$

Solving the above equations for p_e, q_e, and r_e then the relative equilibria states RES1, RES2, and RES3 are given by:

$$\text{RES1} \qquad q_e = 0, \qquad p_e = \frac{-(B_1 - \lambda) + \sqrt{(B_1 - \lambda)^2 + 4B_3^{\,2}}}{2B_3} r_e \tag{4.82}$$

$$\text{RES2} \qquad q_e = 0, \qquad p_e = \frac{-(B_1 - \lambda) - \sqrt{(B_1 - \lambda)^2 + 4B_3^{\,2}}}{2B_3} r_e \tag{4.83}$$

$$\text{RES3} \qquad p_e = 0, \; r_e = 0, \; q_e \neq 0 \tag{4.84}$$

Now the values of p_e, q_e, and r_e in Eqs. (4.82), (4.83), (4.84) must be determined. Before expanding Eq. (4.82), the term of the square root can be given in a series form as:

$$(a+b)^n = a^n + na^{n-1}b + \frac{n(n-1)}{2!}a^{n-2}b^2$$

Using above relation, and it is known that from Appendix-A that both B_1 and B_3 are functions of ε, then Eq. (4.82) can be expanded as follows:

$$p_e = \frac{-1 + \sqrt{1+U^2}}{U} r_e \cong \frac{-1 + \left(1 + \frac{1}{2}U^2\right)}{U} r_e \cong \frac{B_3}{(B_1 - \lambda)} r_e \cong \frac{-B_3}{\lambda} r_e = \frac{-\varepsilon G(b_1 + b_2)}{\lambda} r_e \tag{4.85}$$

where

$$U = \frac{2B_3}{(B_1 - \lambda)}$$

The sign of p_e depends on the sign of λ. Equation (4.85) implies that $r_e = f(1)$ and $p_e = f(\varepsilon)$. The physical meaning for this relative equilibrium is that the spacecraft spin about the *z*-axis and the *z*-axis precesses steadily about the angular momentum vector with small or residual constant nutation angle θ_r which satisfies:

$$\tan\theta_r = \frac{h_t}{h_z} = \frac{\sqrt{\left[(A+I_u+I_{u'})p_e-(I_{uz}+I_{u'z'})r_e\right]^2+\left[(A+I_v+I_{v'})q_e\right]^2}}{(C+2I_z)r_e-(I_{uz}+I_{u'z'})p_e+C_p\dfrac{\Omega_p}{\Omega}} \tag{4.86}$$

where h_t and h_z are the transverse and spin axis angular momentum respectively and θ_r is the residual nutation angle.

Considering that ($\lambda >> \lambda_s$) and substituting for $q_e = 0$ from Eq. (4.82), then Eq. (4.86) becomes:

$$\tan\theta_r = \frac{(A+I_u+I_{u'})p_e-(I_{uz}+I_{u'z'})r_e}{(C+2I_z)r_e-(I_{uz}+I_{u'z'})p_e} \tag{4.87}$$

Substituting for p_e from Eq. (4.85), then Eq. (4.87) becomes:

$$\tan\theta_r = \frac{-\left(1+f(\varepsilon)\right)\varepsilon G(b_1+b_2)-\lambda\varepsilon G(b_1+b_2)}{\lambda\left(\sigma+f(\varepsilon)\right)+\varepsilon^2G^2(b_1+b_2)^2} = \frac{-\varepsilon G(b_1+b_2)(1+\lambda)}{\lambda\sigma} = \frac{-\varepsilon G(b_1+b_2)}{(\sigma-1)} \tag{4.88}$$

For the relative equilibrium state RES2, Eq. (4.83), can be expanded by similar steps followed in the analysis for RES1, then Eq. (4.83) may given by:

$$r_e = \frac{U}{-1-\sqrt{1+U^2}}\,p_e \cong \frac{-U}{2}\,p_e \cong \frac{-B_3}{(B_1-\lambda)}\,p_e \cong \frac{\varepsilon G(b_1+b_2)}{\lambda}\,p_e \tag{4.89}$$

Equation (4.89) implies that $p_e = f(1)$ and $r_e = f(\varepsilon)$. The associated physical meaning is that the spacecraft spin about the *u*-axis and the *u*-axis precesses steadily about the angular momentum vector with a constant residual angle which it is given by:

$$\tan\theta_r = \frac{h_t}{h_z} = \frac{\lambda}{\varepsilon G(b_1+b_2)} \tag{4.90}$$

The third relative equilibrium state described, by Eq. (4.84), in which the values of p_e and r_e are equal to zero. The configuration of the third relative equilibrium state indicates that the spacecraft is in pure spin about v-axis and there is no precession and no residual nutation angle.

4.4 Damping Constant

The damping constant is one of the important characteristics of the nutation dampers. Where, the dimensionless parameters of the given system (spacecraft and nutation dampers) are defined unless the damping constant (η). A consideration of the fluid dynamics of the problem is necessary, since the motion of the fluid is different in the two modes.

For the nutation-synchronous mode the velocity of the fluid is constant with respect to the satellite or ring. The approach suggested is to model the motion of the fluid as steady laminar flow in a pipe [2].

Solution of the Navier-Stokes equations with a flux of;

$$Q_{flux} = \pi r^2 R\dot{\alpha} \tag{4.91}$$

where $R\dot{\alpha}$ is the velocity of the fluid relative to the ring and r is the ring radius, gives:

$$u_f = 2R\dot{\alpha}\left[1-\left(\frac{r_i}{r}\right)^2\right] \tag{4.92}$$

where r_i is the distance from the center of the pipe.

The shear stress at any point is:

$$\tau_{shear} = \mu\frac{\partial u}{\partial r_i} \tag{4.93}$$

where μ is the fluid viscosity. Thus the total viscous force is;

$$F_v = (2\pi r)(R\delta)\tau_{shear}\Big|_{r_i=r} = 8\pi\mu R^2\dot{\alpha}\delta \tag{4.94}$$

where δ is the fullness of the ring and its equal to (2π), (the ring is totally filled).

The damping force from dynamical analysis is:

$$F_v = C_f V_f = C_f R\dot{\alpha} = \eta m\Omega R\dot{\alpha} \tag{4.95}$$

After equating this equation with Eq. (4.94), the damping constant is given by:

$$\eta_n = \frac{8\nu}{r^2\Omega} \tag{4.96}$$

where ν is the kinematic viscosity of the fluid.

In the present study a mixture of glycerin oil with water [(75%) glycerin and (25%) water] is used as a viscous liquid because it gives minimum weight of the damper and maximum energy dissipation [19].

In the spin-synchronous mode the velocity of the fluid is not constant but oscillatory with respect to the ring, so that the approach is used to calculate the damping constant in the nutation-synchronous mode is not available, therefore, the experimental approach is dependent by many researches [2,6,19]. Hameed [19] calculated the damping constant in this mode by empirical relation and it is found to be equal (0.15) which is adopted in this research.

CHAPTER FIVE

Results & Discussion

5.1 Introduction

The analyses of the attitude motion of an axisymmetric dual spin spacecraft provided with two ring nutation dampers are obtained. They are based on the zero-order approximation method to obtain the differential equations for the nutation angle rate and the time constant in the nutation-synchronous and spin-synchronous modes in terms of dimensionless parameters of the spacecraft and the nutation dampers. Also the angular velocities components of the spacecraft are obtained.

In this chapter, the analytic results for the nutation angle and the time constants for the both modes of motion are compared with those found by using computer simulation programs. The effects of the spacecraft and nutation dampers parameters on the dynamic behavior, dynamic characteristics and the residual nutation angle are studied and the results are shown graphically.

5.2 Numerical Determination of the Time Constant

The time constant is one of the important dynamic characteristics of the nutation damper, hence it represents the speed of the response at which that the spacecraft returns to its initial position by the effect of the nutation dampers. It is shown that, the spacecraft has two distinct modes of motion, thus the time constant of each mode has its own characteristics. The analytic expressions of the time constant on both modes of motion are obtained by using an approximate solution (zero order approximation) and in order to compare the analytic solution of the equations of motion with the numerical solution, it is required to determine the time constants numerically. The time constants can be found numerically by using the numerical solution of the nutation angle (θ) obtained from the computer simulation programs.

The data obtained from a numerical solution or from an experimental test, by a variety methods, is used to determine the time constants. The numerical data is plotted in a semi-log manner in order to get a better estimate of the time constant [14]. This method may be described as follows; It is known that an exponential decaying system may be expressed in a general form as [14]:

$$Y = C_i e^{-\frac{\tau}{\tau_c}} \tag{5.1}$$

where Y is the response of the system, C_i is a constant, τ is the time or dimensionless time and τ_c is the time constant of the system. The above equation can be rewritten as:

$$\frac{Y}{C_i} = e^{-\frac{\tau}{\tau_c}} \tag{5.2}$$

Now defining,

$$X = \ln\left(\frac{Y}{C_i}\right) \tag{5.3}$$

Then

$$X = -\frac{\tau}{\tau_c} \tag{5.4}$$

Differentiating the variable X with respect to time τ, then Eq.(5.4), becomes:

$$\frac{dX}{d\tau} = -\frac{1}{\tau_c} \tag{5.5}$$

or

$$\tau_c = -\frac{1}{dX/d\tau} \tag{5.6}$$

Thus if X is plotted versus τ, then the slope of a getting straight line is equal to $1/\tau_c$. This method gives a more accurate estimation of (τ_c) since the best line through all data points is used. In regarding to the time constant in both modes, the nutation-synchronous mode and spin-synchronous mode, it is known that each time constant has its own special characteristics. Thus the numerical determination of the time constants in both modes, using the above mentioned procedure may be summarized as follows:

In the nutation-synchronous mode, it is known that the solution of the nutation angle (θ) is obtained in terms of ($\cos\theta$) rather than the nutation angle (θ) itself. Thus, the time constant is obtained by assuming an exponential behavior of ($\cos\theta$), for the solution obtained by a numerical integration of the exact equations of motion. Consequently, the variable X represent the natural logarithm of ($\cos\theta$), and the time constant can be calculated by the procedure mentioned above.

In the spin-synchronous mode, it is shown that the solution of the nutation angle (θ) is the superposition of an oscillation and an exponential decay with a time constant τ_{cs}. Thus, the time constant is obtained by numerical integration of the exact equations of motion assuming exponential behavior for the maximum values of the nutation angle (θ) during each oscillation.

5.3 Comparison between Analytical Solution and Computer Simulation Results

The analytic solution for the equations of motion, nutation angle, and time constants is dependent on the numerical solution to verify. The numerical solution is obtained by a simulation programs which built using a package in **Matlab program /7**, called **Simulink**. Simulink is a powerful package to model, simulate, and analyze the dynamic systems [39].

The schematic diagrams which illustrate the general form of the programs constructed by the package for the problem are presented in Appendix D. The simulink programs involved the numerical solution (ode 45 Dorman-Prince method of numerical integration) of the exact equations of motion in chapter four, i.e. Eqs.(4.20), (4.21), (4.22), and (4.23), using double nutation dampers mounted with equal center offsets.

The design parameters of the axisymmetrical dual spin satellite provided with double nutation ring dampers adopted in the present study are shown in table (5.1).

Table (5.1) Design parameters [23].

	parameters	***value***
Satellite Parameters	**A**	**36 kg.m^2**
	C	**43.2 kg.m^2**
	C_p	**0.2 kg.m^2**
	Ω	**10.5 rad/sec**
	Ω_P	**0.00007272 rad/sec**
	σ	**1.2**
Rings Parameters	**R**	**250 mm**
	r	**9.5 mm**
	d	**50 mm**
	ε	**0.0009**
Fluid Parameters	m	**0.5186 kg**
	ρ_f	**1164.5 kg/m^3**
	μ	**67.9** $\left(\dfrac{N.\sec}{m^2}\times 10^{-3}\right)$
	ν	**58.31 mm^2/sec**

Figure (5.1) shows the typical nutation angle time history (experimental work) given by Alfreind [2].

Figure (5.2) shows a comparison between the analytical and numerical solutions of the nutation angle time histories for both nutation-synchronous mode and spin-synchronous mode. The general trend of this case is well predict in comparison with that given by Alfreind [2]. It is seen that the analytical results are in good agreement with the numerical results for both modes of motion. The dimensionless value of time constant decay, for nutation-synchronous mode, obtained analytically according to equation (4.62) is found to be (6772.3) and its numerical value is found to be (7496.95). These values indicate that the percentage difference is less than (11%), which may considered to be acceptable. For spin-synchronous mode, the analytical dimensionless value of the time constant decay estimated according to equation (4.74) is found to be (266.4557) and numerically (307.76), so that the percentage difference is (16%) which indicate that the analytical solution is good.

In general, these results reveals that the assumption adopted in the analysis is good for fluid motion in nutation-synchronous and spin-synchronous modes, and this conclusion is well agreed with that provided by [2,6,16].

Figure (5.3) shows the comparison of the analytical solution of the nutation angle time histories for nutation-synchronous mode for the present work and that of reference [3]. It is can be seen that the nutation angle decay is decreased by (50%) compared with that of reference [3], because of the addition of the second nutation ring damper on the system.

Figure (5.4) shows the comparison of the analytical solution of the nutation angle time histories for nutation-synchronous mode for the present work and that of references [2,19], after using the same spacecraft parameters. It is clearly can be seen that there is a great difference between the responses, where the nutation angle decay of the present work is quite faster compared with that given by [2,19].

5.4 Parametric Study

The parametric study included the investigation of the influence of the spacecraft and nutation dampers parameters on the dynamic characteristics of the nutation damping system. Also the study is extended to include the effects of these parameters on the residual nutation angle of the spacecraft.

5.4.1 Influence of the spacecraft and Nutation Dampers Parameters on the Dynamic Characteristics

In the subsequent sections, the influences of the various parameters of the spacecraft and nutation dampers are investigated on the overall performance and the dynamic characteristics of the nutation damping system proposed in the present study.

5.4.1.1 Influence of The Inertia Ratio (σ)

In figures (5.5) and (5.6), the variation of the time constant with the inertia ratio for nutation-synchronous mode and spin-synchronous mode are shown respectively. It can be seen that the time constant increases as the inertia ratio tend to (1), while in figure (5.6), the time constant for spin-synchronous mode decreases as the inertia ratio approaches unity. Also these figures show, for ($\sigma > 1$) the time constant in the nutation-synchronous mode decreases and that of spin-synchronous mode increases with increasing the inertia ratio, this result means that there is a contrast in the design problem requirements of the nutation dampers with respect to the inertia ratio.

Consequently, this may be attributed to the fact that the expressions are valid only for ($\sigma > 1$) according to the stability condition (major axis rule) derived from stability analysis, and the spacecraft with spherical shape or equal principal moments of inertia is not considered throughout the analysis. Comparison also shows that the analytical solution of the time constant given by Eq. (4.62) is good.

5.4.1.2 Influence of Rotor Spin Rate (Ω)

The variation of the time constant with the rotor spin rate (Ω) for nutation-synchronous and spin-synchronous modes are shown in figures (5.7) and (5.8) respectively. Hence increasing the rotor spin rate causes decreasing in the value of the damping constant which leads to increase the time constant for both modes. In physical meaning, the higher the spin rate of a spinning body, for the same moments of inertia, causes higher gyroscopic stiffness of the spinning body, thus more time is needed to return the body to its initial state. Again, comparison between the analytical and numerical solutions of the time constant reveals that the approximate solution is an acceptable one.

5.4.1.3 Influence of Ring Mean Radius (*R*)

Figures (5.9) and (5.10) show the variation of the time constant with the ring mean radius in nutation-synchronous mode and spin-synchronous mode. These figures show that the time constant decreases with increasing the ring mean radius, and this decrease can be understood throughout the dimensionless parameter ε. Hence, the parameter ε directly proportional to the square power of the ring mean radius, at the same time the analytical expression of the time constant, Eq. (4.62), shows that the time constant is inversely proportional to the parameter ε, which interprets the decrease occurs in the time constant with increasing the ring mean radius.

Finally, these figures show that the decrease in the time constant reaches an asymptotic value in each case and behind this value there is no appreciable decrease occurs.

5.4.1.4 Influence of Ring Radius (*r*)

The time constant for nutation-synchronous mode and spin-synchronous mode decreases with increasing the ring radius as shown in figures (5.11) and (5.12). Where, the parameter

(ε), which appears in the time constant terms, is directly proportional with the square power of the ring radius, and it is given by:

$$\varepsilon = \frac{mR^2}{A} = \frac{2\pi^2 r^2 R^3 \rho_f}{A} \tag{5.7}$$

where A is the total transverse principal moment of inertia of the spacecraft.

It can be seen that the effect of (r) has the same effect of ring mean radius.

5.4.1.5 Influence of the Damping Constant

Figures (5.13) and (5.14) show the variation of the time constant with the damping constant for nutation-synchronous mode and spin-synchronous mode respectively. It is shown that the time constant for nutation-synchronous mode decreases with increasing the damping constant and becomes asymptotically at certain value of the damping constant. While, the time constant for spin-synchronous mode is a concave up function of the damping constant and has a minimum, however, such as behavior of the time constant indicates that at the same value of the time constant there are two corresponding values of the damping constant. It can be thought that these two values of the damping constant corresponding to two different types of damping fluids of different properties. So that, the damping fluid type should be selected carefully especially from the view point of saving in the weight of nutation damper and to give passive nutation damper system with good performance.

5.4.1.6 Influence of Ring Height to Ring Mean Radius Ratio (b_1)

In figure (5.15), the time constant variation for spin-synchronous mode with the dimensionless parameter (b_1) is shown. It can be seen that the time constant decreases with increasing the parameter (b_1), where the analytical expression of the time constant in spin-synchronous mode shows that the time constant inversely proportional to the parameter

(b_1), whereas the time constant in nutation-synchronous mode is independent of the parameter (b_1).

The effect of the parameter (b_1) may be interpreted physically as follow, the driving oscillatory forces for the nutation damper are proportional to the acceleration of any point in the spacecraft coordinate system and the latter is directly proportional to the position of the point in the space, as mentioned by [19]. Therefore, the damper on the plane perpendicular to the spin axis should be placed as far as possible from the center of mass of the spacecraft to get better damping performance.

5.4.1.7 Influence of Ring Center Offset (*d*)

Figure (5.16) shows the variation of the time constant for spin-synchronous mode with the center offset distance of the ring. It is seen that the time constant decrease as (d) increased until reach a value where there is not noticeable decreasing beyond it. The position of the damper may be considered to be a very important design parameter when a partially viscous ring nutation damper is used, especially the amount and plane of the offset center of the nutation damper [2,35], where that the spin mode may be not exist if the ring is not offset from the spin axis [2]. Takaichi et al. [35] was referred to that the time constant can be decreased effectively with increasing the offset center distance of the nutation damper. Thus, the appearance of (d) in the time constant spin-synchronous mode term is a good result and it is support the above conclusion.

Finally, the value of the offset distance must be selected carefully and should be within a reasonable value because the increase in its value may be led to what is called time-varying inertia properties.

5.4.2 Influence of Spacecraft and Nutation Dampers Parameters on the Residual Nutation Angle

The residual nutation angle and the time constant of the nutation damper are two of the important indexes for designing the nutation dampers, where the value of that angle must be less than the pointing accuracy of the satellite [31]**.** However, the pointing accuracy of spin stabilized satellite lying between $(0.3\text{-}1)^{o}$ [31].

The residual nutation angle is induced when the nutation motion can not excite the essential relative motion between the damper and the spacecraft, and the energy dissipation rate is ceased.

5.4.2.1 Influence of Inertia Ratio (σ)

In figure (5.17) the residual nutation angle is increased with increasing the inertia ratio, then it will approach very large value when the inertia ratio approaches (1). For ($\sigma > 1$) the residual angle will decrease because the spacecraft with relatively large inertia ratio, and the nutation frequency become higher. Hence large driving force for the damping fluid will be induced, so that much energy will dissipate and small residual nutation angle induced.

5.4.2.2 Influence of R, r & b_1 parameters

Figures (5.18), (5.19), and (5.20) show the variation of the residual nutation angle with the parameters b_1, R, and r. Physically, that the increase in the residual nutation angle may be interpreted as that the increasing in the above parameters, the inertia properties of the nutation dampers will be increased which result in increasing the necessary driving forces for the relative motion of the nutation dampers, so that a larger nutation angle will be induced.

CHAPTER SIX

Conclusions & Suggestions for Future Work

6.1 Conclusions

Based on the results obtained in the present study, several conclusions may be drawn. These may be summarized as follow:

1- The agreement between the analytical results and the numerical results indicates that the proposed configuration of nutation dampers is an acceptable one as a passive nutation damping system. Also, the results show that the addition of second nutation ring damper on the spacecraft is greatly affecting the dynamic characteristics of the nutation damping system. In other words, the time constant specially for nutation-synchronous mode decrease by the half compare with using unique nutation ring damper.

2- The problems of the spreading out on the internal wall, separation into several slugs, and sloshing of the viscous fluid which occur in the partially filled viscous ring nutation dampers are avoided in the fully filled with offset center dampers.

3- The inertia ratio parameter is appreciably affecting the time constant for nutation-synchronous and spin-synchronous modes, and for ($\sigma > 1$), the increase in the inertia ratio results in decreasing the residual nutation angle. So that the design of the nutation damper should be handled carefully with respect to the inertia parameter.

4- The time constant for nutation-synchronous mode decreased with increasing the damping constant, while for spin-synchronous mode, the time constant is a concave function of the damping constant and has a minimum.

5- The parameter (b_1) is appreciably affecting the time constant in the spin-synchronous mode, while in the nutation-synchronous mode, there is no any influence for it on the time constant. Also, the increase in this parameter results in increasing linearly the residual nutation angle of the spacecraft.

6- The increase in the ring center offset distance results in decreasing the time constant in the spin-synchronous mode, while it has nothing to do for the time constant in the nutation-synchronous mode.

6.2 Suggestions for Future Work

The following suggestions may be considered as an extension for the present work:

1- Measurement of the dynamic performance of the proposed dampers configuration experimentally via using an artificial satellite ground test apparatus.
2- Study the stability and the effects of the dynamic unbalance and asymmetry arise in the rotor and the platform on the dynamic characteristics of the system (the spacecraft and nutation dampers).
3- Utilizing nutation ring damper with a circular ring cross-section partially or completely filled with a viscous fluid.